STUDIES ASSESSING INSULIN SIGNALING DEPENDENT NEURONAL MORPHOLOGY AND NOVEL ANIMAL SORTING METHODS IN A *C. ELEGANS* MODEL

By

Skyler C. Hunter, B.S.

A Thesis Submitted in Partial Fulfillment of the Requirements
for the Degree of

Master of Science
in
Biological Sciences

University of Alaska Fairbanks
December 2018

APPROVED:

Dr. Abel Bult-Ito, Committee Co-Chair
Dr. Barbara Taylor, Committee Co-Chair
Dr. Andrej Podlutsky, Committee Member
Dr. Elena Vayndorf, Committee Member
Dr. Diane Wagner, Chair
Department of Biology and Wildlife
Dr. Leah Berman, Dean
College of Natural Science and Mathematics
Dr. Michael Castellini, *Dean of the Graduate School*

GENERAL ABSTRACT:

The purpose of this work is two-part. The primary goal of this thesis is to identify a list of significant target insulin-like peptides (ILPs) that influence the maintenance of neuronal morphology in an aged animal model of *Caenorhabditis elegans* (*C. elegans*) and determine whether or not morphological changes have bearing on neuronal function. The second goal is to address and devise a solution for a common laboratory difficulty encountered within the research community, difficulty maintaining large age-synchronous populations of the model organism, *C. elegans*.

Chapter 1 discusses the importance of insulin signaling and how it pertains to the morphology of aging neurons. A reverse genetic screen was conducted to knockdown the expression of individual ILPs in a *C. elegans* model. The results identify a subfamily of ILPs that play significant roles in maintaining regular morphology of aging mechanosensory neurons. These data corroborate previously published work demonstrating that aberrant morphology of mechanosensory neurons does not directly influence their function and that these two parameters, morphology and function, can be uncoupled and considered mutually exclusive.

Chapter 2 describes a main difficulty associated with using *C. elegans* as a model organism; the problem of maintaining a large age-synchronous population on solid media. To address this difficulty a novel piece of equipment, named the *Caenorhabditis* Sieve, and an accompanying methodology for its application, were created to mechanically sort and clean *C. elegans*. The use of this new device facilitates the implementation of assays with animals cultivated on solid media that are normally cost and resource prohibitive. Presented with the protocol for device construction and implementation, are standard experiments that were conducted to verify "proof of concept" of the tool's efficacy. The results demonstrate that the *Caenorhabditis* Sieve effectively transfers animals from one culture plate to the next in a manner that does not influence common markers of physiological stress; thus validating the sieve's use in future experiments among the research community, as well as highlighting the success of creating a cost-effective, efficient, fast, and simple process to mitigate difficulties and ease progress in research fields using small model organisms.

TABLE OF CONTENTS

List of Figures

Page

List of Tables

Page

GENERAL INTRODUCTION:

Insulin Ligands Influence Morphology of Mechanosensory Neurons

Aging human brain tissue is subject to normal restructuring over time, and this overall restructuring has been proposed as an underlying cause of cognitive decline with advancing age and neurodegeneration[1-4]. This brain restructuring comprises synapse deterioration, neuronal sprouting and restructuring with little if any cell loss, and this restructuring is seen as a normal age-related occurrence[1-3]. Outside of normal, healthy, aging of brain tissue, there are neurodegenerative diseases such as Alzheimer's disease (AD), which affects over 5 million Americans[5], Parkinson's disease (PD), affecting almost 1 million Americans[6], and Amyotrophic Lateral Sclerosis (ALS), affecting 30,000 Americans[7]. These diseases are age-related with all three, on average, being diagnosed in subjects over 50 years of age[5-8]. These case numbers are projected to increase as modern medicine progresses and geriatric population numbers continue to grow[5-8]. Under the neurodegenerative conditions of these diseases, an increase in protein mis-folding is observed and causes cellular stress, eventually leading to protein aggregation in brain tissue[9]. Over time this cellular stress and protein aggregation can lead to morphology changes in brain structures, atrophy, and degeneration in the affected regions[10].

A major regulator of the aging process, both at the organismal and cellular levels, is the insulin and insulin-like signaling (IIS) pathway, which influences lifespan, health quality, and life stage progression[11,12]. This pathway is conserved in metazoans ranging from *Drosophila*[13] to humans and in the latter, a single nucleotide polymorphism (SNP) of the FOXO transcription factor (DAF-16 in *Caenorhabditis elegans* (*C. elegans*)), an insulin signaling target, can help predict whether an individual will reach the age of 100 years[14]. This IIS pathway has also been shown to influence neuronal morphology in a *C. elegans* model[15-17], yet no correlation has been found between the number of neuronal morphological changes linked to the IIS pathway modulation and changes in neuronal function or lifespan[17]. Interestingly, these morphological changes at the neuronal level appear to be independent from neuron function and organismal lifespan.

Understanding IIS and its influence on the morphology of healthy, normal, aging neurons, helps build a foundation of knowledge that can be used to understand IIS in age-related neurodegenerative conditions. By establishing a baseline for the morphological changes seen in healthy brains and neurons, researchers can reference a metric to compare neurodegenerative conditions. This is important because of the projected increase in age-related neurodegenerative conditions that will parallel the increase in the geriatric population[5-8]. Understanding IIS in healthy neurons is important also because neurodegenerative conditions such as AD have been correlated with dysregulation of normal insulin and insulin-like growth factor expression in the central nervous system (CNS) of humans[18,19]. Indeed, some researchers have proposed a relatively new "type III" diabetes to reflect the neurodegenerative pathogenesis seen in AD patients[19]. If neurodegeneration can be triggered over time in what is thought to be healthy, non-disease carrying individuals, then prevention, mitigation and possible reversal are all the more important. Others have already shown that gain of function mutations in IIS pathway constituents in models

where their respective upstream activator molecules are missing can help to recover dysregulated signaling[20-22]. Thus, this is a potentially fruitful route to explore therapeutic targets.

The nematode worm *C. elegans* is a premier model organism whose genome has been fully sequenced[23]. The cellular fate of all 959 cells has also been mapped in the *C. elegans* hermaphrodite, including its 302 neurons[24,25]. Because of its ease of culturing, relatively quick life cycle and simplified nature of complex tissues like intestine, reproductive, and nervous systems, *C. elegans* is a common model system for the study of aging, molecular pathways and neurodegeneration[26-31]. A key feature for *C. elegans* use in aging studies is that it utilizes the previously mentioned conserved IIS pathway for cellular signaling with 40 species specific insulin-like peptides (ILPs)[32]. While humans produce 10 ILPs and rely on a vascular system for intercellular insulin transportation, *C. elegans* secretes some 40 ILPs primarily from neurons[32-25]. These ILPs affect neighboring cells, or diffuse into a fluid-filled body cavity called a "pseudocoelom" that bathes *C. elegans* tissues and organs and serves to function in place of a respiratory and circulatory system for cases outside of local cell-to-cell secretion and signaling[36-38].

Currently the IIS pathway has been mapped with respect to its major participants and targets[28,30,32,39]. The structure of both the insulin ligands and the insulin receptor (IR), a receptor tyrosine kinase (RTK) are known, as well as the specific binding sites on the receptor and the general mechanism that induces conformation change upon ligand binding which allows for tyrosine phosphorylation of substrate[40,41]. The IIS pathway, as depicted by Murphy and Hu, comprises the ILP ligands, the IR (DAF-2 in *C. elegans*), primary messengers such as AGE-1 and phosphoinositide-3 kinases (PI3), secondary messengers such as PDK-1 and AKT-1, and transcription factors HSF-1, DAF-16/FoxO, and SKN-1/Nrf (**Figure I.1**)[32].

Upon agonist ligand binding at the IR, the IIS pathway is activated which results in the phosphorylation of pro-longevity transcription factors HSF-1, DAF-16, and SKN-1. Phosphorylation of these transcription factors inhibits their translocation to the nucleus, where they function to upregulate downstream pro-longevity genes. Antagonist ligand binding at the receptor or other resultant decrease in IR activity would have the opposite effect and cause a "disinhibition" of the transcription factors, allowing them to translocate to the cell nucleus and activate pro-longevity genes[30,32,39].

The insulin ligands themselves are peptide ligands composed entirely of amino acids with two major functional domains, the A and B peptide domains[34,42]. These A and B peptide regions are α helices and give ILPs a basic helix-loop-helix folded structure[34,40-42]. In addition to this basic structure, the known ILPs have been subdivided into three major subfamilies based on their sequence and structural similarity, the α, β, and γ subfamilies[34,42]. The γ subfamily is characterized by canonical disulfide bonds found in mammalian and most all other insulin ligands, and the α subfamily by nonpolar substitutions at the 6/11 disulfide bond positions on the A peptide[35]. The β subfamily is characterized by the three canonical di-sulfide bonds found in mammalian and most other insulin ligands, as well as additional di-sulfide bonds at position 21 of the A peptide and position 22, 23, or 24 of the B peptide[34] (**Figure**

I.2)[36]. These minor alterations in sequence and conserved intra-subfamily sequence variation between ILPs produces subtle changes in structure and variations in the affinity of ILPs for the IR and other interacting molecules[43]. These variations may also influence the ILPs' immediate agonist/antagonist action at the IR's binding sites as the relative binding affinities of ILPs and their immediate binding roles as either agonist or antagonist are still largely unknown. In fact, agonist or antagonist activity is not conserved across ILP subfamilies with both activities seen in a given subfamily[34,44-46]. Several researchers have investigated the agonistic and antagonistic roles of ILP function in *C. elegans* models but have done so with endpoint-specific results that did not utilize local intra-IIS pathway constituents. The agonistic/antagonistic role of individual ILPs was determined by downstream endpoints such as dauer arrest (a larval stage diapause)[34,35,37,44,46,47], olfactory learning[45], downstream marker regulation[37,46], or ILP-to-ILP interactions[28,45,46], to name a few. Additionally, different tissues and developmental time points can vary the specific ILPs present and their expression levels[35,37,48]. While incredibly insightful, these studies do not focus on ligand/receptor activation or blocking at the molecular level, albeit a more difficult operation considering the many ILPs present in the *C. elegans* model. These variations in ILP sequence, conformation and potential binding affinity have led to beliefs of functionally redundant ILPs in cases of compromised expression of an individual ILP[34,35,37,49] and/or that different subfamilies and each individual ILP has different roles and expression patterns based on given environmental and metabolic stress conditions[35,47].

The IR is a homodimer with each monomer consisting of three main regions, an extracellular domain, transmembrane domain, and a cytosolic domain[40,41]. As represented by Colin Ward, the extracellular domains are shaped in "upside down Vs" that, when dimerized through disulfide bonds, rest side-by-side against one another, facing 180 degrees opposite the other with eclipsed side silhouettes (**Figure I.3**)[40]. Each monomer has a primary binding site (S1) for ILPs on the distal V arm and a secondary, weaker, region that binds ILPs on the V arm proximal to the transmembrane region (S2), meaning that each side of the IR's extracellular domain has a primary binding site (S1) and a secondary site on the opposing IR monomer (S2') that lies next to it[40,41]. Upon ILP binding to a primary (S1) IR site, the IR dimers are rotated together to allow the ILP's secondary site to bind the opposing monomer's complimentary secondary site (S2')[40-41]. This is illustrated by Colin Ward as a two-step action that occurs on either side of the IR's extracellular region (**Figure I.4**)[40]. This rotation causes a conformational change through the transmembrane region that leads to an unrolling of coiled tyrosine kinase (TK) regions on the cytosolic region of the IR homodimers (**Figure I.3**)[40]. This IR dimer rotation also pulls the other set of primary and secondary ILP binding regions apart on the opposing side of the IR's extracellular domain (**Figure I.4**)[40]. When the TK regions unwind, there are thirteen potential phosphorylation sites along each cytosolic domain of the IR. These docking sites are thought to be for SH2 and PTB-domain containing proteins, which are signal and RNA binding proteins, respectively[40].

While the vast majority of the research conducted to date investigates the pathway itself and its primary downstream constituents, there has been relatively limited research conducted on the signaling molecules upstream of the IR that bind and activate it in regards to neuronal aging processes. In *C. elegans*, many studies have been conducted with

individual ILPs to ascertain the effects of their absence or overexpression in specific tissues or on specific events[34,44-46], but collective studies on the ILP family as a whole have been limited. These studies concentrate primarily on the expression interactions ILPs have on one another and the relative spatiotemporal expression of each in a nematode model[35,47,48], or on protein aggregation regulators in disease models[31]. The specific ligands and the phenotypic growth they regulate in neurons are still unclear. Furthermore, the classification of ILPs into subfamilies[34,42] has not been investigated for correlation with phenotypic regulation. By correlating specific ILPs or a particular ILP subfamily with neuronal morphology phenotypes, researchers may be able to use those ILP expression levels and actions in neurons to gauge neuronal health and neurodegeneration, and additionally use them to build a baseline metric for neurodegenerative conditions when seeking therapeutic treatments.

The objective of Chapter 1 was to modulate the IIS pathway in an aged *C. elegans* model, via individual knockdown of 39 of the 40 ILP ligands expressed, to identify key ILPs responsible for maintaining neuronal morphology and function with the hypothesis that the different efficacies within the ILP families will dictate their regulatory importance on the neuronal aging process. Results were expected to point to similar ILPs, relative to sequence/structure as being important players in this role. The intent was to use the identified ILPs and potential findings to contribute to the greater understanding of healthy neuronal aging and use this to seek therapeutic targets that are within, or modulatory to, the IIS pathway or the upstream ILP ligands and their expression to help regulate or correct any dysregulation of the pathway that could lead to irregular neuronal aging and neurodegeneration.

***Caenorhabditis* Sieve: A Low-Tech Instrument and Methodology for Sorting Small Multicellular Organisms**

Chapter 2 introduces the development of a novel laboratory tool designed to sort *C. elegans* and other small organisms by body size. This endeavor grew out of the identification of difficulties in maintaining age synchronous populations of *C. elegans* during previous work on ILPs influence on neuronal morphology and identifying these same difficulties in the work of others within the *C. elegans* research community. Many assays require large numbers of age synchronous populations to be maintained to prolonged time points (e.g., DNA extraction, RNA extraction, lifespan and other age-dependent experiments such as those involving neurodegeneration).

Previous protocols that separate or sort *C. elegans* by body size have been related to utilizing liquid culture media and have unknown outcomes on animal health and stress[50]. Culturing *C. elegans* in liquid media has its own specific requirements compared to culturing with solid nematode growth media (NGM)[27]. The liquid conditions require closer monitoring as starvation and overcrowding are common and can lead to dauer formation, an arrested developmental stage during the Larval 3 growth phase[27].

Culturing *C. elegans* on solid NGM on the other hand requires less monitoring, and allows for harvest and separation of specific individual animals for assays such as gentle touch response[27,51]. The drawback of solid NGM is the limited surface area/volume available which limits the number of animals that can be sustained on a single

plate before starvation and overcrowding occurs. This requires that animals be cultured on larger and larger plates or multiple plates per group to achieve an appropriate population size if large numbers of animals are required for a given assay.

When the food supply runs low, *C. elegans* must be transferred to new plates to maintain environmental conditions[27]. This becomes problematic when multiple generations of animals at different life stages are mixed on the NGM plates. Current methods of sorting animals are picking by hand, fluorodeoxyuridine (FUDR) dissolved in NGM, and microfluidic sorting. Picking by hand is very accurate but time consuming and inefficient when transferring large numbers of animals on multiple plates per group with multiple groups per experiment. FUDR, a chemical that inhibits cell proliferation, is toxic, and can lead to possible epigenetic contamination of animals. Furthermore, its use is limited to adult animals[52-56]. Microfluidic sorting utilizes machines with fine capillary tubes and optical data processing to sort animals[57]. These microfluidic methods require that animals be prepared in fluid and run through the microfluidic devices. While accurate, it is a complex method that relies on advanced technology and the microfluidic channels can become clogged with debris[58]. In addition to their complexity, microfluidic devices can be cost prohibitive to many research groups.

The goal of work reported in Chapter 2 was to create an efficient, fast, affordable, simple to make and simple to use/learn device to assist in common laboratory experiments by sorting *C. elegans* and/or other small organismal models by body size. The device and protocol created aimed to teach the scientific community how to manufacture and implement such a device to maximize the yield of return on animals sorted and exhibit its efficacy as a safe alternative to several current sorting methods.

FIGURES:

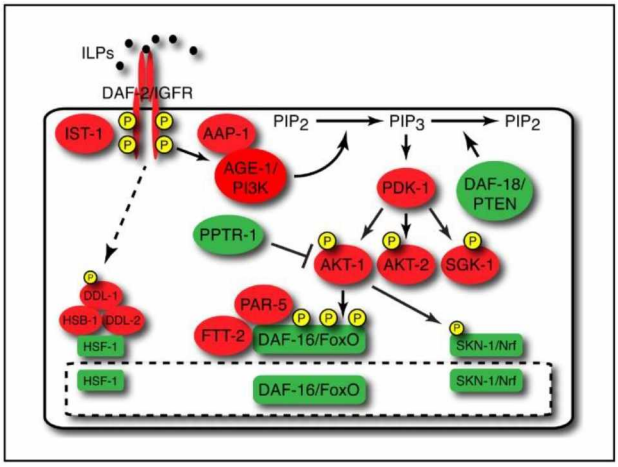

Figure I.1. Insulin and insulin-like signaling (IIS) pathway in *C. elegans*. Graphic from Murphy and Hu, 2013 (Figure 1)[32]. Insulin-like peptides (black circles) bind to the extracellular domain of the DAF-2 receptor located in the cellular membrane. Intracellular pathway constituents that promote positive IIS signaling are colored red, and pathway constituents that antagonize or are antagonized by positive IIS signaling are colored green. Agonist binding to the DAF-2 receptor functions to inhibit translocation into the nucleus (indicated by the dotted line) of the pro-longevity transcription factors HSF-1, DAF-16, and SKN-1, while antagonist binding to the DAF-2 receptor functions to dis-inhibit their translocation.

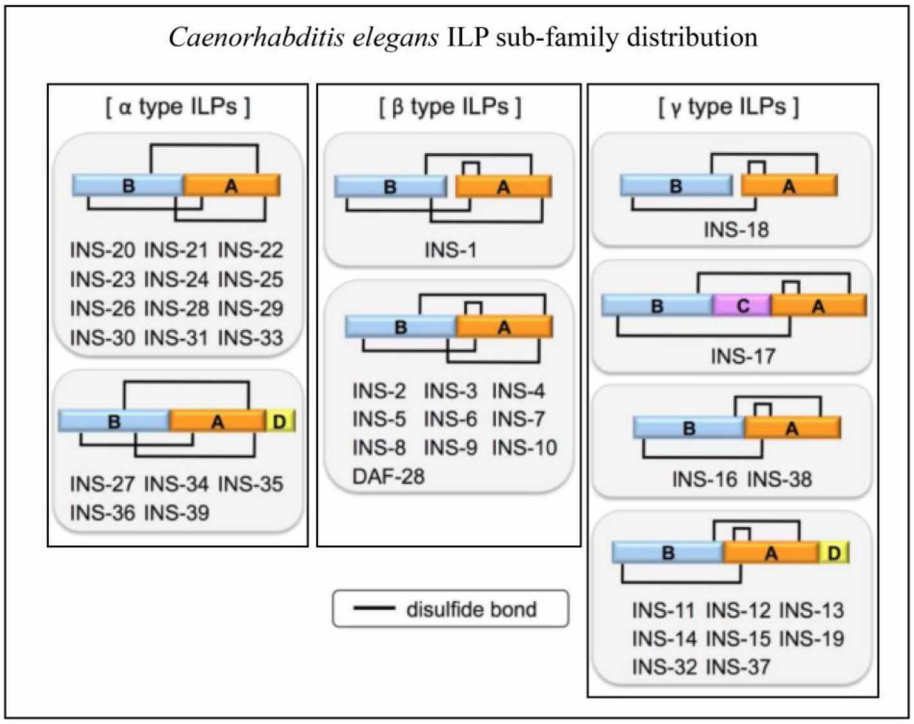

Figure I.2. *Caenorhanditis* elegans ILP sub-family distribution. Graphic from Matsunaga et al., 2017 (figure 1)[36]. Categorization of the 40 *C. elegans* ILPs into α, β, and γ sub-families. Colored blocks represent peptide sequences and black bars represent structural disulfide bonds.

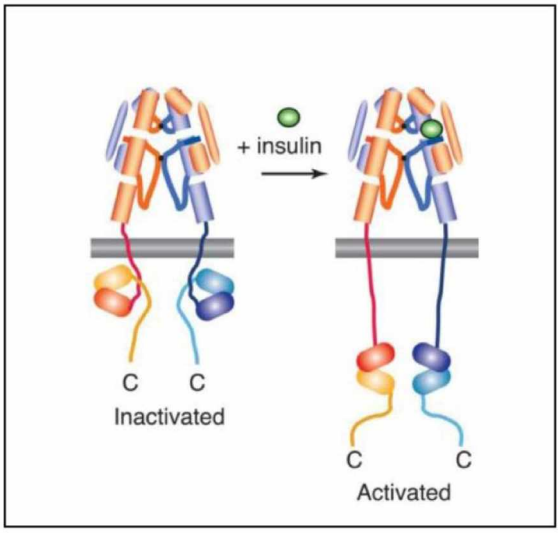

Figure I.3. Insulin receptor structure and conformational change. Graphic from Ward, Menting and Lawrence, 2013 (Figure 5A)[40]. Insulin receptor (IR) structure shown in side-view in the inactivated and activated conformations. Upon ligand binding to complementary binding regions on the extracellular domain, the cytosolic receptor tyrosine kinase (RTK) unrolls to allow for substrate docking.

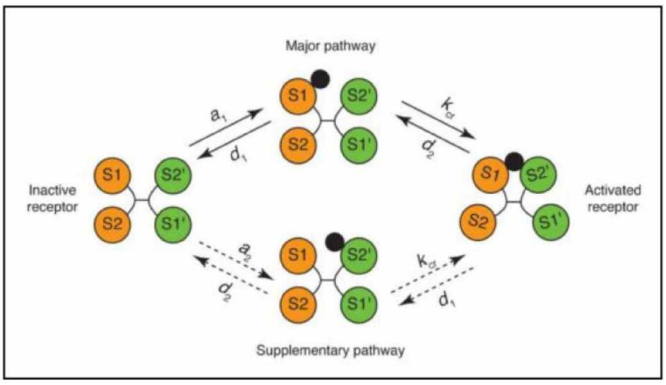

Figure I.4. ILP binding and disassociation at complimentary homodimer binding sites. Graphic from Ward, Menting, and Lawrence, 2013 (Figure 1)[40]. Top view illustration of ILP binding at the insulin receptor. ILP (black circle) binds at the S1 site and triggers crosslinking to S2' site of adjacent monomer. Dashed arrows depict alternate association and disassociation routes for the same S1 and S2' pair. This association and dissociation model can occur at the S2 and S1' sites as well.

CHAPTER 1:

Insulin Ligands Influence Morphology of Mechanosensory Neurons[1]

1.1 ABSTRACT:

Insulin signaling plays a key role in the aging of organisms ranging from yeast to mice, and there is evidence that in humans, single nucleotide polymorphisms (SNPs) of the insulin transcription factor, FOXO, can predict whether an individual will reach the age of 100. In *Caenorhabditis elegans* (*C. elegans*), insulin-like peptides (ILPs) are regulators of both organismal and neuronal aging. In humans, healthy neuronal aging is characterized by neuronal sprouting, synaptic deterioration and restructuring with little to no neuronal cell loss. However, the physiological factors that affect the decline of neuronal morphology and structure over time in their native context remain poorly understood. This is particularly true at the single cell level. *C. elegans* ILPs belong to three major subfamilies based on their sequence and structure. The goal of this study was to determine how ILPs, individually or as a group, influence the morphology of aging mechanosensory neurons. To investigate the relationship between ILPs and neuronal morphology and function, a reverse genetic screen of insulin ligands in *C. elegans* with fluorescently labeled mechanosensory neurons was conducted. RNAi was used to individually knock down expression of insulins 1 through 38 and DAF-28, and structural and functional data were collected for anterior lateral mechanosensory (ALM) and posterior lateral mechanosensory (PLM) neurons. ILPs of interest were rescreened for a total of three replicates compared to empty vector controls. The results highlight ILPs whose absence correlated with specific neuronal aberrations and functional outcomes, and showed that neuronal morphology may be influenced by ILPs in a subfamily dependent manner. Specifically, the β subfamily may be particularly important in producing somatic outgrowths seen in normal neuronal morphology. The results also agree with previous research that demonstrated neuronal morphology aberrations were not influential on functional capacity, in that no relationship was seen between neuronal aberration occurrence and mechanosensory neuron function. These data implicate a subfamily of ILPs and their ensuing IIS pathway response as possible therapeutic targets in the fight against aging and neurodegeneration.

1.2 INTRODUCTION:

Aging related diseases are numerous, many of which are neurodegenerative. Currently 5 million Americans have Alzheimer's disease (AD)[1], almost 1 million have Parkinson's disease (PD)[2], and almost 30,000 have Amyotrophic Lateral Sclerosis (ALS)[3]. These diseases are age-related with all three, on average, being diagnosed over the age of 50 years[1-4]. These incidences of these diseases are projected to increase as modern medicine progresses and geriatric population numbers continue to grow.

Aging of healthy brains is characterized by neuronal sprouting, synaptic deterioration and restructuring with little to no cell loss[5]. As neurons age there is an increase in the occurrence of this cellular restructuring[5,6]. Similar to this

[1] Citation: Hunter, S., Vayndorf, E., Driscoll, M., Taylor, B.E., Bult-Ito, A. Insulin ligands influence morphology of mechanosensory neurons. Manuscript completed in preparation for submittal.

age-related brain restructuring in humans, the nematode worm *Caenorhabditis elegans* (*C. elegans*) exhibits structural aging in neurons without cell loss[6-8]. This structural aging in *C. elegans* neurons resolves as morphological aberrations in the form of new somatic, axonal, and dendritic branching[6] The insulin and insulin-like signaling (IIS) pathway, a conserved receptor tyrosine kinase pathway among metazoans, has a definitive role in influencing the aging processes of *C. elegans,* impacting lifespan, health quality reporters such as motility, metabolism and stress response, as well as life stage progression[9-11]. The primary components of this pathway in *C. elegans*, as depicted by Scerbak et al.[12], comprise the insulin and insulin-like peptide (ILPs) ligands, the insulin receptor DAF-2, primary messenger AGE-1, phosphoinositide-3 kinases, secondary messengers AKT-1/AKT-2 and the transcription factor DAF-16 (**Figure 1.1**)[12]. Under normal operation, positive DAF-2 signaling functionally inhibits the translocation of pro-longevity transcription factor DAF-16. This conserved pathway is important to most organisms including other nematodes, *Drosophila*[13] and even humans. In the latter, a single nucleotide polymorphism (SNP) of the FOXO transcription factor (DAF-16 in *C. elegans*), an insulin signaling target, can predict whether an individual will reach the age of 100 years[14].

Modulation of the IIS pathway has been shown to influence the occurrence of age-related neuronal aberrations in *C. elegans* mechanosensory neurons[6-8]. Reduced IIS pathway activity through knockdown of the sole known insulin receptor in *C. elegans*, DAF-2, has been shown to decrease the occurrence of neuronal aberrations, while knockdown of the DAF-2 downstream target DAF-16 (FOXO in humans), a pro-longevity transcription factor, results in an increase in these aberrations[6,8]. In addition to regulating neuronal aberrancy, the IIS pathway plays a role in neuronal synapse development and axon regeneration. Decreasing the activity of the DAF-2 receptor reduces the occurrence of aberrant synaptic development in motor neurons[15] and causes an increase in axon regeneration levels after laser ablation[16]. Modulation of the IIS pathway also influences lifespan, with DAF-2 receptor suppression increasing lifespan and DAF-16 transcription factor suppression decreasing lifespan[6,8,16]. Interestingly, the role the IIS pathway plays in neuronal morphology and remodeling and its role in lifespan operate independently. The influence exhibited by the IIS pathway on both the occurrence of neuronal aberrations and level of axon regeneration are not coupled with lifespan, neuronal morphology and lifespan display a heterogeneity in occurrence that makes them independent of one another[6,8]. The presence of neuronal aberrations in *C. elegans* mechanosensory neurons also does not indicate any influence in their function, meaning that these two metrics appear to operate independently as well[6].

Because the IIS pathway is so involved in multiple facets of the aging process, the role ILPs binding DAF-2 play in neuronal aging was investigated. *C. elegans* have 40 ILPs; INS-1 through INS-39 and DAF-28[17,18]. These ILPs have been grouped into three major subfamilies, α, β and γ, based on their sequence and structure[17,19].

While several genetic screens against *C. elegans* ILPs have been conducted, they pertain primarily to the ILP-to-ILP interactions and relationships and ILP expression levels. These previous screens encompass all 40 *C. elegans* ILPs but do not investigate the morphological outcomes on neurons when ILPs are knocked down. Prior screens have

focused on using the dauer phenotype to determine ILP function, spatiotemporal expression patterns of ILPs in different tissues at set developmental time-points[20,21], or whole animal ILP mRNA expression over only the first 60 h after embryo hatching[22]. Researchers have conducted genome-wide RNAi screens in *C. elegans* searching for regulators of polyglutamine aggregation in neurodegenerative models[23], but currently no genetic screens have been conducted that focus on the roles individual ILPs have on neuronal morphology in healthy models. To investigate the roles ILPs play in the neuronal aging process, a reverse genetic screen of 39 of 40 *C. elegans* ILPs using RNAi was conducted, with the hypothesis that knockdown of similar ILP subfamily members will result in similar phenotypic aberrations in neurons. This is based on the similar sequence and structure within the insulin subfamilies[17,19] and the possibility of similar binding affinities and redundancy within subfamilies.

1.3 MATERIALS AND METHODS:

1.3.1 *C. elegans* strain and maintenance

The strain used in this study, P_{mec-4} GFP, $P_{unc-119}$ SID-1, $P_{unc-119}$ YFP, P_{mec-6} mec-6 known as mec-4::gfp, was created by Dr. Elena Vayndorf in the laboratory of Dr. Monica Driscoll at Rutgers University, New Jersey. This mec-4::gfp strain has green fluorescent protein (GFP) expressed in the mechanosensory neurons allowing for whole neuron visualization under fluorescent microscopy, and contains neuronal SID-1 channels that allow for dsRNA uptake. Standard methods to maintain and manipulate a mec-4::gfp population of *C. elegans* were used[24]. The stock population was cultured at 25°C on Nematode Growth Media (NGM) agar plates (1 L NGM: 2.5 g peptone, 17 g agar, 3 g NaCl, 975 mL double distilled water, 1 mL 5 mg/mL cholesterol, 1 mL 1 M $CaCl_2$, 1 mL 1 M $MgSO_4$, 25 mL 1 M $KHPO_4$, and 0.5 mL 100 mg/mL streptomycin) seeded with live bacteria (*E. coli* strain OP50-1) cultured in Luria Broth with 100 mg/mL streptomycin that were allowed to form a lawn for 48 h at room temperature and then stored at 4°C until use, as per the standard Wormbook protocol[25]. The stock population was maintained at 25°C through at least 3 generations of offspring without starvation, mitigating the effects of environmental stress on gene expression. All age-synchronous *C. elegans* populations were created using the egg lay method , i.e., allowing 20-30 gravid adults to lay eggs for 4-6 h, then removing the adults, and were cultured at 25°C until day 5 of adulthood[26]. Maintaining *C. elegans* at 25°C is well known to accelerate metabolism and the aging process[27-31] as is evidenced by the decrease in the gentle touch response[32]. This accelerated aging process through growth at 25°C better simulates an aging model for the purposes of age-related neurodegeneration, as it allows researchers to advance animal age at specific time points in comparison to growth at 20°C. Day 5 of adulthood for *C. elegans* was chosen as a designated time point for animal harvesting and data collection in all following assays as apparent differences in touch response and neuronal morphology has previously been shown to occur by day 4 of adulthood in *C. elegans* when matured at 20°C and maintained at 24°C[6].

1.3.2 RNAi plate making

Once a stock population had been obtained and stabilized, RNAi treatment plates were made as per the Wormbook protocol[33] (1 L NGM: 2.5 g peptone, 17 g agar, 3 g NaCl, 975 mL double distilled water, 1 mL 5 mg/mL

cholesterol, 1 mL 1 M CaCl2, 1 mL 1 M MgSO4, 25 mL 1 M KHPO4, 0.5 mL 50 mg/mL carbenicillin, and 1 mL 1M isopropyl β-D-1-thiogalactopyranoside (IPTG)). Bacterial cultures were established for each RNAi treatment clone of *E. coli* strain HT115 via the Wormbook protocol[25]. HT115 is a strain used to contain the plasmid vector L4440. Each treatment clone has an L4440 plasmid that produces dsRNA for a single target ILP's mRNA. Bacterial cultures were inoculated in 15 mL tubes and incubated overnight in Luria Broth with 100 mg/mL carbenicillin. RNAi plates were seeded with a micropipette under sterile technique with 200 µL of live treatment bacteria. After seeding, RNAi plates were allowed to form a lawn for 48 h at 25°C and then stored at 4°C until use. 48 h prior to use, RNAi plates were brought back to 25°C to allow the bacteria to produce fresh dsRNA[32].

1.3.3 Ageing acceleration and L4440 vector validation

The temperature accelerated aging process was confirmed along with validation that the L4440 plasmid did not influence mechanosensory neuron morphology or function. To verify the effects of temperature and the validity of the HT115 strain containing the L4440 vector, RNAi plates with an L4440 empty vector clone, producing no dsRNA, were seeded. Two populations of mec-4::gfp animals were age-synchronized and maintained on NGM plates at 20°C and two populations on NGM plates at 25°C, for a total of four groups. At the L4 stage two groups were transferred to new OP50-1 NGM plates, one at 20°C and one at 25°C. The other two groups were transferred to RNAi plates seeded with the L4440 clone, one group maintained at 20°C and the other at 25°C. At day 3 of adulthood all groups were transferred to new respective plates and maintained at their respective temperatures. On day 5 of adulthood, 30 animals from all four groups were tested for their anterior and posterior gentle touch response with two-way analysis of variance (ANOVA) with $\alpha = 0.05$ followed by a Bonferroni multiple comparison post-test with $\alpha = 0.05$. Animals were then harvested for fluorescent imaging to compare mechanosensory neuron morphology. Anterior and posterior morphology aberrations per animal were combined to create a "total anterior aberrations" and "total posterior aberrations" categories to achieve a more normal data distribution than seen when analyzing individual aberration types and to consolidate multiple individual control analysis. These same four groups were compared using a two-way ANOVA with $\alpha = 0.05$ followed by a Bonferroni multiple comparison post-test with $\alpha = 0.05$.

1.3.4 RNAi arrival to mechanosensory neurons

To verify that RNAi treatments were arriving at and influencing the mechanosensory neurons, an RNAi clone specifically targeting a mechanosensory neuron gene was used. Several RNAi plates were seeded with the L4440 vector, and several plates were seeded with an HT115 *mec-7* clone, this is a clone containing an L4440 plasmid that produces dsRNA targeting the *mec-7* gene, a gene required for proper mechanosensory neuron function[34-37], and two populations were age-synchronized onto NGM both at 25°C. Groups were grown normally until the L4 stage. At the L4 stage animals were transferred to L4440 or *mec-7* treatment plates. At day 3 of adulthood, both groups were transferred to new plates with their respective treatments, upon day 5 of adulthood 15 to 20 animals from both groups were assayed for the anterior and posterior gentle touch response. The mean anterior and posterior responses of the L4440 empty vector control and *mec-7* knockdown were compared using a two-tailed T-test with $\alpha=0.05$.

1.3.5 RNAi screen

ILP treatment groups were age-synchronized by conducting egg lays from the stock population of mec-4::gfp onto NGM plates at 25°C as described above[26]. Synchronized eggs were allowed to hatch and grow normally until the L4 stage. Once the L4 stage was reached, 40 animals from each synchronized treatment group were transferred to an RNAi treatment plate using an eyelash pick. Eyelash picks consisted of a sterilized hair bonded to the end of a glass pipet that allowed for gentle transfer of worms[38,39]. L4 worms were maintained on the same RNAi treatment plate until day 3 of adulthood at which time they were transferred to a new RNAi treatment plate, via eye-lash pick, to avoid starvation. On day 5 of adulthood, 30 animals were harvested for fluorescent imaging to compare mechanosensory neuron morphology. After statistical analysis of fluorescent imaging, RNAi clone treatments producing significant results were DNA sequenced (**Supplementary Table 1.5**) and repeated two more times for a total of three individual replicates per each initial significant RNAi treatment. The touch response data were collected on each animal for the subsequent rescreens of ILPs of interest with statistical analysis conducted using a one-way ANOVA with $\alpha = 0.05$ and Dunnett's post-test with $\alpha = 0.05$ to compare both anterior and posterior touch response of RNAi treatments to L4440 control. A second frozen batch of mec-4::gfp animals, due to the time separation between the first and second rounds was thawed and used for the rescreening rounds of RNAi.

1.3.6 Fluorescent imaging of mechanosensory neuron morphology

Animals were harvested with an eye-lash pick and mounted to a cover slip on 1μL of 36% pluronic solution. Mounted animals were then sandwiched between another cover slip and mounted to a standard glass microscopy slide before being placed in an Olympus FSX100 fluorescent microscope. Animals were viewed using a FITC filter with 20x magnification and approximately 1/15 s of exposure. Four neurons were evaluated per worm, the two *Anterior Lateral Mechanosensory* (ALM) and the two *Posterior Lateral Mechanosensory* (PLM) neurons. Neuron evaluation consisted of counting and tallying a list of predetermined morphological aberration categories for each neuron. These categories were *Somatic Outgrowths*, *Extended Somatic Outgrowths* and *Neurite Branches* (**Figure 1.2**). *Somatic Outgrowths* are processes extending from the cell soma independently from the primary axon/neurite, *Extended Somatic Outgrowths* are *Somatic Outgrowths* that are at least 2x the length of the cell soma from which they originate, and *Neurite Branches* are atypical processes that extend from the primary axon/neurite[6,32]. Morphological aberrations data were collected in a scaled count for *Somatic Outgrowth*, *Extended Somatic Outgrowth* and *Neurite Branches* categories. Mechanosensory neurons were segregated as either anterior or posterior, giving two anterior and two posterior neurons per animal, for total anterior and posterior neuron sample sizes of two times the number of animals used per treatment group. Comparison of RNAi induced morphological aberrations was analyzed using a Kruskal-Wallis test with $\alpha = 0.05$ followed by a Dunn's multiple comparison post-test with $\alpha = 0.1$ in each *Somatic Outgrowths'*, *Extended Somatic Outgrowths'* and *Neurite Branches'* anterior and posterior categories ($\alpha = 0.1$ was used to reduce type II errors due to raw data values being smaller than expected and right skewed with Poisson distribution).

1.3.7 Touch Response

The gentle touch response was performed based on the methods described by Calixto et al.[38].The anterior and posterior touch response was recorded by gently stroking an eyelash pick perpendicularly across the head or tail (5 times each, alternating head and tail) of the animals. Halting or movement in the opposite direction of the stroke earned the animal a point and each animal's response was scored on a scale of 0 to 5 for both anterior and posterior response.

1.3.8 Relationship between neuronal morphology and function

For RNAi screen replicates 2 and 3, where both aberration and touch response data was collected, Spearman correlation was utilized to search for a relationship between neuronal aberration occurrences and mechanosensation capacities. A two-tailed Spearman correlation was performed to determine a Spearman correlation coefficient (r_s) for the mean occurrence of morphology aberrations versus mean anterior and posterior gentle touch response of each RNAi knockdown treatment.

1.4 RESULTS:

1.4.1 Ageing acceleration and L4440 vector validation

To verify accelerated aging of the *C. elegans* model when maintained at 25°C, and that the L4440 plasmid vector did not influence the function of mechanosensory neurons, both anterior and posterior gentle touch response of four treatment groups, fed either OP50-1 or L4440 and maintained at both 20°C and 25°C, were compared using two-way ANOVA. The anterior touch response was significantly depressed in animals reared at 25°C relative to those reared at 20°C ($p = 0.000$, $DFn = 1$, $DFd = 116$, $F = 13.36$). Food source, OP50-1 or L4440, had no influence on anterior touch response ($p = 0.491$, $DFn = 1$, $DFd = 116$, $F = 0.478$) (**Figure 1.3A**). Animals reared at 25°C had no significant change in posterior touch response when compared to those reared at 20°C ($p = 0.731$, $DFn = 1$, $DFd = 116$, $F = 0.119$), but L4440 as a food source did produce a decrease in posterior gentle touch response when compared to OP50-1 as a food source ($p = 0.017$, $DFn = 1$, $DFd = 116$, $F = 5.824$) (**Figure 1.3B**).

To validate that the L4440 plasmid vector did not influence the morphological structure of mechanosensory neurons, the occurrence of morphological aberrations in animals at day 5 of adulthood, fed and maintained on OP50-1 were compared to animals fed the L4440 RNAi clone, at both 20°C and 25°C. Animal rearing at 25°C had no influence on anterior neuronal aberration occurrence when compared to rearing at 20°C ($p = 0.157$, $DFn = 1$, $DFd = 116$, $F = 2.03$) and L4440 as a food source had no influence on anterior total aberration occurrence when compared to OP50-1 as a food source ($p = 0.601$, $DFn = 1$, $DFd = 116$, $F = 0.28$) (**Figure 1.4A**). Animal rearing at 25°C resulted in a significant increase in posterior neuronal aberration occurrence when compared to rearing at 20°C ($p = 0.003$, $DFn = 1$, $DFd = 116$, $F = 9.06$) and L4440 as a food source had no influence on posterior neuronal aberration occurrence when compared to OP50-1 as a food source ($p = 0.489$, $DFn = 1$, $DFd = 116$, $F = 0.48$) (**Figure 1.4B**).

1.4.2 RNAi arrival to mechanosensory neurons

To verify that the RNAi was arriving at and influencing the four mechanosensory neurons of interest, the anterior and posterior gentle touch response of animals treated with a mec-7 RNAi clone was compared to animals treated with the L4440 empty vector RNAi clone. There were statistically significant decreases in both the anterior (p = 0.0022, t = 3.371, df = 28) and posterior (p = 0.004, t = 3.098, df = 28) gentle touch responses from the mec-7 treatment group when compared to the L4440 control group (**Figure 1.5**), thus, showing that the RNAi treatment process was effective at targeting and knocking down genes of interest.

1.4.3 RNAi screen

The RNAi screen of 39 of 40 *C. elegans* ILPs was conducted in a three-part fashion to narrow in on ligands of interest. The first round was a screen of *ins-1* through *ins-38* and *daf-28* (an *ins-39* RNAi clone was not available). After this initial round was completed, knockdown targets that resulted in significant changes in the occurrence of morphological aberrations were chosen for RNAi clone sequencing and two more rounds of repeat screening for validation.

The initial round of RNAi screening resulted in eight ILPs that showed significant differences in aberrant neuronal morphology when compared to the L4440 control; *ins-1*, *ins-2*, *ins-3*, *ins-4*, *ins-9*, *ins-16*, *ins-30,* and *ins-38* (**Table 1.1**). The knockdown of *ins-1*, *ins-4,* and *ins-30* resulted in significant decreases in *Somatic Outgrowths* in PLMs compared to control (Kruskal-Wallis $p < 0.0001$, H = 169), while knockdown of *ins-38* resulted in a significant increase in *Somatic Outgrowths* in ALMs (Kruskal-Wallis p = 0.002, H = 68.71). Knockdown of *ins-2*, *ins-9* and *ins-16* resulted in decreases in *Extended Somatic Outgrowths* in ALMs, while knockdown of *ins-3* resulted in an increase in *Extended Somatic Outgrowths* in ALMs (Kruskal-Wallis $p < 0.0001$, H = 189.8) and a decrease in *Neurite Branches* in PLMs (Kruskal-Wallis $p < 0.0001$, H = 121.5).

The second round of screening produced no significant changes in neuronal aberration occurrence across the 7 selected genes, other than the *ins-4* treatment, but did reveal changes in gentle touch response across multiple treatments **(Table 1.2)**. The *ins-4* knockdown treatment resulted in the decrease in *Neurite Branches* in ALMs (Kruskal-Wallis p = 0.004, H = 20.69), while touch response scores showed a significant increase in the anterior portion of animals (one-way ANOVA p = 0.031, F = 2.276) from the *ins-9* treatment group and significant increase in the posterior portion of animals (one-way ANOVA p = 0.003, F = 3.274) from the *ins-3*, *ins-4*, *ins-16*, and *ins-30* treatment groups (**Figure 1.6**). Spearman correlation showed no relationship between any relative neuronal aberration occurrences and touch response in either anterior or posterior portions of animals from the seven rescreened treatment groups (**Figure 1.7**).

The third round of screening again resulted in several of the genes of interest showing significant changes in neuronal morphology, similar to the initial round (**Table 1.3**). The *ins-1* treatment resulted in a significant increase in *Somatic Outgrowths* in ALMs (Kruskal-Wallis p = 0.021, H = 16.51), while the *ins-3*, *ins-4*, *ins-9*, and *ins-30*

treatment groups resulted in significant decreases in *Extended Somatic Outgrowths* in ALMs (Kruskal-Wallis $p < 0.0001$, $H = 33.95$). Gentle touch response scores for the third round showed significant decreases in the anterior portion of animals (one-way ANOVA $p = 0.045$, $F = 2.097$) in the *ins-9* and *ins-16* treatment groups (**Figure 1.8**). Spearman correlation showed no relationship between any relative neuronal aberration occurrences and touch response in either anterior or posterior portions of animals from the seven rescreened treatment groups (**Figure 1.9**).

1.5 DISCUSSION:

1.5.1 Results interpretation

The results presented show that there are specific insulin ligands that play a role in maintaining the normal morphology of mechanosensory neurons. Interestingly, the results also suggest the possibility that insulin ligands modulate neuron morphology in a subfamily-dependent manner. The insulins that presented themselves as significant contributors in maintaining neuronal morphology during the first round of RNAi screening were *ins-1, ins-2, ins-3, ins-4, ins-9, ins-16, ins-30, and ins-38* and the knockdown of these genes (except *ins-38*) in an individual manner produces morphological aberrations at a lower rate than control, meaning that their presence may be important for producing, or at least contributing to, what we define as aberrancies.

The results from the second round of RNAi screening were unexpected as experimental protocols were conducted without change. The lack of significant change in neuronal morphology and the parallel significant change in mechanosensory neuron function is somewhat counter intuitive to the first round results. These anomalous results are most likely explained by the variability in doses of RNAi treatments, an inherent design variable in the RNAi bacterial feeding method. A copy of the mec-4::gfp *C. elegans* strain was thawed and used for both the second and third RNAi rounds. If there were a failure to respond by the animals, these same results would be expected in the third round of RNAi, which was not the case. The only explanation we can propose is the possibility of a partial or incomplete incubation of RNAi *E. coli* clones on the second round treatment plate media prior to administration, leading to a decreased level of dsRNA for *C. elegans* uptake.

Results from the third round of RNAi screening were more consistent with the first round results in that significant changes were seen in the rescreen candidate treatments. The results, while similar, were slightly divergent from the first rounds'. *ins-1* treatment produced a reversal of aberration occurrence with an increase in *Somatic Outgrowths*. *ins-2* and *ins-16* produced no significant change in morphology. The remaining *ins-3*, *ins-4*, *ins-9*, and *ins-30* treatment groups produced decreases in *Extended Somatic Outgrowths*, while not the standard *Somatic Outgrowths* seen in the first round, they were a type of *Somatic Outgrowth* and their occurrence was reduced along the lines of the first round, if we look at *Somatic Outgrowths* as a whole (**Figure 1.10**). Nevertheless, six of the seven rescreen candidates produced significant morphological changes again.

When investigating the results for any correlations, it first appears that there was a relationship between the presence of aberrations and the improvement of mechanosensory neuron function. During the second round of RNAi screening, morphological aberration occurrence increased (though statistically insignificant) in relation to the first round with a corresponding increase in touch response score, while during the third round of RNAi there was a significant decrease in morphological aberrations and a corresponding decrease in some touch response scores. Upon Spearman correlation analysis between morphological aberration occurrence and respective touch response score, there was no relationship between the frequency of neuronal aberrations and touch response score. This lack of a relationship between "form and function" of mechanosensory neurons actually supports the uncoupled nature of neuronal morphology and function by DAF-2/DAF-16 modulation from previous research[6-8].

Using these data from the RNAi screen, we searched for overlapping shifts in neuronal aberrations and gentle touch response over treatment rounds. We searched for overlap by consolidating anterior and posterior regions of animals for each neuronal aberration type and overlaid these results from each RNAi round using a Venn diagram. This visualization of RNAi response helps consolidate the separate responses and highlight any re-screen candidate ILPs as potential modulators of neuronal morphology. There was significant overlap when investigating all outgrowth types over the three RNAi rounds pointing to mainly β sub-type ILPs (**Figure 1.10**). When investigating overlap of regular *Somatic Outgrowths* (**Figure 1.11**) or *Extended Somatic Outgrowths* (**Figure 1.12**), the overlap of neuronal aberration decreases but still points to β sub-type ILPs as producing repeat shifts on event occurrence. When repeating this process for all *Neurite Branches* there is no overlap, but the two treatments from separate RNAi rounds where there were shifts in this aberration type both targeted β sub-type ILPs (**Figure 1.13**). This process was repeated for gentle touch response scores taken from the second and third rounds of RNAi, keeping anterior (**Figure 1.14A**) and posterior (**Figure 1.14B**) regions of animals separate. Overlap of gentle touch response scores indicated only the *ins-9* treatment as having any overlap between the second and third RNAi rounds. This treatment group displayed shifts in opposite direction between the second and third RNAi rounds.

1.5.2 ILP subfamilies and complex expression nature

ins-1, *ins-2*, *ins-3*, *ins-4* and *ins-9* are part of the same subfamily of insulin ligands, the β subfamily[17]. *ins-16* and *ins-30* are part of the γ and α subfamilies, respectively[17]. The γ subfamily is characterized by the canonical disulfide bonds found in mammalian and most all other insulin ligands, and the α subfamily by nonpolar substitutions at the 6/11 disulfide bond positions on the A peptide[21]. The β subfamily on the other hand is characterized by the three canonical di-sulfide bonds found in mammalian and most other insulin ligands, as well as additional di-sulfide bonds at position 21 of the A peptide and position 22, 23 or 24 of the B peptide[17]. This β subfamily contains *C. elegans ins-1* through *ins-10*, with *ins-1* thought to be the closest in structure to mammalian insulin peptide based on computer modelling[19]. Notable sequence alterations within the β subfamily of *C. elegans* ILPs are in the functional A and B peptides, with *ins-1* having a 20 amino acid long C peptide that is cleaved contributing to its closest similarity to mammalian insulin, and *ins-10* containing a cysteine substitution at position 15 of the B peptide thought to produce an additional disulfide bond[17]. Outside of these notable variations, the β subfamily remains largely

similar and homologous across the functional A and B peptides, with trivial residue variation most likely having no effect or leading to minor fluctuation in structure and binding affinity at the DAF-2 receptor[40].

The grouping and specificity of the observed results is not entirely unexpected. The β subfamily of ILPs contains those that are closest to mammalian insulin, a major metabolic and growth regulator. Under normal laboratory conditions, as seen in this study, this subfamily may contain the standard ILPs utilized for normal adult growth and metabolism in mechanosensory neurons. Ashlyn Ritter discusses a "block design" for spatiotemporal ILP expression that could very well explain the observed pattern grouping of significant ILPs seen here as well as the reason *C. elegans* have 40 ILPs as opposed to the 10 seen in humans[21]. This concept operates on the idea that each *C. elegans* tissue type taps into specific groups and combinations of ILPs under different environmental conditions and, importantly, developmental stages. Environmental cues would allow differential access to ILPs that have a tailored use or combination with a suite of genes, possibly juxtaposed genomically, for said environmental conditions. Indeed many ILPs are in fact grouped in clusters according to their subfamily delineations across *C. elegans* chromosomes[17]. Different environmental and cellular conditions would call upon different lists of ILPs and associated gene expression to meet metabolic requirements and necessary changes. Since *C. elegans* is a very robust and hardy organism subject to extreme environmental and metabolic shifts, the expanded ILP family observed in their genome could be seen as a mechanism for fine tuning tissue growth and metabolism under various environmental conditions. This also appears to be the case for developmental stages wherein specific ILP expression is required to alter, progress, or halt development. Such is the case in dauer formation, an arrested development occurring during the larval 3 stage. Specific ILPs have been shown to enhance dauer entry or be upregulated during the dauer phase to maintain this specific life stage, while other ILPs have been shown to mitigate entry into dauer[17,20,22,41,42]. This life stage-specific expression is also seen throughout animal development wherein certain ILPs have variable expression based on specific time points in life throughout multiple tissue types[21,22]. This research into variable ILP expression provides a broad understanding of spatiotemporal IIS but specific quantitative data on whole worm ILP expression over time relative to other ILPs in age matched animals, or tissue specific ILP expression over time relative to other ILPs, has not been acquired. This spatiotemporal variability in ILP expression lends credence to the complex and specific expression dynamics of the greater *C. elegans* insulin signaling mechanism and to the possibility that what has been observed in this study is the knockdown influence of individual ILPs on only a single, conditional expression pattern for healthy aging animals in one tissue type, the mechanosensory neurons.

Complementing the spatiotemporal expression of ILPs, is the fact that these ligands can bind as either agonists or antagonists at the DAF-2 receptor, to either activate or inactivate signaling, respectively[43]. By modulating the relative concentrations of ILPs, the resulting competitive binding equilibrium at the DAF-2 receptor acts to regulate the frequency, interval, and duration of signaling. If cellular conditions result in high expression of antagonist relative to agonist expression, then DAF-2 signaling frequency is reduced and vice versa. Additionally, an ILP with a relatively high binding affinity will out-compete other ILPs at the receptor site and produce its agonistic/antagonistic effects relative to the other ILPs it is outcompeting. In fact, there is evidence that agonist ILPs

outcompete antagonist ILPs for access to the IR binding sites[42]. While the relative binding affinities of ILPs is largely unknown, specific amino acid substitutions at sites along ILP functional domains and even those nonbinding domains that influence ILP dimerization and tertiary structure, can impact receptor affinity and dissociation rate[40]. This behavior may help explain the unexpected results from the second round of RNAi screening, assuming the proposed explanation of incomplete treatment bacteria incubation and low RNAi doses are correct. This proposed explanation would be supported if the rescreen candidate genes act as agonists to the IR. Under proper dosage, RNAi would knockdown agonist ILPs. This would reduce IIS pathway signaling directly by removing the stimulus, and indirectly by removing competition from antagonist ILPs that reduce IIS. Under these conditions IIS would decrease overall, leading to a decrease in neuronal morphology aberrations. If low doses of RNAi were administered, then a failure to knockdown or incomplete knockdown of the candidate genes would result in continued expression of those agonist ILPs. This continued expression of agonist ILPs would activate/increase IIS pathway signaling directly through IR binding, and indirectly by outcompeting antagonist ILPs. Under these "failure to knockdown" conditions, IIS continues, resulting in a relative increase in neuronal aberration occurrence back to normal control wildtype levels. This may be a plausible explanation as modulating the IIS pathway for an overall increase in signaling is known to induce neuronal morphology aberrations[6-8]. Additionally, agonist ILPs outcompeting antagonist ILPs could help explain the overall decrease and the relative lack of increase in neuronal aberration seen in this study. If agonist ILPs outcompete antagonist ILPs[42], then RNAi knockdown of antagonists should have little influence on the overall rate of IIS. While agonist ILPs establish binding dominance, reducing expression of the lower affinity antagonist ILPs will have little change on the established agonist ILP binding dominance. If knockdown of a high affinity, or highly expressed antagonist ILP were to occur, activated IIS may increase without restriction leading to an increase in neuronal aberration. This is most likely to have been the case with the ins-1 treatment group in RNAi round 3 where there was an increase in somatic outgrowth, INS-1 being a known antagonist ILP[17,42].

The relative binding affinities of ILPs and their immediate binding roles as either agonists or antagonists is still largely unknown and in fact agonist or antagonist activity is not entirely conserved across ILP subfamilies with both activities seen in a given subfamily[15,17,43,44]. Several, but unfortunately not all, of the agonistic/antagonistic roles of *C. elegans* β sub-family ILPs are known[15,17,18,37,41,42,45-48]. The β sub-family comprises *ins-1* through *ins-10*, and *daf-28*. Not all of the known agonist ILPs are in the β sub-family, although based on the results of this study, those agonists pertaining to neuronal morphology are. Ins-1 has shown both agonist and antagonist behavior. INS-1 acts as an agonist during salt chemo-tactic learning[49]. As an antagonist, INS-1 as well as its human homolog *human insulin*, act antagonistically on intestinal DAF-2 receptor to enhance dauer formation[17], and INS-1 is secreted from neurons to suppress DAF-2 activity in thermos-tactic learning[50]. INS-2, INS-3, INS-4, INS-6 and DAF-28 are known to act from neurons as agonists on intestine to prevent dauer formation[42]. INS-4 and INS-6 again act as agonists in sensory and motor neurons to regulate neuromuscular junction synapse development[15]. INS-7 has exhibited both agonist and antagonist characteristics depending on the experimental endpoint. As an agonist influencing lifespan and dauer formation[41], and as an antagonist in RIA head neurons that blocks DAF-2 activity to repress olfactory learning[44].

INS-9 only appears in ASI and ASJ amphid neurons, and acts as an agonist to regulate dauer formation[51]. The function and binding roles of INS-5, INS-8, and INS-10 are still unknown, but INS-5 and INS-10 are thought to have agonist behavior based on their influence on dauer formation[20,45]. Outside of the β sub-family, binding roles of many ILPs are known but remain unclear. For example; INS-12, INS-17, INS-18, and INS-23 act antagonistically to promote dauer formation and/or longevity[17,42,46,48,52,53], yet INS-12 has displayed both agonist or antagonist behavior depending on dauer exit or entry, respectively[20,42], as an experimental endpoint. INS-33 has displayed both agonist and antagonist behavior[48] as well, as an agonist in germline proliferation[54], and as an antagonist in regulating dauer formation[55]. INS-35 has displayed contradictory agonist[20] and antagonist[55] behavior when it comes to dauer formation. The ILPs with known agonist and/or antagonist roles are summarized in **Table 1.4** including the RNAi re-screen candidates with their respective changes in neuronal morphology compared to any known agonist/antagonist role.

Previously published ILP activity, regarding agonist and/or antagonist roles, largely agrees with results from this study. As stated previously, five of the seven re-screen candidate ILPs fall within the β sub-family. When INS-1 was knocked down we observed an initial decrease in neuronal aberration consistent with agonist behavior, but upon re-screen we observed an increase in aberration consistent with knocking down a significant antagonist, which INS-1 is known to be[17,42](**Table 1.4**). This supports the dual binding behavior that other researchers have described[17,50]. When INS-2, INS-3, and INS-4 were knocked down we observed a decrease in neuronal aberration events, as would be expected when knocking down agonist ILPs. INS-2 through INS-4 are also known to be agonists that prevent dauer formation[42]. INS-9 is thought to be an agonist that regulates dauer control by secretion from specific neurons51, and RNAi data from this study reports results consistent with agonist activity, a decrease in neuronal aberration when knocked down. We therefore propose that INS-9 is an agonist ILP. INS-16 and INS-30 are γ and α sub-types, respectively. The function and agonistic role of these ILPs is still unknown but they may be possible agonist ILPs as well, seeing as they produced decreases in neuronal aberrations when knocked down. While several γ ILPs have been shown to act as antagonists, binding roles are not conserved across sub-families, like as seen with the dual binding roles of INS-1 and INS-7 in the β sub-family.

Complicating the roles of ILPs further is the fact that they can initiate self-feedback loops and can mediate ILP-to-ILP interactions with one another. An example of the first scenario is that INS-18 is the sole ILP expressed in Hermaphrodite Specific Neurons (HSNs) and acts antagonistically on DAF-2 to upregulate DAF-16 nuclear translocation[43]. DAF-16, once translocated, activates *ins-18* transcription, creating an *ins-18 positive antagonistic feedback loop* in HSNs. Another such case is INS-7 acting as an agonist that contributes to normal development and prevention of dauer formation. Upon agonist binding at DAF-2, DAF-16 translocation which normally downregulates INS-7 production is prevented, thus leading to an increase in INS-7 production and an *ins-7 positive agonist feedback loop*[41]. An example of ILP-to-ILP interaction is INS-6 functioning to repress INS-7 in URX neurons[15] or that loss of INS-7 can upregulate INS-8 approximately 15 fold in endogenous whole animal expression[21].

To further investigate the agonist and antagonist roles of individual ILPs we propose a study with a more direct IIS pathway response than what has been conducted in previous work. We propose a study similar to what we have done here, a reverse genetic screen of ILPs. The natural starting point being to knockdown the ILPs whose agonist/antagonist roles are thought to be known. This proposed screen would use a *C. elegans daf-16::gfp* reporter mutant with ubiquitous SID-1 channels. RNAi would then be used to knockdown ILPs and the nuclear translocation activity of *daf-16::gfp* reporter would be discerned. This would allow us to build a more accurate representation of ILP's binding roles on the IR, as *daf-16::gfp* translocation is a more immediate IIS pathway response than the previously used dauer diapause. Knockdown of agonist ILPs would lead to an increase in *daf-16::gfp* translocation, while a knockdown of antagonists should result in a decrease of *daf-16::gfp* translocation. In treatments where *daf-16::gfp* is already low, a heat-shock treatment to raise *daf-16::gfp* expression could be used in conjunction with RNAi knockdown to determine a relative decrease in *daf-16::gfp* expression occurs. This study also has tissue specific implications as *daf-16::gfp* translocation could be determined in different tissue regions, helping to clarify some of the self-contradicting binding behavior of certain ILPs like INS-7[41,44].

Additionally, we propose studies quantifying ILP mRNA expression levels similar to that conducted by Ryan Baugh[22]. In particular, by using age-synchronous, unmixed populations, to determine ILP mRNA expression levels at multiple time points, reaching past the 60 h of total life as previously reported. Knowing these relative expression levels of ILPs over time would help determine long term versus episodic ILP expression and which ILPs to focus on during the later stages of life when cognitive decline and neurodegeneration become prevalent.

1.5.3 Concluding remarks

It is clear that IIS signaling is still a very complex and conditionally specific molecular topic and that there is still much more to explore in regards to individual ILP's roles and relationships to one another in each tissue type of expression. With this in mind, perhaps what this study has shown is a glimpse into insulin signaling and its morphological outcome on regular neuronal sprouting/regeneration in healthy aged neurons. This knowledge can be used as a basis for identifying specific ILPs or their respective subfamilies, the β subfamily in this case, that play foundational roles in regular neuronal morphology and neurodegeneration. Knowing how normal, healthy neurons utilize IIS to maintain health and function will be important in the future of human health as genetic factors may play roles in neurodegeneration, such as family history of AD being correlated with higher levels of circulating IGF-1 in mice[56], and impaired IIS and expression of IIS pathway constituents being implicated as a mechanism in human AD[57], one of the major forms of neurodegeneration seen in the growing geriatric population.

1.6 ACKNOWLEDGEMENTS:

Research reported in this publication was supported by an Institutional Development Award (IDeA) from the National Institute of General Medical Sciences of the National Institutes of Health under award number P20GM103395. The content is solely the responsibility of the authors and does not necessarily represent the official views of the National Institutes of Health.

1.7 DISCLOSURES:

The authors have nothing to disclose. The authors declare that the research was conducted in the absence of any commercial or financial relationships that could be construed as a potential conflict of interest.

1.8 REFERENCES

1. https://www.alz.org/alzheimers-dementia/facts-figures

2. http://parkinson.org/Understanding-Parkinsons/Causes-and-Statistics/Statistics

3. http://www.alsa.org/about-als/facts-you-should-know.html

4. https://www.cdc.gov/DiseasesConditions/

5. Yankner, B., Lu T., Loerch, P. The aging brain. The Annual Review of Pathology: *Mechanisms of Disease*. (3), 41–66 (2008). DOI: 10.1146/annurev.pathmechdis.2.010506.0920442008

6. Toth, M. et al. Neurite Sprouting and Synapse Deterioration in the Aging *Caenorhabditis elegans* Nervous System. *The Journal of neuroscience: the official journal of the Society for Neuroscience*. **32** (26), 8778–8790 (2012). DOI: 10.1523/JNEUROSCI.1494-11.2012

7. Pan, C., Peng, C., Chen, C., McIntire, S. Genetic analysis of age-dependent defects of the *Caenorhabditis elegans* touch receptor neurons. *Proceedings of the National Academy of Sciences of the United States of America*. **108** (22), 9274-9 (2011). DOI: 10.1073/pnas.1011711108

8. Tank, E. M. H., Rodgers, K. E., Kenyon, C. Spontaneous Age-Related Neurite Branching in *Caenorhabditis elegans*. *The Journal of neuroscience: the official journal of the Society for Neuroscience*. **31** (25), 9279-88 (2011). DOI: 10.1523/JNEUROSCI.6606-10.2011

9. Tissenbaum H. Genetics, life span, health span, and the aging process in *Caenorhabditis elegans*. *Journals of Gerontology - Series A Biological Sciences and Medical Sciences*. **67A** (5), 503-510 (2012). PMID: 22499764

10. Samuelson, A., Carr, C., Ruvkun, G. Gene activities that mediate increased life span of *C. elegans* insulin-like signaling mutants. *Genes and Development*. **21** (22), 2976-2994 (2007). DOI: 10.1101/gad.1588907

11. Kaletsky, R., Murphy, C. The role of insulin/IGF-like signaling in *C. elegans* longevity and aging. *Disease models & mechanisms*. **3** (10), 415-419 (2010). DOI: 10.1242/dmm.001040

12. Scerbak C., et al. Insulin signaling in the aging of healthy and proteotoxically stressed mechanosensory neurons. *Frontiers in Genetics*. **5** (July), 1-14 (2014). DOI: 10.3389/fgene.2014.00212

13. Kannan, K., Fridell, Y. Functional implications of *Drosophila* insulin-like peptides in metabolism, aging, and dietary restriction. *Frontiers in physiology*. **4** (October), 288 (2013). DOI: 10.3389/fphys.2013.00288

14. Suh, Y. et al. Functionally significant insulin-like growth factor I receptor mutations in centenarians. *Proceedings of the National Academy of Sciences of the United States of America*. **105** (9), 3438-3442 (2008). DOI: 10.1073/pnas.0705467105

15. Hung, W. et al. Attenuation of insulin signaling contributes to FSN-1-mediated regulation of synapse development. *The EMBO journal*. **32** (12), 1745-60 (2013). DOI: 10.1038/emboj.2013.91

16. Byrne A. et al. Insulin/IGF1 signaling inhibits age-dependent axon regeneration. *Neuron*. **81** (3), 561-73 (2014). DOI: 10.1016/j.neuron.2013.11.019

17. Pierce, S. et al. Regulation of DAF-2 receptor signaling by human insulin and ins-1, a member of the unusually large and diverse *C. elegans* insulin gene family. *Genes and Development*. **15** (6), 672-86 (2001). DOI: 10.1101/gad.867301

18. Li, W., Kennedy, S., Ruvkun, G. daf-28 encodes a *C. elegans* insulin superfamily member that is regulated by environmental cues and acts in the DAF-2 signaling pathway. *Genes and Development*. **17** (7), 844-858 (2003). DOI: 10.1101/gad.1066503

19. Duret L., et al. New Insulin-Like Proteins with Atypical Disulfide Bond Pattern Characterized in *Caenorhabditis elegans* by Comparative Sequence Analysis and Homology Modeling. *Genome Research*. **1998** (8), 348-353 (1998). DOI: 10.1101/gr.8.4.348

20. Fernandes de Abreu, D.A. et al. An Insulin-to-Insulin Regulatory network Orchestrates Phenotypic Specificity in Development and Physiology. *PLOS Genetics*. **10** (3), e1004225 (2014). DOI: 10.1371/journal.pgen.1004225

21. Ritter, A., et al. Complex expression dynamics and robustness in *C. elegans* insulin networks. *Genome Research*. **23** (6), 954-65 (2013). DOI: 10.1101/gr.150466.112

22. Baugh, R.L., Kurhanewicz, N., Sternberg, P.W. Sensitive and Precise Quantification of Insulin-Like mRNA Expression in *Caenorhabditis elegans*. *PloS one*. **6** (3), 18086 (2011). DOI: 10.1371/journal.pone.0018086

23. Nollen, E. et al. Genome-wide RNA interference screen identifies previously undescribed regulators of polyglutamine aggregation. *Proceedings of the National Academy of Sciences*. **101** (17), 6403-6408 (2004). DOI: 10.1073/pnas.0307697101

24. Brenner S. The genetics of *Caenorhabditis elegans*. *Genetics*. May **77** (1), 71-94(1974). PMID: 4366476

25. Stiernagle, T. Maintenance of C. elegans (February 11, 2006), WormBook, ed. The *C. elegans* Research Community, WormBook, doi/10.1895/wormbook.1.101.1, http://www.wormbook.org

26. Corsi, A.K., Wightman, B., and Chalfie, M. A Transparent window into biology: A primer on *Caenorhabditis elegans* (June 18, 2015), WormBook, ed. The C. elegans Research Community, WormBook, doi/10.1895/wormbook.1.177.1, http://www.wormbook.org.

27. Klass, M. Aging in the nematode *Caenorhabditis elegans*: Major biological and environmental factors influencing life span. *Mechanisms of Ageing and Development*. **1977** (6), 413-429 (1977).

28. Lee, S., Kenyon, C. Regulation of the Longevity Response to Temperature by Thermosensory Neurons in *Caenorhabditis elegans*. *Current Biology*. **19** (9), 715-722 (2009). DOI: 10.1016/j.cub.2009.03.041

29. Wu, D., Rea, S.L., Cypser J.R., Johnson, T.E. Mortality shifts in *Caenorhabditis elegans*: remembrance of conditions past. *Aging Cell*. **8** (6), 666-675 (2009). DOI: 10.1111/j.1474-9726.2009.00523.x.Mortality

30. Xiao, R. et al. A genetic program promotes *C. elegans* longevity at cold temperatures via a thermosensitive TRP channel. *Cell*. **152** (4), 806-817 (2013). DOI: 10.1016/j.cell.2013.01.020

31. Zhang, B. et al. Environmental Temperature Differentially Modulates *C. elegans* Longevity through a Thermosensitive TRP Channel. *Cell Reports*. **11** (9), 1414-1424 (2015). DOI: 10.1016/j.celrep.2015.04.066

32. Vayndorf, E. et al. Morphological remodeling of *C. elegans* neurons during aging is modified by compromised protein homeostasis. *npj Aging and Mechanisms of Disease*. **2** (June), 16001 (2015). DOI: 10.1038/npjamd.2016.1

33. Ahringer, J., ed. Reverse genetics (April 6, 2006), WormBook, ed. The *C. elegans* Research Community, WormBook, doi/10.1895/wormbook.1.47.1, http://www.wormbook.org

34. Chalfie, M., Thomson, N. Structural and Functional Diversity in the Neuronal Microtubules of *Caenorhabditis elegans*. *The Journal of Cell Biology*. **93** (April), 15-23 (1982).

35. Chalfie, M., et al. The Neural Circuit for Touch Sensitivity in *Caenorhabditis elegans*. *The Journal of neuroscience: the official journal of the Society for Neuroscience*. **5** (4), 956-64 (1985). DOI: 3981252

36. Bounoutas, A., O'Hagan, R., Chalfie, M. The Multipurpose 15-protofilament Microtubules in *C. elegans* Have Specific Roles in Mechanosensation. *Current Biology*. **19** (16), 1362-1367 (2009). DOI: 10.1016/j.cub.2009.06.036.

37. http://www.wormbase.org

38. Calixto, A., Chelur, D., Topalidou, I., Chen, X., Chalfie, M. Enhanced neuronal RNAi in *C. elegans* using SID-1. *Nature Methods*. **7** (7), 554-9 (2010). DOI: 10.1038/nmeth.1463

39. Chalfie, M., Sulston, J. Developmental Genetics of the Mechanosensory Neurons in *Caenorhabditis elegans*. *Developmental Biology*. **82** (2), 358-370 (1980). DOI: 10.1016/0012-1606(81)90459-0

40. Varewijck, A.J., Janssen, J.A.M.J.L. Insulin and its analogues and their affinities for the IGF1 receptor. *Endocrine-Related Cancer*. **19** (5), F63-F75 (2012). DOI: 10.1530/ERC-12-0026

41. Murphy, C. et al. Genes that act downstream of DAF-16 to influence the lifespan of *Caenorhabditis elegans*. *Nature*. **424** (6946), 277-83 (2003). DOI: 10.1038/nature01789

42. Hung, W., Wang, Y., Chitturi, J., Zhen, M. A *Caenorhabditis elegans* developmental decision requires insulin signaling-mediated neuron-intestine communication. *Development*. **141** (8), 1767-1779 (2014). DOI: 10.1242/dev.103846

43. Matsunaga, Y., Gengyo-Ando, K., Mitani, S., Iwasaki, T., Kawano, T. Physiological function, expression pattern, and transcriptional regulation of a *Caenorhabditis elegans* insulin-like peptide, INS-18. *Biochemical and biophysical research communications*. **423** (3), 478-83 (2012). DOI: 10.1016/j.bbrc.2012.05.145

44. Chen, Z. et al. Two insulin-like peptides antagonistically regulate aversive olfactory learning in *C. elegans*. *Neuron*. **77** (3), 572-585 (2013). DOI: 10.1016/j.neuron.2012.11.025

45. Chen, Y., Baugh, R.L. Ins-4 and daf-28 function redundantly to regulate *C. elegans* L1 arrest. *Developmental Biology*. **394** (2), 314-326 (2014). DOI: 10.1016/j.ydbio.2014.08.002

46. Matsunaga, Y. et al. A *Caenorhabditis elegans* Insulin-Like Peptide, INS-17: Its Physiological Function and Expression Pattern. *Bioscience, Biotechnology, and Biochemistry*. **76** (11), 2168-2172 (2012). DOI: 10.1271/bbb.120540

47. Hua, Q. et al. A divergent INS protein in *Caenorhabditis elegans* structurally resembles human insulin and activates the human insulin receptor. *Genes and Development*. **17** (June), 826-831 (2003). DOI: 10.1101/Gad.1058003

48. Matsunaga, Y., Iwasaka, T., Kawano, T. Diverse insulin-like peptides in *Caenorhabditis elegans. International Biology Review*. **1** (1), 1-15 (2017). DOI: 10.18103/ibr.v1i1.1276

49. Tomioka, M. et al. The Insulin/PI3-Kinase Pathway Regulates Salt Chemotaxis Learning in *Caenorhabditis elegans*. *Neuron*. **51** (5), 613-625 (2006). DOI: 10.1016/j.neuron.2006.07.024

50. Kodama, E. et al. Insulin-like signaling and the neuronal circuit for integrative behavior in *C. elegans*. *Genes and Development*. **20** (21), 2955-2960 (2006). DOI: 10.1101/gad.1479906

51. Delaney, C. et al. A histone H4 lysine 20 methyltransferase couples environmental cues to sensory neuron control of developmental plasticity. *Development*. **144** (7), 1273-1282 (2017). DOI: 10.1242/dev.145722

52. Matsunaga, Y., Ito, H., Kawano, T. Proceedings: Physiological Function of INS-12, one of the Type-γ Insulin-like peptides, in *C. elegans*. *Peptide Science*. **2009**, 459-462.

53. Matsunaga, Y., Matsukawa, T., Iwasaki, T., Nagata, K., Kawano, T. Comparison of physiological functions of antagonistic insulin-like peptides, INS-23 and INS-18, in *Caenorhabditis elegans*. *Bioscience, Biotechnology and Biochemistry*. **82** (1), 90-96 (2018). DOI: 10.1080/09168451.2017.1415749

54. Michaelson, D., Korta, D., Capua, Y., Hubbard, E. Insulin signaling promotes germline proliferation in *C. elegans*. *Development*. **137** (4), 671-680 (2010). DOI: 10.1242/dev.042523

55. Liu, T., Zimmerman, K., Patterson, G. Regulation of signaling genes by TGFbeta during entry into dauer diapause in *C. elegans*. *BMC Developmental Biology*. **4** (11), (2004). DOI: 10.1186/1471-213X-4-11

56. van Exel, E. et al. Insulin-like growth factor-1 and risk of late-onset Alzheimer's disease: findings from a family study. *Neurobiology of Aging*. **35** (2014), 725.e7-725.e10 (2014). DOI: 10.1016/j.neurobiolaging.2013.08.014

57. Steen, E. et al. Impaired insulin and insulin-like growth factor expression and signaling mechanisms in Alzheimer's disease- is this type 3 diabetes? *Journal of Alzheimer's Disease*. **7** (2005), 63-80. DOI: 10.3233/JAD-2005-7107

58. Kawano, T., Nagatomo, R., Kimura, Y., Gengyo-Ando, K., Mitani, S. Disruption of ins-11, a *Caenorhabitis elegans* Insulin-Like Gene, and Phenotypic Analysis of the Gene-Disrupted Animal. *Bioscience, Biotechnology, and Biochemistry*. **70** (12), 3084-3087 (2006). DOI: 10.1271/bbb.60472

1.9 FIGURES AND TABLES

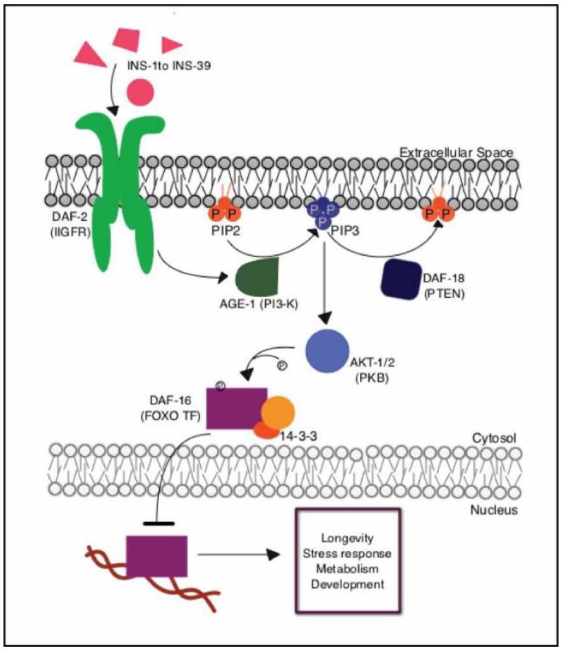

Figure 1.1. Insulin and Insulin-like Signaling (IIS) pathway. Graphic from Scerbak et al, 2014 (Figure 1)[12]. Graphical depiction of the IIS pathway and major molecules involved in signal transduction, human homologues in parantheses. ILP ligands bind to DAF-2 receptor, this induces a phosphorylation sequence that results in the targeted inhibition of DAF-16 nuclear translocation. DAF-16 is a prolongevity transcription factor. Under normal operation agonist binding at DAF-2 inhibits DAF-16 translocation and antagonist binding at DAF-2 dis-inhibits DAF-16 translocation.

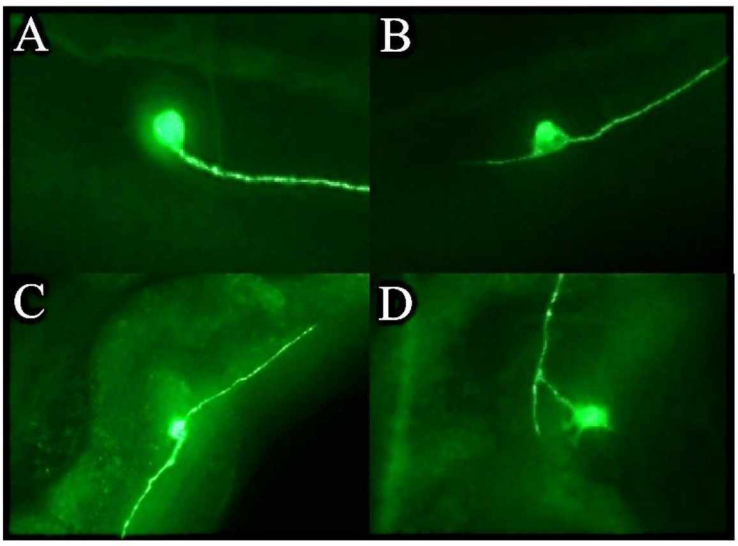

Figure 1.2. Morphological aberration categories. Representative images of a healthy neuron and its morphology (**A**) compared to those with morphological aberrancy; in the form of Somatic Outgrowths (**B**), Extended Somatic Outgrowths (**C**) and Neurite Branches (**D**).

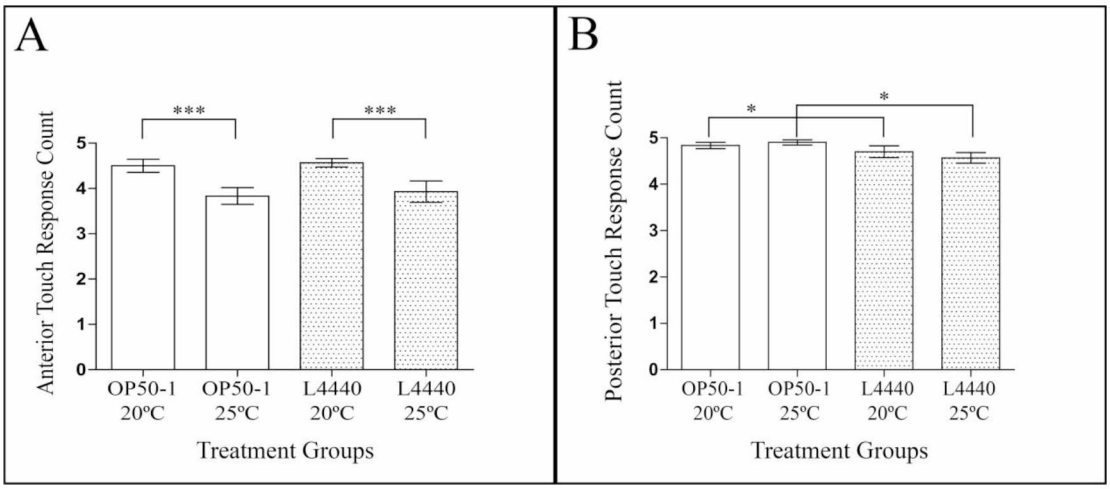

Figure 1.3. Gentle touch response temperature and L4440 vector validation. Anterior (**A**) and posterior (**B**) touch response scores of L4440 treatment vector versus the standard OP50-1 *E. coli* food source at both 20°C and 25°C. L4440 treatment is an *E. coli* clone containing an empty L4440 plasmid that is used in clones hosting RNAi knockdown treatment. Significant decrease in anterior touch response in both OP50-1 and L4440 treatments when conducted at 25°C compared to 20°C, indicating a decrease in functional health. Analysis reported L4440 as a source of significant differencein in posterior touch response when compared to OP50-1 at both 20°C or 25°C. n=30 animals for each treatment group, (* = $p < 0.05$), (* = $p < 0.01$), (*** = $p < 0.001$).

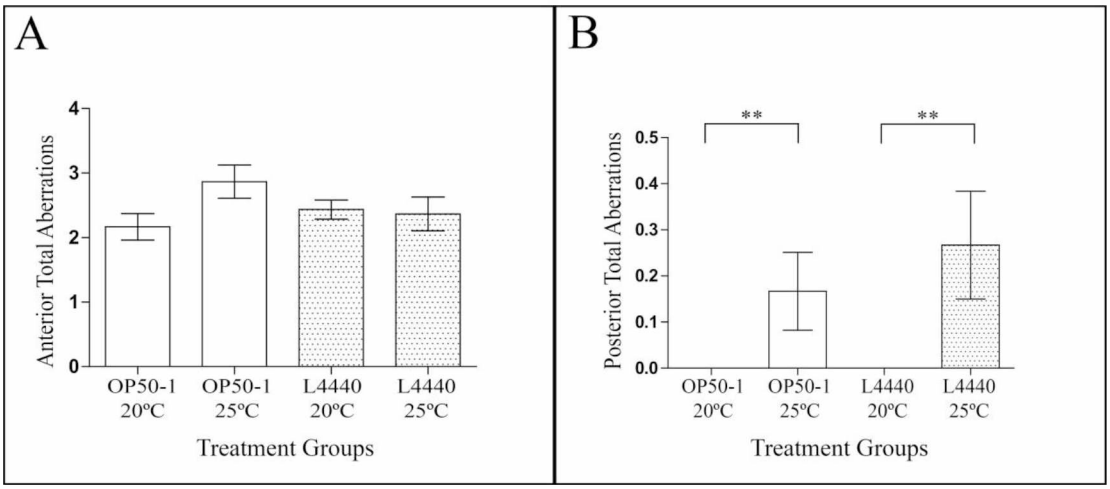

Figure 1.4. Mean total aberrations temperature and L4440 vector validation. Mean anterior (**A**) and posterior (**B**) total aberrations per animal when fed L4440 treatment vector versus the standard OP50-1 *E. coli* food source at both 20°C and 25°C. L4440 treatment is an *E. coli* clone containing an empty L4440 plasmid that is used in clones hosting RNAi knockdown treatment. No significant change in mean anterior total aberrations from either increased temperature or from L4440 vector. L4440 was not a significant source of variation in mean posterior total aberrations at either 20°C or 25°C. A higher temperature was reported to be a significant source of variation in mean posterior total aberrations within OP50-1 and L4440 groups. n=30 animals for each treatment group, (** = $p < 0.01$).

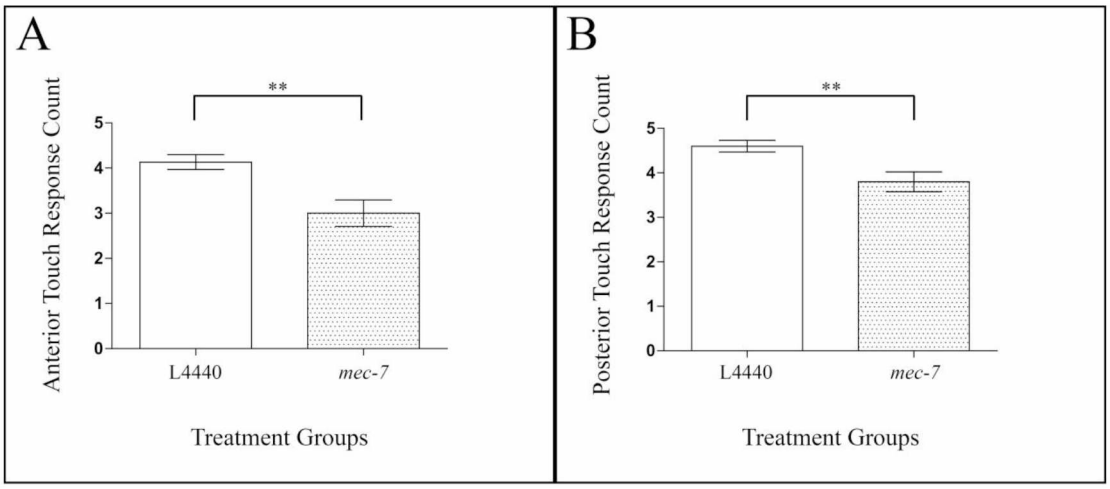

Figure 1.5. RNAi influences target mechanosensory neurons. Anterior (**A**) and posterior (**B**) touch response of *mec-7* knockdown treatment versus L4440 control. *mec-7* is a required gene for proper mechanosensation. Statistically significant decreases in both anterior and posterior touch response of *mec-7* treatment group, showing the arrival and influence of the RNAi treatment on the neurons of interest. n=30 animal for each treatment group (** = $p < 0.01$).

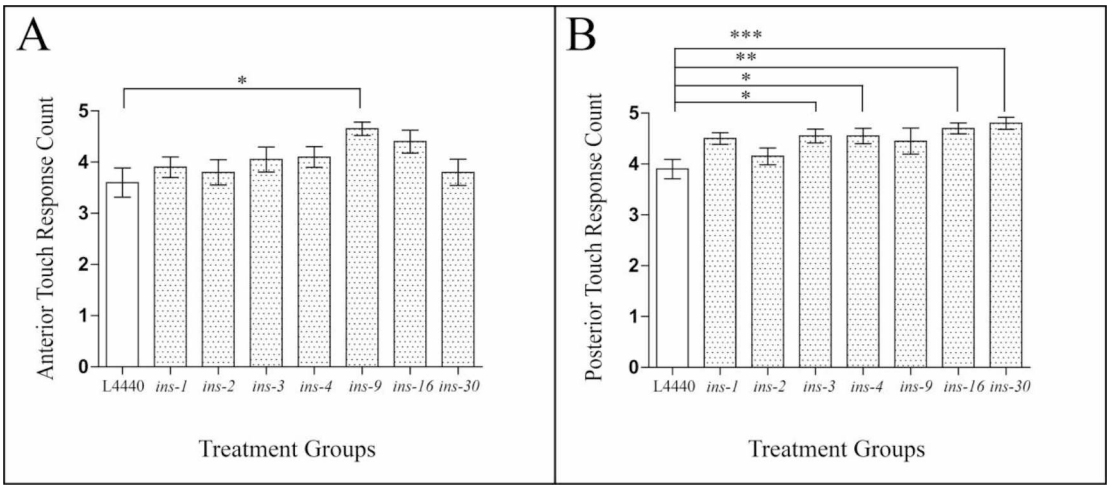

Figure 1.6. Second round RNAi screen mechanosensory function. Mean anterior (**A**) and posterior (**B**) gentle touch response of treatment groups for seven ILPs of interest compared to L4440 control. *ins-9* treatment saw a statistically significant increase in anterior touch response. *ins-3*, *ins-4*, *ins-16*, and *ins-30* treatment groups saw statistically significant increases in posterior touch response. Approximately n=30 animals for each treatment group, * = $p<0.05$, ** = $p<0.01$ and *** = $p<0.001$.

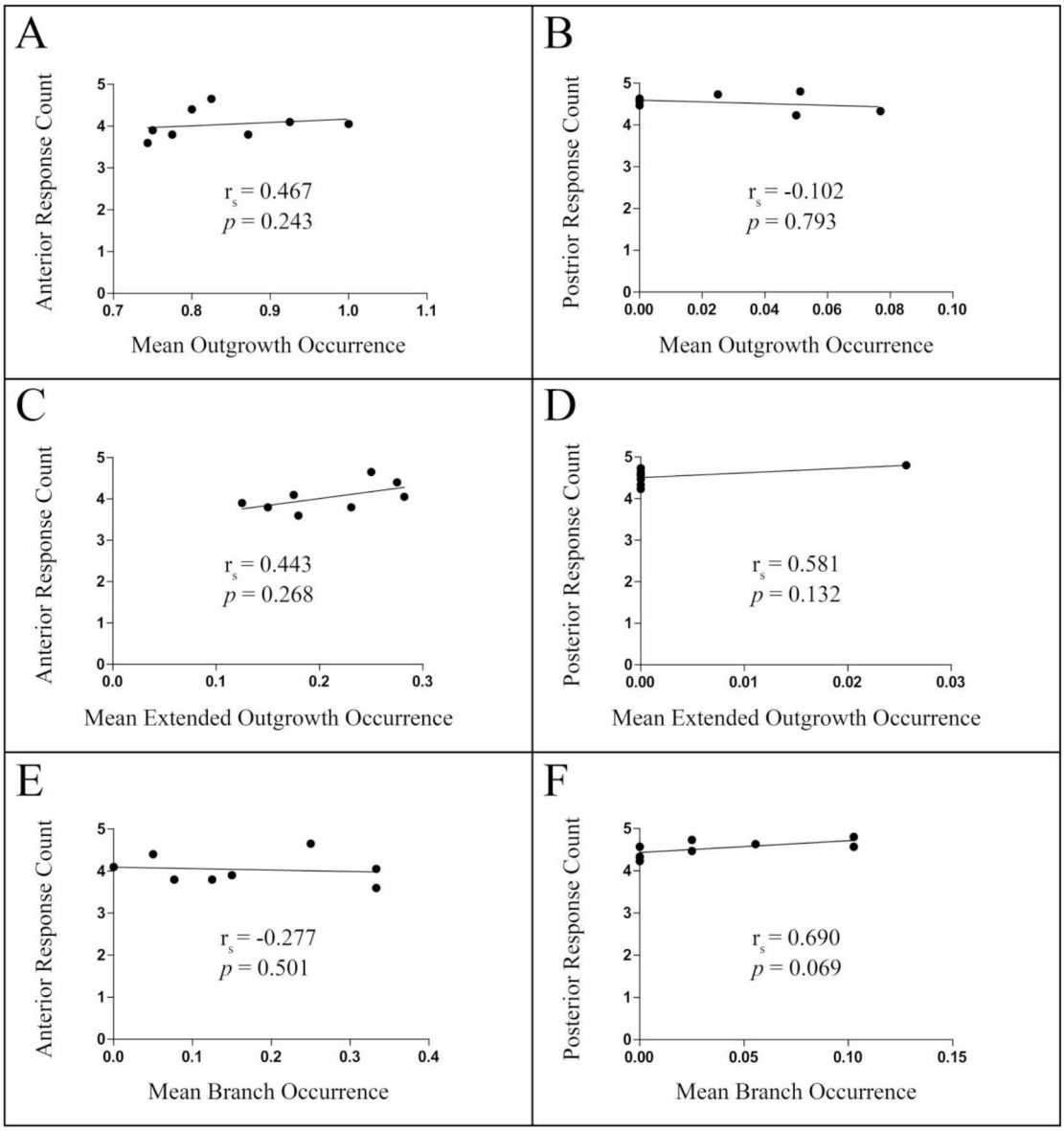

Figure 1.7. Second round RNAi screen neuronal aberration and touch response correlation. Spearman correlation analysis of mean morphological aberration occurrence versus gentle touch response score of each treatment group. Mean anterior (**A**) and posterior (**B**) touch response of L4440 and seven selected treatment groups versus their respective *somatic outgrowths* occurrence. Mean anterior (**C**) and posterior (**D**) touch response scores of control and seven selected treatment groups versus their respective *Extended Somatic Outgrowths* occurrence. Mean anterior (**E**) and posterior (**F**) touch response scores of L4440 and seven selected treatment groups versus their respective *Axonal Branches* occurrence. r_s-values indicated no correlation between touch response score and aberration occurrence in anterior or posterior mechanosensory neurons.

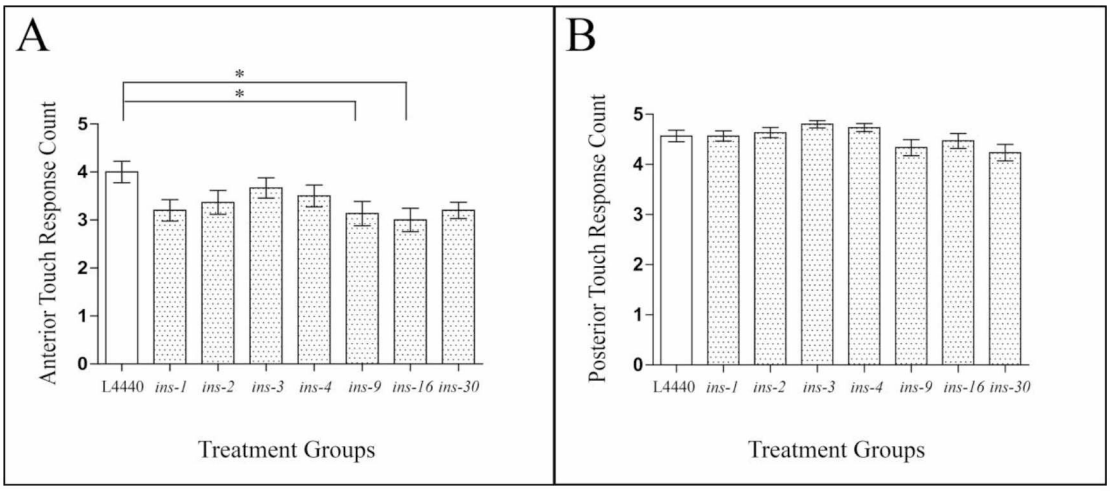

Figure 1.8. Third round RNAi screen mechanosensory function. Mean anterior (**A**) and posterior (**B**) gentle touch response of treatment groups for seven ILPs of interest compared to L4440 control. *ins-9* and *ins-16* treatments saw statistically significant increases in anterior touch response. No statistically significant difference in posterior touch response for any treatment group. Approximately n=30 animals for each treatment group, * = $p<0.05$.

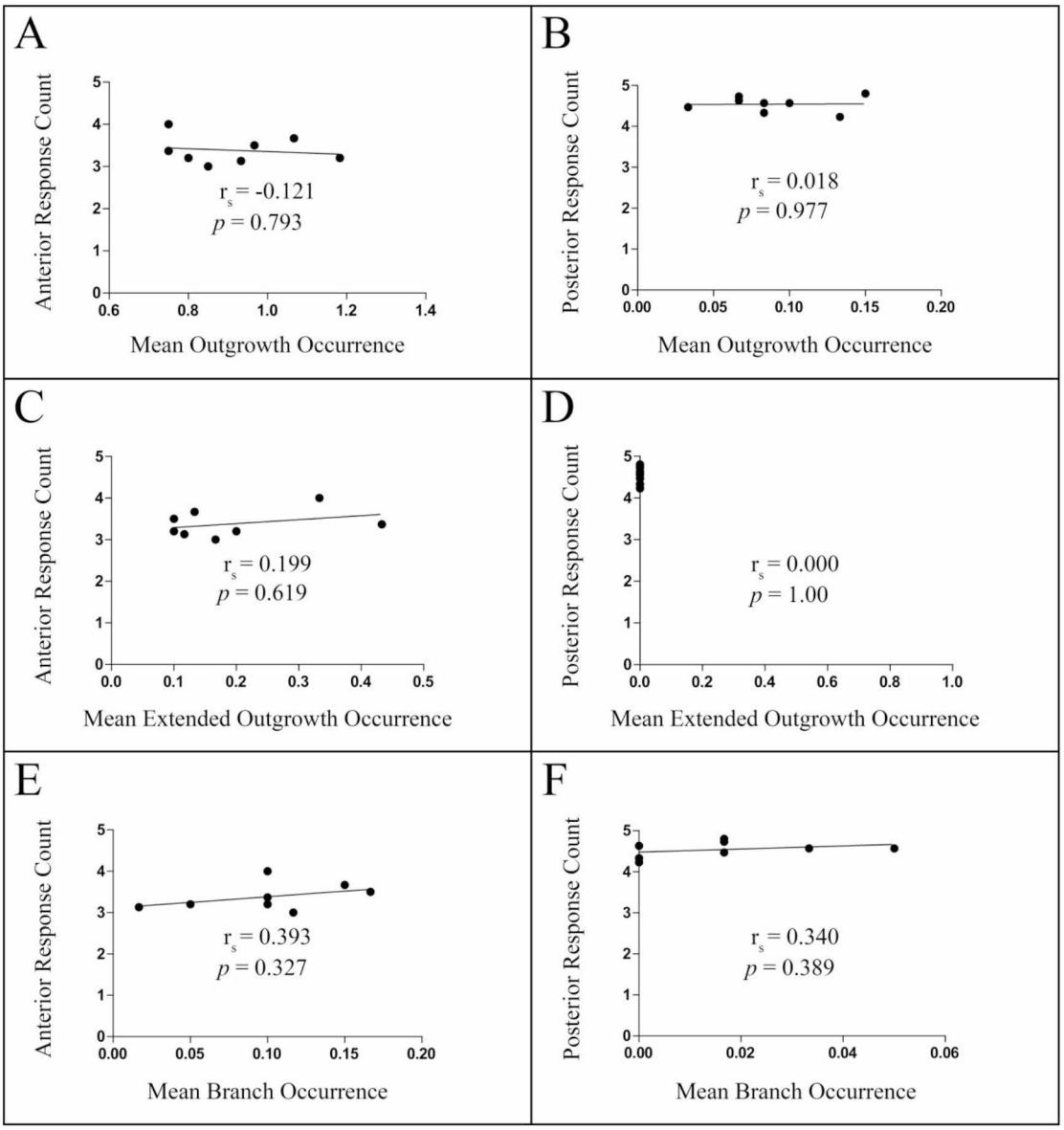

Figure 1.9. Third round RNAi screen neuronal aberration and touch response correlation. Spearman correlation analysis of mean morphological aberration occurrence versus gentle touch response score of each treatment group. Mean anterior (**A**) and posterior (**B**) touch response of L4440 and seven selected treatment groups versus their respective *Somatic Outgrowths* occurrence. Mean anterior (**C**) and posterior (**D**) touch response scores of control and seven selected treatment groups versus their respective *Extended Somatic Outgrowths* occurrence. Mean anterior (**E**) and posterior (**F**) touch response scores of L4440 and seven selected treatment groups versus their respective *Neurite Branches* occurrence. r_s-values indicated no correlation between touch response score and aberration occurrence in anterior or posterior mechanosensory neurons.

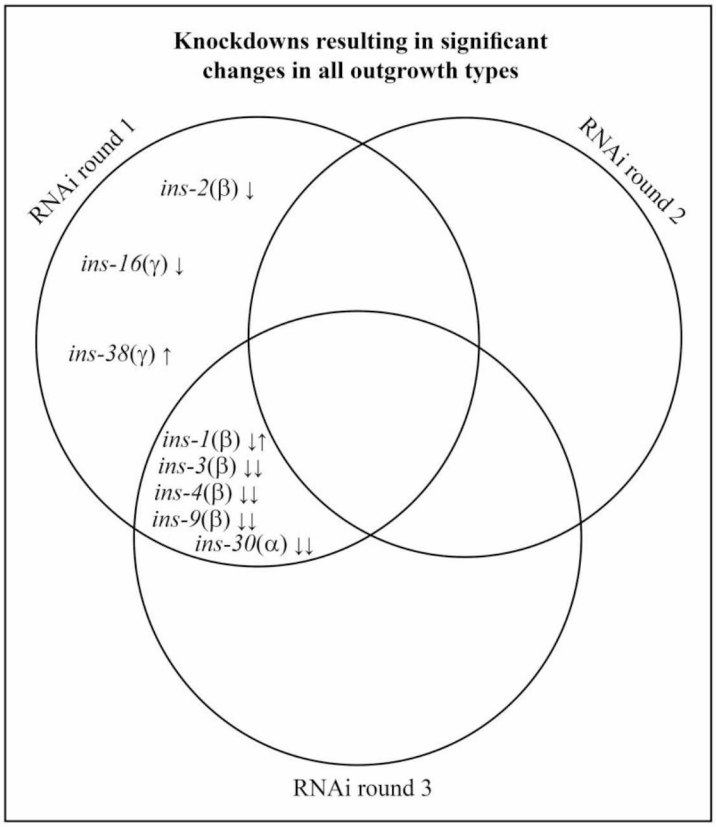

Figure 1.10. ILP knockdown treatments displaying significant changes in all somatic outgrowth types. Venn diagram illustrating overlap of RNAi knockdown treatments that produced significant changes in any outgrowth type. *Somatic Outgrowth* and *Extended Somatic Outgrowth* have been merged anterior and posterior regions have been merged as well. ILP sub-family is in parentheses, arrows sequentially depict relative shift in aberration occurrence.

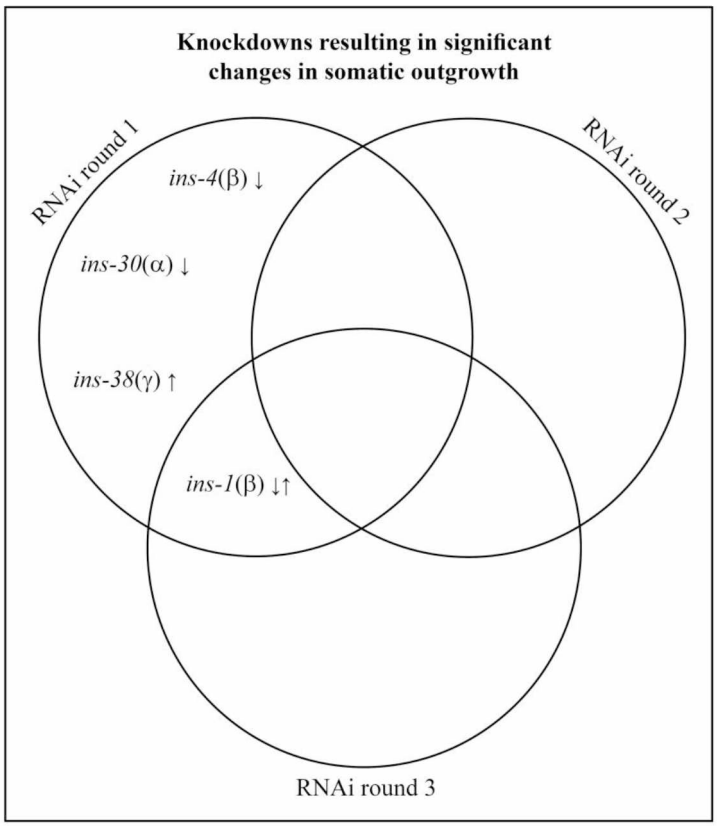

Figure 1.11. ILP knockdown treatments displaying significant changes in somatic outgrowth. Venn diagram illustrating overlap of RNAi knockdown treatments that produced significant changes in somatic outgrowth. Anterior and posterior have been merged. ILP sub-family is in parentheses, arrows sequentially depict relative shift in aberration occurrence.

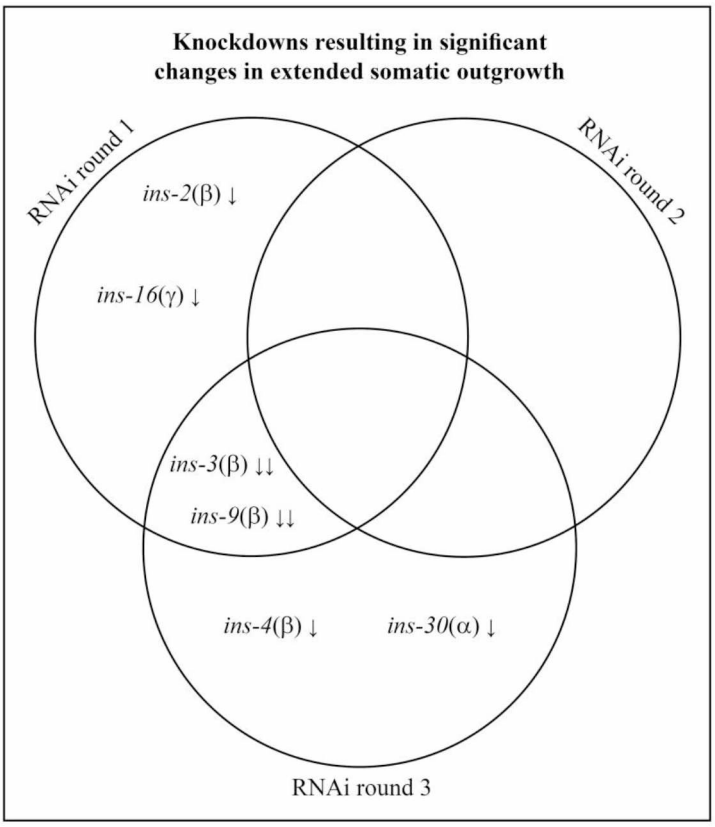

Figure 1.12. ILP knockdown treatments displaying significant changes in extended somatic outgrowth. Venn diagram illustrating overlap of RNAi knockdown treatments that produced significant changes in *extended somatic outgrowth.* Anterior and posterior have been merged. ILP sub-family is in parentheses, arrows sequentially depict relative shift in aberration occurrence.

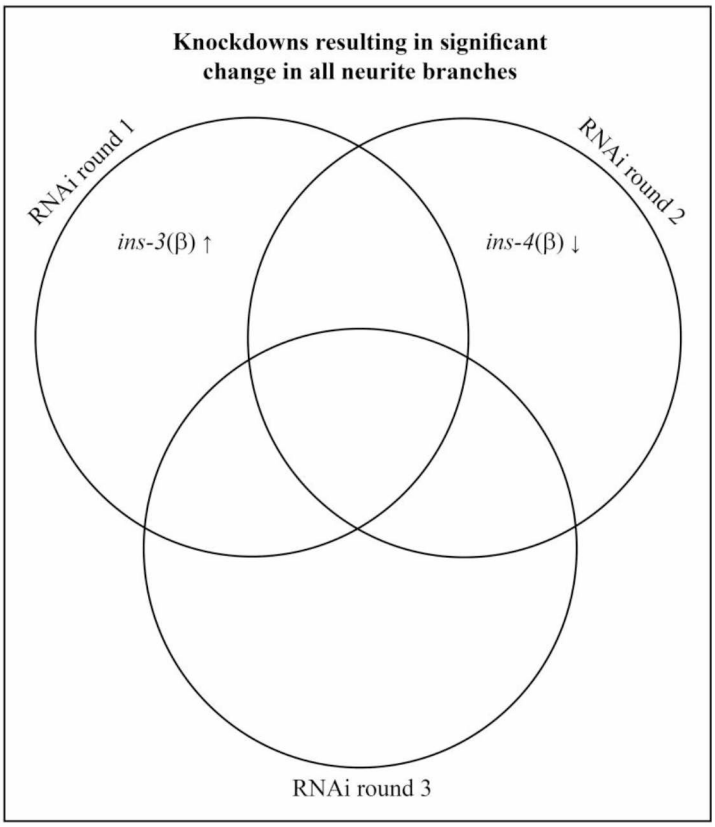

Figure 1.13. ILP knockdown treatments displaying significant changes in all neurite branches. Venn diagram illustrating overlap of RNAi knockdown treatments that produced significant changes in all *neurite branches*. Anterior and posterior have been merged. ILP sub-family is in parentheses, arrows sequentially depict relative shift in aberration occurrence.

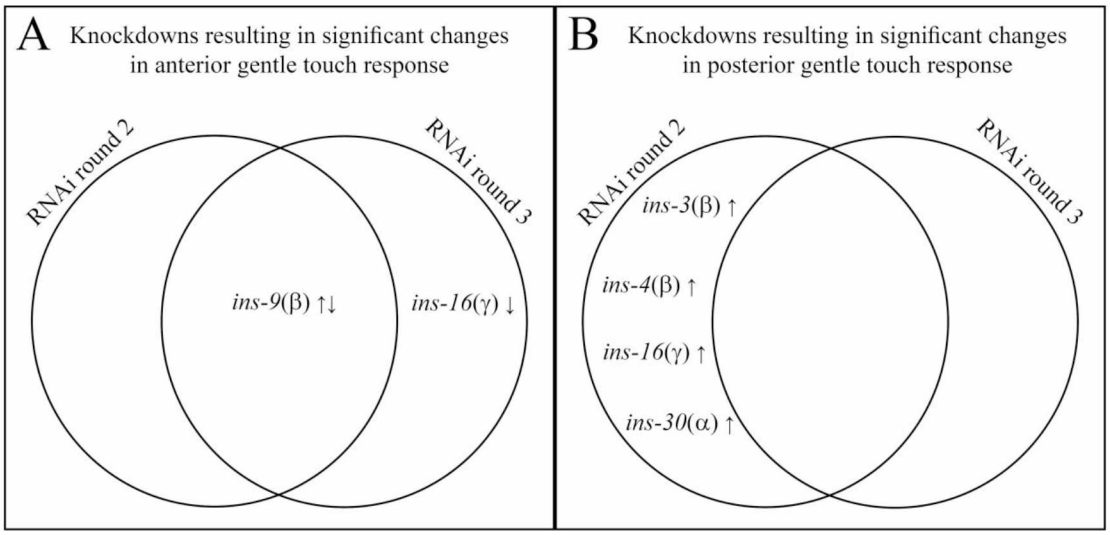

Figure 1.14. ILP knockdown treatments displaying significant changes in gentle touch response. Venn diagram illustrating overlap of RNAi knockdown treatments that produced significant changes in anterior (A) and posterior (B) gentle touch response. ILP sub-family is in parentheses, arrows sequentially depict relative shift in aberration occurrence.

RNAi Treatment	Outgrowths		Extended Outgrowths		Branches	
	Anterior	Posterior	Anterior	Posterior	Anterior	Posterior
L4440	0.836	0.241	0.400	0.056	0.400	0.259
ins-1 ↓	0.829	0.000	0.098	0.000	0.122	0.400
ins-2 ↓	0.983	0.035	0.033	0.000	0.356	0.754
ins-3 ↓↑	1.050	0.068	↓0.1	0.000	0.283	↑1.034
ins-4 ↓	0.706	0.000	0.118	0.000	0.078	0.146
ins-5	1.071	0.093	0.196	0.000	0.446	0.426
ins-6	0.933	0.068	0.250	0.000	0.117	0.203
ins-7	1.133	0.133	0.300	0.000	0.767	0.417
ins-8	0.833	0.043	0.125	0.000	0.104	0.196
ins-9 ↓	0.966	0.035	0.017	0.000	0.121	0.140
ins-10	0.915	0.104	0.390	0.000	0.356	0.229
ins-11	1.036	0.204	0.327	0.000	0.346	0.315
ins-12	1.085	0.220	0.153	0.051	0.458	0.441
ins-13	1.175	0.286	0.351	0.020	0.368	0.490
ins-14	1.054	0.083	0.268	0.021	0.286	0.042
ins-15	1.300	0.200	0.283	0.017	0.250	0.333
ins-16 ↓	1.018	0.130	0.091	0.000	0.164	0.093
ins-17	0.860	0.105	0.526	0.000	0.211	0.386
ins-18	1.000	0.136	0.250	0.034	0.083	0.136
ins-19	0.818	0.093	0.227	0.000	0.205	0.047
ins-20	0.900	0.067	0.150	0.000	0.283	0.100
ins-21	1.200	0.186	0.267	0.017	0.500	0.610
ins-22	0.950	0.203	0.383	0.000	0.583	0.373
ins-23	1.000	0.121	0.317	0.052	0.100	0.241
ins-24	1.229	0.292	0.417	0.021	0.229	0.596
ins-25	1.172	0.351	0.276	0.000	0.466	0.281
ins-26	1.278	0.333	0.352	0.037	0.500	0.315
ins-27	1.300	0.316	0.300	0.035	0.167	0.404
ins-28	1.033	0.339	0.517	0.034	0.267	0.153
ins-29	1.043	0.250	0.340	0.045	0.404	0.546
ins-30 ↓	0.880	0.000	0.180	0.000	0.260	0.160
ins-31	0.897	0.362	0.603	0.052	0.552	0.362
ins-32	1.183	0.383	0.517	0.017	0.683	0.233
ins-33	1.149	0.208	0.277	0.021	0.298	0.271
ins-34	1.017	0.123	0.203	0.018	0.203	0.175
ins-35	0.814	0.250	0.627	0.000	0.136	0.367
ins-36	1.179	0.214	0.339	0.054	0.411	0.214
ins-37	1.152	0.242	0.258	0.061	0.424	0.152
ins-38$^{\Psi}$ ↑	1.294	0.182	0.162	0.000	0.191	0.152
daf-28	0.932	0.184	0.271	0.000	0.170	0.190

Table 1.1. RNAi screen of 39 *C. elegans* ILPs. Mean event occurrence of morphology aberrations per ALM or PLM. All 39 available *C. elegans* ILPs targeted and compared to L4440 control, highlighted in light grey. Occurrences with $p<0.1$ are highlighted in dark grey. Arrows in treatment column denote the relative shift in aberration occurrence compared to L4440 control. Anterior and posterior categories are composed of both ALMs or PLMs from each animal, for approximately 60 ALMs and PLMs counted per treatment group. Ψ *ins-38* not selected as a rescreen candidate in an initial data analysis that selected for genes with "significant" and "almost significant" shifts in more than one category/location, nonetheless *ins-38* knockdown did show a statistically significant shift in aberration occurrence.

RNAi treatment	Outgrowths		Extended Outgrowths		Branches	
	Anterior	Posterior	Anterior	Posterior	Anterior	Posterior
L4440	0.744	0.000	0.180	0.000	0.333	0.000
ins-1	0.750	0.000	0.125	0.000	0.150	0.103
ins-2	0.872	0.000	0.231	0.000	0.077	0.056
ins-3	1.000	0.051	0.282	0.026	0.333	0.103
ins-4 ↓	0.925	0.025	0.175	0.000	0.000	0.025
ins-9	0.825	0.077	0.250	0.000	0.250	0.000
ins-16	0.800	0.000	0.275	0.000	0.050	0.025
ins-30	0.775	0.050	0.150	0.000	0.125	0.000

Table 1.2. Second round RNAi screen of *C. elegans* ILPs of interest. Mean event occurrence of morphology aberrations per ALM or PLM in treatment groups for ILPs of interest. Seven *C. elegans* ILPs targeted and compared to L4440 control, control highlighted in light grey. *p*-values of <0.1 are highlighted in dark grey. Arrows in treatment column denote the relative shift in aberration occurrence compared to L4440 control. Anterior and Posterior categories were comprised of both ALMs or PLMs from each animal, for approximately 60 ALMs and PLMs counted per treatment.

RNAi Treatment	Outgrowths		Extended Outgrowths		Branches	
	Anterior	Posterior	Anterior	Posterior	Anterior	Posterior
L4440	0.750	0.083	0.333	0.000	0.100	0.050
ins-1 ↑	1.183	0.100	0.200	0.000	0.100	0.033
ins-2	0.750	0.067	0.433	0.000	0.100	0.000
ins-3 ↓	1.067	0.150	0.133	0.000	0.150	0.017
ins-4 ↓	0.967	0.067	0.100	0.000	0.167	0.017
ins-9 ↓	0.933	0.083	0.117	0.000	0.017	0.000
ins-16	0.850	0.033	0.167	0.000	0.117	0.017
ins-30 ↓	0.800	0.133	0.100	0.000	0.050	0.000

Table 1.3. Third round RNAi screen of *C. elegans* ILPs of interest. Mean event occurrence of morphology aberrations per ALM or PLM in treatment groups for ILPs of interest. Seven *C. elegans* ILPs targeted and compared to L4440 control, control highlighted in light grey. p-values of <0.1 are highlighted in dark grey. Arrows in treatment column denote the relative shift in aberration occurrence compared to L4440 control. Anterior and Posterior categories were comprised of both ALMs or PLMs from each animal, for approximately 60 ALMs and PLMs counted per treatment.

ILP gene	ILP sub-family	Known ILP Agon./Antag. activity	Neuronal aberration changes observed by RNAi round						RNAi result as agonist/ antagonist consistent with published literature?
			Outgrowths		Extended Out-growths		Branches		
			Anterior	Posterior	Anterior	Posterior	Anterior	Posterior	
Hulns	γ	Antagonist[17]	---	---	---	---	---	---	N/A
ins-1	β	Ag[49]/Ant[17,42,50]	3↑	1↓	N.S.	N.S.	N.S.	N.S.	Y (Ant.Out.)[17,42,49,50]
ins-2	β	Agonist[42]	N.S.	N.S.	1↓	N.S.	N.S.	N.S.	Y[42]
ins-3	β	Agonist[42]	N.S.	N.S.	1↓ 3↓	N.S.	N.S.	1↑	Y (Ext.Out.)[42]
ins-4	β	Agonist[15,42]	N.S.	1↓	3↓	N.S.	2↓	N.S.	Y[15,42]
ins-5	β	Agonist[20,45]	---	---	---	---	---	---	N/A
ins-6	β	Agonist[15,42,47,48]	---	---	---	---	---	---	N/A
ins-7	β	Agon[43]/Antag[44]	---	---	---	---	---	---	N/A
ins-9	β	Agonist[51]	N.S.	N.S.	1↓ 3↓	N.S.	N.S.	N.S.	Y[51]
ins-10	β	Agonist[20,45]	---	---	---	---	---	---	N/A
ins-11	γ	Ag[20,45]/Ant[58,45]	---	---	---	---	---	---	N/A
ins-12	γ	Antagonist[49]	---	---	---	---	---	---	N/A
ins-14	γ	Agonist[20,45]	---	---	---	---	---	---	N/A
ins-16	γ	N/A	N.S.	N.S.	1↓	N.S.	N.S.	N.S.	N/A
ins-17	γ	Antagonist[46]	---	---	---	---	---	---	N/A
ins-18	γ	Antag[17,42,46]	---	---	---	---	---	---	N/A
ins-20	α	Antag[20,45]	---	---	---	---	---	---	N/A
ins-21	α	Agonist[20,45]	---	---	---	---	---	---	N/A
ins-22	α	Agonist[20,45]	---	---	---	---	---	---	N/A
ins-23	α	Antagonist[53]	---	---	---	---	---	---	N/A
ins-26	α	Agonist[20,45]	---	---	---	---	---	---	N/A
ins-27	α	Agonist[20,45]	---	---	---	---	---	---	N/A
ins-30	α	N/A	N.S.	1↓	3↓	N.S.	N.S.	N.S.	N/A
ins-33	α	Agon[54]/Antag[55]	---	---	---	---	---	---	N/A
ins-35	α	Ag[20,45]/Ant[55]	---	---	---	---	---	---	N/A
daf-28	β	Agonist[18,20,42]	---	---	---	---	---	---	N/A

Table 1.4. Known agonist/antagonist ILP activity and RNAi re-screen candidate morphology changes. List of ILPs with known agonist and/or antagonist roles at the DAF-2 IR in *C. elegans*. RNAi re-screen candidates (highlighted grey) are included with their respective changes in neuronal aberrations listed for cross-referencing with any previously known agonist/antagonist activity. Changes in neuronal morphology are represented by the RNAi round number with an arrow showing the relative shift in aberration occurrence when the target ILP was knocked down. In RNAi treatment aberration categories where there is no significant change, "N.S" is used. "N/A" represents information that is not available. References for known agonist and antagonist behavior are included as superscript numbers.

RNAi Clone	Sequence Read
L4440	GGCNCTAGNCNTNNANACTCGNNCGAAGGGNAGTCGCTCTACCTTCTGCCCANNNTACTTCGTGATATNNNT-CATTTCCTCCCATTTCACNGCACCAGTCAGCAATNNCTGCTCCTTTCTGGATAAATTTTGCNTCNCTTTCATTTCCNNAANNNNCCTCT-CATAACNATCAGAAAGNAGNCNGTAACAATTTNNNAGCTCTCGACCTTNANTTTCCGGCNNANAANCGTAAAGTTTTCCGATTTCCNNGN-CATTTNANACGCGATNCNNGNGGTCAACCTACGGCGTGAATCTAGAATTGACNGAAGGANATATTTTNACGANNNCAAAAAACATA-AANANNNAATCAANTNNACAAAGTTNNNTNCGTCCGCCACCACAGANNNGCTCGACTTCGTCTTTCAGATGNNATNNGCGNNACTC-GCTCNNNAGAGTGTCGTAATACTNNAGCAGCCGAGATCAAGTTNNTCAANNAGANNNAANNTGCNNNNNCNNNNNTNNNNNNNGN-TACCGATTCCTATCAANNNGAGGGTGCCGGNNNNTTTTNATNGGANNCNNNTTNATTACGNNCGACATAAANNGGGAACGTA-ATGCCTAAATNANNNAGAANNGCGATAAACNGNNNNNANNTNCGNNNNCTGNNNTACNNTCCAATNNATGAAGNNNNTNTN-NATNNNNACTNNNNNNCAACCACGTTGATGAGTNNNCAAT
ins-1	NCCNANCTNTNTAGGGCGATTGGGTACCATTATCGTCCTGATTGCAGCAGAATGTTTTGAGATATGCAAATGAACATCGCTTCTCACAA-CATTCTGTCGCAATTCCGCCTCGCTTTTGTTGGTGGTGAATGTGAAAAAGATCGCGAGTTGTTGGTGCATAGGATTGGTCGGCGGAAC-GTTTGAAAGCGGTTAATCCAGTGCACAGCTGATTCCGGCATACTGCTAAAAGGGTTGTTGTGAGACGTGATCCACATAGTCGAATCGATGC-GTCTGAAGGCGTCGGCGACGAGAGGAGAAGGATCGCGAGAAAGCCAAAGAAGAACGAGGGTCTGTAAACTTGACGAAACCAGTACAT-GCGGCCGCCACCGCGGTGGAGCTCGAATTCATCGATGATATCAGATCTGCCGGTCTCCCTATAGTGAGTCGTATTAATTTCGATAAGCCAG-GTTGCTTCCTCGCTCACTGACTCGCTGCGCTCGGTCGTTCGGCTGCGGCGAGCGGTATCAGCTCACTCAAAGGCGGTAATACGGTTATC-CACAGAATCAGGGGATAACGCAGGAAAGAACATGTGAGCAAAAGGCCAGCAAAAGGCCAGGAACCGTAAAAAGGCCGCGTTGCTG-GCGTTTTTCCATAGGCTCCGCCCCCCTGACGAGCATCACAAAAATCGACGCTCAAGTCAGAGGTGGCGAAACCCGACAGGACTATAAA-GATACCAGGCGTTTCCCCCTGGAAGCTCCCTCGTGCGCTCTCCTGTTCCGACCCTGCCGCTTACCGGATACCTGTCCGCCTTTCTCCCTTCG GGAAGCGTGGCGCTTTCTCATAGCTCACGCTGTAGGTATCTCAGTTCGGTGTAGGTCGTTCGCTCCAAGCTGGGCTGTGTGCAC-GAACCCCCCGTTCAGCCCGACCGCTGCGCCTTATCCGGTAACTATCGTCTTGAGTCCAACCCGGTAAGACACGACTTATCGCCACTGGCAG-CAGCCACTGGTAACAGGATTAGCAGAGCGAGGTATGTAGGCGGTGCTACAGAGTTCTTGAAGTGGTGGCCTAACTACGGCTACACTAGAA-GAACAGTATTTGGTATCTGCGCTCTGCTGAAGCCAGTTACCTTCGGAAAAAGAGTTGGTAGCTCTTGATCCGGCAAAAANCCACCGCTG-GTAACGGTGGTTTTTTTGTTTGCAAGCAGCNGATTACCNGCAGAAAAAANGGATCTCAGAANNNTCCTTTGATCTTTNCTACGGGGTCT-GANNGNNNNTGGAANNNAANCTCCNGTTAAGGGATTTGGNCCNGAGATTNNCNAAANGGNNNTTCCNNAANTCCTTTNAATTAAAANG-GNGNTTNCAACCACCCNAANNANNTNNNAANNCATTGNNTNNNNCGTTNNNNCTGCTTAATGCGNGGNN
ins-2	NNNNNNNNNNNNNNNNNNNNGANNNNNNNNNNGGNNNNNNNNNNNNNNNNNNNNNNNNNNNNNNNNNNNNNNNNNNNNNNNNNNNNNNNNG-TATTAAGAAAACTAACATTTTGAAAAGTTAATGATAGTACGATANGTCCATAACTATTTTCTAAATGAATTCGGGCAGCAGACTCTGAT-GATATCTTGAACGTCACATNGTTTTATGCAGCAAATATGCGAAAGGTCTTCTGATGAATCTGAAATGTATCATATGTTTAAAGGGTGAAC-GTTTGAAACAGTATGAAAAACAATAGTTGGACTTTTTGACGTCCTGAAAATTCTTATAAATGTATGCCTGCCTTCAATGCGATCAACGCAT-GCAATGCGTAGACATGTACGGCGCGTTTTGTTGAAGTATTAATTTTCAGAAACAAAAAATCTTTCCAGAATAAATTGACAATTTCAAAATT-TAATTTTTAATAGTAATCATTTTATTAACTCAAAATTTTCTAGAATTGAATGAATTTCCATTAAAGTTTTACGTTCAAAAATAATTTTAATACT-TAAAAAAAAAGTCGTACCTGTATCACATTCTCCACATGTTGCAAGCATGAATAAAATAAGACGTCTTCCGCATAGACGTTTCTGGACTCTT-GAGGCACGGTTTGGAGTTGGAGTTGACTCAACTGGTATGATATCAAGTTGATTGATGATCAAATGTTCATTTCTGTGTTCTATTCCTTTTC-CGAAAACTTCATAAGTGGCAGTGACAGTTGTGAAGAGGAGACAGAAGATTATAGCGTTCATGGTAGATTTTAGAATGGAAAGGAAAGAA-CATCTACGGCACTTTTTGTTTTTATACCGTTTTTAAACGTAGGGAGGGCGTGGCAGGAGGCATCGTTTTTGGGATTAGGTAGAAATGGGAC GACAATCAGATCTGCCGGTCTCCCTATAGTGAGTCGTATTAATTTCGATAAGCCAGGTTGCTTCCTCGCTCACTGACTCGCTGCGCTCG-GTCGTTCGGCTGCGGCGAGCGGTATCAGCTCACTCAAAGGCGGTAATACGGTTATCCACAGAATCAGGGNATAACGCAGGAANGACCT-GTGAGCAAANGCCAGCANAAGGCNNGAACCGTANAAGGCCGCGTTGCTGGCGTTTTTCCTAGGCTCCGCCCCCTGACAGACATCA-CAAANTNCANNCTCAATTCGAAGTGGNCAAACCCCNNGGANNNAANAANCCNGNGNTTTCCCNTGGAAATCCCCCCNGNGNCTNC-CGTTNCNNACCGGCCNTNNNACGAACACNCNNCCNNCTTCCNTTCCGGAAGNNNGGTTTTNCNANNCNCTANNNCCNGNNT-CAACNNNNGNAANNNGNCNNNNNNNCCNGGNNCNNNN
ins-3	NNNCAANCNTNCCTANGGNCGANTGGNNNCTCTTGANGGNCAGCACTTNGTAGTTATNTCTTCCATTGTGCACATTTTTTCACAGCATTCT-GTAGCGATGTTCTCATTCGTTGATGAACATTCTCCTCCACACATTACCATCACCATTTTCAGAACTTTTGTACCACAAATCTTCACTTT-GTCTCCTCTTCTTGATCTGGCCATCAGGGAGTGAATGTTATGGAATCCAATTTCCGAATCATCATAATCGTGTTCCAATTCTTTCTCAAAATC-GAACATCCAGTTACGCATAAGACTTGCAGCTCCAAGTTGGAAAATAATGAAAAGTGCAAGAACAACGGAGAGTTTCATGCGGCCGC-CACCGCGGTGGAGCTCGAATTCATCGATGATATCAGATCTGCCGGTCTCCCTATAGTGAGTCGTATTAATTTCGATAAGCCAGGTTGCTTC-CTCGCTCACTGACTCGCTGCGCTCGGTCGTTCGGCTGCGGCGAGCGGTATCAGCTCACTCAAAGGCGGTAATACGGTTATCCACAGAAT-CAGGGGATAACGCAGGAAAGAACATGTGAGCAAAAGGCCAGCAAAAGGCCAGGAACCGTAAAAAGGCCGCGTTGCTGGCGTTTTTC-CATAGGCTCCGCCCCCCTGACGAGCATCACAAAAATCGACGCTCAAGTCAGAGGTGGCGAAACCCGACAGGACTATAAAGATACCAG-GCGTTTCCCCCTGGAAGCTCCCTCGTGCGCTCTCCTGTTCCGACCCTGCCGCTTACCGGATACCTGTCCGCCTTTCTCCCTTCGGGAAGC-GTGGCGCTTTCTCATAGCTCACGCTGTAGGTATCTCAGTTCGGTGTAGGTCGTTCGCTCCAAGCTGGGCTGTGTGCACGAACCCCCC-GTTCAGCCCGACCGCTGCGCCTTATCCGGTAACTATCGTCTTGAGTCCAACCCGGTAAGACACGACTTATCGCCACTGGCAGCAGC-CACTGGTAACAGGATTAGCAGAGCGAGGTATGTAGGCGGTGCTACAGAGTTCTTGAAGTGGTGGCCTAACTACGGCTACACTAGAAGAA-CAGTATTTGGTATCTGCGCTCTGCTGAAGCCAGTTACCTTCGGAAAAAGAGTTGGTAGCTCTTGATCCGGCAAACAACCACCGCTGG-TAGCGGTGGTTTTTTTGTTNGCAAGCANNNNATTACCNGCAAAAAAANGGATNTNNNNANANNCNTTTNATCTTTTTNANGGGNTN-NAAGCNNNNTGGAANCAAANNNNCCTTNAAGGNNTTGTGNNNGCAGATTATTACAANGATGTTNCCNNNAATTNNTTTTNANNN-NAAAANNANNTTTNAACANNCCNNNAACTAANNGNGNANNACNNNNNTNNN
ins-4	NNNNNNNNNNNNNNNNNNNNGANNNNNNNNNNGGNNNNNNNNNGNNNNNNNNNNNGNNNNGNNNNNNNNNNNGNNNNNN NNNNNNNNNNANNNNNNNNNNNNNAANNNNANNAANNACNNNAATTNCAAGCTCTTCAAAAAGATGGTTAATTTTCATA-ATTTTTCAGAAGTTTTTCAAAAGCTCCAAGAGAATGTTTTCATTCTTTACATATTTCCTTCTCTCCGCACTTCTTCTCTCCGCTTCAT-GTCGACAACCTTCCATGGACACCAGCAAAGCCGATCGTATTCTACGAGAGATCGAAATGGAAACAGAACTCGAAAATCAACTCTCCC-GAGCACGACGAGTCCCAGCTGGAGAGGTTCGTGCCTGTGGAAGACGACTTCTTCTNCTTTGTCTGGTCAACCTGTGGAGAACCAT-GCACGCCACGTACGTTTAATGCTAAAAATTTTTTAAAAAACCTTAATCTGAATTTATTATTTTTCAGAAGAGGACATGGACATTGC CACAGTTTGCTGCACAACACAGTGCACTCCATCATATATAAAACAAGCTTGCTGCCCAGAAAAGTAAAAACAGTCGTCCAACAAGC-CATCTCCGTCGTCAAATAATTTTCAATAGAGTCTAGATTTTCTCCATTCACAAACTTTCCATTTTAATTTCCATGTGCAACCAATTCCTGCTCT-CAAAGTTCCAGGCTTCTCCTACAATCAATCTTCNAAAGATCTCTTTCATCCCGTTACAGTAACTTGTTTTCAAAATGATCTCACTATTTA TTTTT CTGCAATAAAACTTTTTGAATAAAN TTCCTTTCATAATACCCATGTTCAATGATAGAGTGAATAATGA............ (CONTINUED)...........

Supplementary Table 1.5. RNAi clone DNA sequencing.

ins-4	.....(CONTINUED).....TTTTTATTATGAAACGGAGGGACGGTTGTCTTNTTTATCAANAAGGGAAACAACTTTAACTTTTAGATTTTTGATA- NAATTACCTCTTCTATGTACGAGCAAAGAACTTCTGATTTTCCGTTAATATTTTTCTAGATATCAAGAATTTTTTTATTGTTTCAATTTA- ATGAAAGCACTATGCATATACGTAGTCTTAATTTTATATGATGGAAATATTATAATTTGAAATATTAACTTTAAACCCAATTCTTTCAANTC- TAAAAANCAGTCATTATTTGGAATCCTTGTCGTTTTTGAATCAGATCTGCCGGTCTCCNNNNANNGAGTCGTATTAATTTCNNNANNC- CAGGTTGCTTCCTCNCTCACTGAACCCNNNGCGCNNNGGNCGTTCGGNNNGGNNNNANGGGNTNNNNNNTCCNTCCAANAGGNG- GTNNNNNGGNTTNNCCCCNGAANNCNGGGGGNNNAACCCCNGGNANAAAANCTTNTNNNNNNAAANGGNNNNNNAAAANGNNCCNG- GAANCCNNNA
ins-9	GGNCGNNNNCNNNANCNNNNTACCNTNAANNNCCGGGNNGGGNCGGNANNTNNNNNGGGNNANCCCNNAAATTTNTCTG- GTTTCCGNGGCCACNAAGNCCAATNGGNCCTNNNTNTCCCNNNNGNAATTNNNTCNAAACCGTAAAANNGGTTNNC- CANTNNTNNGGGGTTNTNNCCCCACCAAGGCCAACCAAGNCCTTNTANGNANGNNNGNAANNCCCNTTNGGTTTTCCCNGGT- NANCCCCTNAAAANNAAAATTANTTTTTTANTTCCCGNAATTTTTTTCGGAATTTTTTTNANNGAGGAAAACCAAANAACCGNAAT- TAACCTTTNANCCCCCCGNNGGTTTNCNACCAATCGGGGCCNCCCCGGTTTCGGCCAACCGGCCTCGGANTCANGCCNACCAATTC- CANGNTCGGTCAAGNNNGGTTTTTNTTCCTTTTCCCCACCAAGCCNGNGNTNANGAATTTTTTTTTTNCCGAGGTTTTTCCCCAAGGGTT TTCTTTTCCTCCGNCCCCNGAATTTTTCCCATCGNGTCGNATCGNGTGGGGTCGGGGTTGNATTGNATCGAATTTACTCGACGNGNT- GNGNAGNGAATNTNTNCTTCGCNNTNCCATTGNAGNANCNAAATNCNANAATGGNANTTTNANAGAANTNCCATTTTTNCNGNTT- GTTTTNCCAGATNANCNTAGAGNANAAGGGTGGTGCNNCNATTTGNANAGTTCCAANTNGNACAAGNANAAGAAACAAT- CAAAGNTTGNACGATTTCATGCGGNCCCNGCCACCGNCGNNGTGGAAGCTTCNGAATTCANTNCGATGATNANTCAGATTCTNGNCCG- GTCTNCCCNTATAGTGAGTCNGTATTAATTTTCGATAANGCCAGGTTTGCTTCCTCNGCTCACTNGACTCGCTTGCGCTCGNGTCGTTTCG- GCTTGCGGCGAGCGNGTATCAGCTTCACTCAAAGGCGNGTAATACGGNTTATCCACAGAATCAGGGGATAACGCAGGAAAGAACATGT- GAGCAAAAGGCCAGCAAAAGGCCAGGAACCGTAAAAAGGCCGCGTTGCTGGCGTTTTTCCATAGGCTCCGCCCCCCTGACGAGCAT- CACAAAAATCGACGCTCAAGTCAGAAGTGGCGAAACCCGACAGGACTATAAAGATACCAGGCGTTTCCCCCTGGAAGCTCCNTCGT- GCGCTCTCCTGTTCCGACCTGCCGCTTACGGATACCTGTCCNCTTNCTCCNTTCGGAACGTGGCGCTTCTCATACTCNCCTGTAGTATCT- CATTCGTGTAGTCGTCGCTCAGCTGGCTGGTGCCAACCCCGTCACCGACGCTCCNTATCGTANTNCTCTTATCACCGTAACCACTACGCC- GCACACNCGTACGNTCAACAGTGTGCGGTACATCTATGTGCATCGTCNAANCTNTGACGCCGTACGTCTNAAATGATTNCGAACCCGNG- GTTTTNANATCCAAAGTCAACTTTNCGTACCGAANCTAGTNNNNNAGTCACTAAAATANANTAANNNN
ins-16	NNNNNNNNNNNNNNNNGNNNNNNNNNNNNNNNNNNNNNNNNNNNNNNNNNNNNNNNNNNNNNNNNNNNNNNNNN NNNNNNNNNNNNNNNGNNNNNNNNNNNNNNNNNNNNTNNNNNNNNNNNNNNACNNNNNGNNNNNCANANNNCGCNNN NNNNNNNAAAAAGNNNCACAGNNNNACGTNNGAGCTCCCGGCCANGAATNNCCGGCGCAAAAACTGACAGTGTGAG- GAGGCAGGCAAGAATTGGTAGGCTTTGCATGCGGCCGCCACCGCGGTGGAGCTCGAATTCATCGATGATATCAGATCTGCCG- GTCTCCCTATAGTGAGTCGTATTAATTTCGATAAGCCAGGTTGCTTCCTCGCTCACTGACTCGCTGCGCTCGGTCGTTCGGCTGCGGC- GAGCGGTATCAGCTCACTCAAAGGCGGTAATACGGTTATCCACAGAATCAGGGGATAACGCAGGAAAGAACATGTGAGCAAAAGGC- CAGCAAAAGGCCAGGAACCGTAAAAAGGCCGCGTTGCTGGCGTTTTTCCATAGGCTCCGCCCCCCTGACGAGCATCACAAAAATC- GACGCTCAAGTCAGAGGTGGCGAAACCCGACAGGACTATAAAGATACCAGGCGTTTCCCCCTGGAAGCTCCCTCGTGCGCTCTCCT- GTTCCGACCCTGCCGCTTACCGGATACCTGTCCGCCTTTCTCCCTTCGGGAAGCGTGGCGCTTTCTCATAGCTCACGCTGTAGGTATCT- CAGTTCGGTGTAGGTCGTTCGCTCCNAGCTGGGCTGTGTGCACGAACCCCCCGTTCAGCCCGACCGCTGCGCCTTATCCGGTAAC- TATCGTCTTGAGTCCAACCCGGTAAGACACGACTTATCGCCACTGGCAGCAGCCACTGGTAACAGGATTAGCANANCGAGGTATG- TANGCGGTGCTACAGAGTTCTTGAAGTGGTGGCCTAACTACNGCTACNCTAGAAGANAGTATTTGGTATCTGCNCTCTGCTGAAGC- CAGTTACNTTCNNAAAANANTTGGNAGCTCNNGNTNNNGNNNNAAACNCNNTNGNANCNNNNNTTTTNNNNNANNCAGCNNA NNNCNCGCNNNAAAANNNNNNAGANNNNNNTNGATNNNTNNTNNNNNNNNNANNNTNNNNNNNNNAAANNNNNNNNNNNG- NATTNNNNNNNNNNNNNNNCNAAANNNNNTNNNNNNNNNNNNNNNNNNNNANNNNNNNNNNNNNNNNNNNNNNNNNNNNNNGNNNN NNNNNNANNNNNNN
ins-30	GNNTAGNTATNTACATAGGNANGANGGNNTCNCTCTATTCTTCTNCNNNGTTGAAGTTGAGGTTTTGANANTTTCCTCTANTTCACT- GCTCCTGTATATCAGNACGCTTCCCCTTTCTNTATTAATTTTTGCNTNACTTTCAGTTCCANCAAANTNNNNTNNNANNATCA- GATNGNNNNCCGTAAACATTTTNAGAGCCTCACGANCNNNGNGNTTCCGGNACCACAAACGGATNNGTTTTACGNTTCNTTGNCGA- CAATTTGATCCGCGTTNCCNGATGGCGATGNTCTCGTGGTGGCAGCGAGAAATGATCGGAGAAAGATCACNANAANGTCAAAAAACAAC- GAGGGTCTGTAAACTNGACAAAACCAGTATNTNNGNCNGCCCCCNNGNTGGAGCTCGAATTTCTCNCTGATGTCATATGTGCCAGTC- GCCCTATAGAGAGTCGTATTAATTTCGATAANNCAAGTAGGTTCCTCGATCANAGACNCNNTGTGATCGGTCGTTNGGCNGCTGGTAGCG- GTATNANCCCACGCAAAGGTGNNAATACGGTTATCCACCCAATCATNGNATAACGCANNNNNGAACATGTGNGCTAAAGGCCAACATNNT- GCCACCAACCGNAAANNNGACCNNNNNNTCGCNNNNNCNACTANNNNCCNNCCCNAAGACNNNCATNNNNTAANCCNNNNNCNGNNNC AGGTGGTGCANNANNCNNNNCNNNNNNANNCNCNTGGCCCACACCTCCGNNNCCGCTTNGNCCCTC

Supplementary Table 1.5. RNAi clone DNA sequencing. DNA identification sequence reads for RNAi *E. coli* clones selected for additional screening rounds.

CHAPTER 2:

Caenorhabditis Sieve: A Low-tech Instrument and Methodology for Sorting Small Multicellular Organisms[2]

2.1 ABSTRACT:

Caenorhabditis elegans (*C. elegans*) is a well-established model organism used across a range of basic and biomedical research. Within the nematode research community, there is a need for an affordable and effective way to maintain large, age-matched populations of *C. elegans*. Here, we present a methodology for mechanically sorting and cleaning *C. elegans*. Our aim is to provide a cost-effective, efficient, fast, and simple process to obtain animals of uniform sizes and life stages for their use in experiments. This tool, the *Caenorhabditis* Sieve, uses a custom-built lid system that threads onto common conical lab tubes and sorts *C. elegans* based on body size. We also demonstrate that the *Caenorhabditis* Sieve effectively transfers animals from one culture plate to another allowing for a rapid sorting, synchronizing, and cleaning without impacting markers of health, including motility and stress-inducible gene reporters. This accessible and innovative tool is a fast, efficient, and non-stressful option for maintaining *C. elegans* populations.

2.2 INTRODUCTION:

The nematode worm, *Caenorhabditis elegans*, is a premier model organism. In addition to the straightforward and controlled nature of their cultivation in the laboratory, their entire genome is sequenced[1] and the developmental fate of each cell is known[2]. Due to these features, *C. elegans* is a widely used model organism for genetic studies. However, along with these beneficial characteristics come some challenges for researchers. Due to their rapid generation time, *C. elegans* populations can quickly run out of food and/or become mixed populations with multiple generations and developmental stages present at once. Thus, experiments performed on solid nematode growth media (NGM) require researchers to physically move animals to fresh plates before the bacterial food source depletes and new larvae develop. This can be tedious as a frequent transferring of the animals is required to prevent the experimental populations from becoming mixed with offspring generations. Still, some experiments require both large numbers of animals and extended time points (*e.g.*, DNA or RNA extraction in adulthood). This compounds the challenges of accurately maintaining a synchronized population and transferring large numbers of animals.

Current methods of transferring *C. elegans* cultured on NGM are picking or washing the animals from plate to plate; chemically treating the animals (*e.g.*, with the DNA replication inhibitor fluorodeoxyuridine or FUDR); or using flow cytometry to sort the animals in multi-well plates. Picking involves the use of a hand tool, made with either a thin platinum wire or an eyelash, to manually transfer individual or multiple animals[3,4]. This method is accurate but requires both skill and time and is a limitation for studies involving large numbers of animals. Picking may also be physically damaging and stressful to the animals by potentially subjecting individuals to unnatural and inconsistent amounts of disturbance and force. Washing involves rinsing a culture dish with a buffer solution and transferring the

[2] Citation: Hunter, S., Maulik, M., Scerbak, C., Vayndorf, E., Taylor, B.E. *Caenorhabditis* Sieve: A low-tech Instrument and Methodology for Sorting Small Multicellular Organisms. *Journal of Visualized Experiments*. (**137**), e58014, DOI: 10.3791/58014 (2018).

solution with the animals via glass Pasteur pipette to a new culture plate. This method is rapid and efficient but is not accurate as multiple generations and developmental stages of animals are transferred in bulk. Chemical treatments, such as FUDR, can be dissolved in the culturing media to prevent the production of offspring through blocking any DNA replication, and thus, the gamete production and egg development. While effective, this method must be applied after developmental maturation so as to not disrupt the normal developmental processes, and this means that there is still a requirement to transfer the animals prior to its administration[3]. This method also influences multiple cellular signaling pathways, resulting in noticeable effects on the animals as they age (*e.g.*, a lifespan extension or an altered proteostasis) depending on the strain of *C. elegans* used[5-10]. Flow cytometry methods automatically sort and transfer individual *C. elegans* from one multi-well plate to another[11]. While this method is very effective and efficient, flow cytometry equipment is prohibitively expensive and inaccessible to many researchers. An alternative to transferring animals is to use mutant models that are temperature sensitive, such as *fer-15* and *fem-1*, which become sterile with temperature adjustment[12]. While using mutant animals is useful in some situations, these specific strains grow slower than wild-type animals and they rely on an altered genome, serving as poor representatives for aging or healthy worms. In addition, the reliance on a temperature shift to induce sterility also results in the absence of a static environment, and temperature changes have been readily shown to influence gene expressions[13-15]. Research groups have previously published techniques describing the use of a mesh to filter *C. elegans* by size[16]. However, we were unable to find previous work testing for any changes in the overall health outcomes that may be associated with the use of such filters.

There is, thus, a need within the *C. elegans* research community for an affordable, efficient, rapid, and accurate method for transferring large numbers of animals between culture plates. We have developed an improved, accessible piece of equipment (named the *Caenorhabditis* Sieve) and an associated protocol for its manufacture and operation that meets the needs of the *C. elegans* research community. Herein, we share the design of the *Caenorhabditis* Sieve and methods for its use, and we demonstrate that its use does not impact the health or any common stress markers when compared to standard manual picking and a treatment with the commonly-used, fertility-restricting chemical FUDR.

2.3 PROTOCOL:

2.3.1 *Caenorhabditis* Sieve Construction and Use

2.3.1.1 Construction protocol

2.3.1.1.1 Acquire 2 lids from 50 mL conical tubes (**Figure 2.1A**).

2.3.1.1.2 Remove the center area inside the inner lip of the lids (when viewed from the bottom, **Figure 2.1B**) using a Bunsen burner and a hot metal probe or a soldering iron or stepped drill bit.

Note: Using heat to cut the plastic lid is preferable to a blade because there is less risk of injury.

2.3.1.1.3 Clean and sand the cut edges and top the surface with a curved file or a rotary grinding tool (*e.g.*, Dremel). See **Figure 2.1C**.

2.3.1.1.4 Cut the circle of the monofilament mesh to the appropriate diameter (**Figure 2.1D**). For this, trace a lid onto a monofilament nylon mesh sheet and cut just inside the line drawn.

2.3.1.1.5 Cut grooves/slashes into the top surface of the lids to enhance the adhesion of the two lids when glue is applied to the plastic (**Figure 2.1E**).

2.3.1.1.6 Clean the lids with ethanol and let them dry.

2.3.1.1.7 Apply cyanoacrylate glue to the top surface of both lids, keeping to the outer edge.

Note: A little glue goes a long way.

2.3.1.1.8 Lay the monofilament mesh, according to **Table 2.1**, on one glued lid (**Figure 2.1F**). Place the second lid inverted on top of the mesh; both lids must have their tops together. Press firmly together (**Figure 2.1G**). Ensure that the mesh is taut.

Note: As a safety measure, use tweezers to place the mesh on the lids.

2.3.1.1.9 Once the initial layer of glue has dried, apply a ring of cyanoacrylate glue around the outer gap between the lids. Be generous as this adds integrity and prevents any peeling apart or leaking.

2.3.1.1.10 Label the filter with the mesh pore size of the monofilament mesh.

Note: Here, we use two mesh pore sizes—20 µm and 50 µm.

2.3.1.2 Use protocol

2.3.1.2.1 Pre-wet the sieve.

2.3.1.2.1.1 Pipette a saline solution, such as M9 [5 g of NaCl, 6 g of Na_2HPO_4, 3 g of KH_2PO_4, 1 L of ultrapure H_2O, and 1 mL of $MgSO_4$ (1 M)][17], through the center of the sieve until a droplet forms, condenses, and drips off the

center of the filter bottom (**Figure 2.2A**). Optionally, apply a lint-free wipe (*e.g.*, Kimwipe) to the bottom to shape or spread a moisture droplet on the mesh.

2.3.1.2.1.2 Place the sieve over a 50 mL conical tube. Label the tube as 'Waste tube' (**Figure 2.2B**).

2.3.1.2.2 Wash a population of *C. elegans* off an agar plate.

2.3.1.2.2.1 Wash the plate with the M9 buffer and place the worm-containing medium on the topside of the monofilament mesh 1 mL at a time (**Figure 2.2C**). Make sure to operate in the center of the mesh. Wash all worms from the plate.

Note: Typically, 3 mL of M9 for a 60 mm plate is sufficient.

2.3.1.2.2.2 To minimize the number of worms lost in pipetting, use a glass Pasteur pipette to move the worms off the plate and onto the mesh center (repeat as needed).

2.3.1.2.2.3 Rinse the filter with the M9 buffer from the top. Again, make sure to operate in the center of the mesh and rinse all worms in that area. Wash as many times as necessary to ensure that all the bacteria and smaller worms have passed through the mesh.

2.3.1.2.3 Harvest the size-matched animals from the sieve.

2.3.1.2.3.1 Attach a new 50 mL conical tube to the top of the sieve, with the adult worms from step 1.2.2.3 facing the inside of the new collection tube (**Figure 2.2D**).

2.3.1.2.3.2 Remove the first tube (waste tube) and quickly flip over the sieve and new tube to keep the droplet from migrating (**Figure 2.2E**).

Note: If sterility is not required, use a lint-free wipe (e.g., Kimwipe) to wick fluid from bottom of the mesh prior to flipping.

2.3.1.2.3.3 Rinse the mesh with M9 into the new 50 mL tube from the new topside (**Figure 2.2F**). Again, operate in the mesh center and maintain a droplet on the underside of the mesh.

2.3.1.2.3.4 Allow the worms to settle or gently spin them down (*e.g.*, < 16 x g) for approximately 1 min (**Figure 2.2G**).

2.3.1.2.3.5 Aspirate the buffer solution from the pellet of worms, ideally down to > 0.5 mL, or remove as much fluid as possible without disturbing the pellet.

2.3.1.2.3.6 Pipette the worms using a glass Pasteur pipette onto an NGM plate and let them dry. Space multiple droplets out on a new plate so they dry faster (**Figure 2.2H**).

2.3.1.2.4 Clean the sieve.

2.3.1.2.4.1. Rinse the sieve gently and thoroughly with ethanol and reverse-osmosis water. Let it dry.

2.3.1.2.4.2 Store it in a clean container for indefinite future use.

2.3.1.2.4.3 Discard it when the mesh develops a "sag" appearance.

2.4 VALIDATION OF *CAENORHABDITIS* SIEVE SORTING METHOD:

2.4.1 General maintenance

2.1.1. For all experiments, culture worms on a standard Nematode Growth Media[17] (1 L of NGM consists of 2.5 g of peptone, 17 g of agar, 3 g of NaCl, 975 mL of double-distilled water, 1 mL of 5 mg/mL cholesterol, 1 mL of 1 M $CaCl_2$, 1 mL of 1 M $MgSO_4$, 25 mL of 1 M $KHPO_4$, and 0.5 mL of 100 mg/mL streptomycin) at 25°C.

2.4.2 Experimental treatment administration

2.4.2.1 Compare the three treatment groups: pick, fluorodeoxyuridine (FUDR), and *Caenorhabditis* Sieve.

2.4.2.1.1 For the FUDR treatment group, add 100 mg/mL FUDR to the NGM media to a final concentration of 100 μM to prevent any progeny production, and transfer the worms every other day to a fresh NGM plate to avoid food depletion.

2.4.2.1.2 For the pick group, select and transfer the worms manually using a platinum loop.

2.4.2.1.3 For the *Caenorhabditis* Sieve treatment group, follow step 1.2 and pipette the worms onto an NGM plate.

2.4.3 *Caenorhabditis* Sieve percentage yield

2.4.3.1 To quantify how effective the sieve is at sorting *C. elegans*, grow age-synchronous N2 animals to day 1 of adulthood at 25°C (*i.e.*, 48 h after egg laying) and then transfer them by picking them to fresh NGM plates (totaling N = 50 or N = 100 animals per treatment group).

2.4.3.2 After 24 h of recovery, transfer the population to new NGM plates with the *Caenorhabditis* Sieve following the above protocol (see step 1.2) and count the number of successfully transferred animals.

2.4.3.3 Calculate the percentage yield as the ratio of the number of animals transferred in comparison to the starting number at the beginning of the transfer multiplied by 100 (%).

2.4.4 Healthspan assays

Note: Score healthspan parameters of the motility class, the pharyngeal pump rate, and both the anterior and the posterior gentle touch response on days 2, 4, 6, and 8 of adulthood for age-synchronized N2 animals maintained at 25°C.

2.4.4.1 Motility tracking

2.4.4.1.1 Assign motility scores based on a class-based system (classes A, B, and C) following the methods of Herndon *et al.*[18]. Compare the effects of the three experimental groups using an ordinal logistic statistics model in statistical analysis software.

Note: Class A individuals move spontaneously in a normal, sinusoidal pattern. Class B individuals move in markedly non-sinusoidal movements and may require prodding to encourage movement. Class C individuals move their head and/or tail in response to prodding but are unable to move across the agar.

2.4.4.2 Pharyngeal pump rate

2.4.4.2.1 Count the grinder movement of the animal's terminal pharyngeal bulb visually under a stereomicroscope at a 600X final magnification for 1 min.

2.4.4.2.2 Conduct a statistical analysis with a one-way ANOVA with $\alpha = 0.05$ and Bonferroni post-tests with $\alpha = 0.05$.

2.4.4.3 Touch response

2.4.4.3.1 Record a gentle touch response and compare between the three treatment groups. Perform the assays based on the methods described by Calixto *et al.*[19].

2.4.4.3.2. Record the anterior and posterior touch response by gently stroking an eyelash pick perpendicularly across the tail or the head (5x each, alternating head and tail) of the animals.

2.4.4.3.3 Score any movement in the opposite direction of the stroke as 1 point on a scale of 0 to 5 for both the anterior and the posterior response.

2.4.4.3.4 Conduct statistical analysis with a one-way ANOVA with $\alpha = 0.05$ and Bonferroni post-tests with $\alpha = 0.05$.

2.4.5 Fecundity assay

2.4.5.1 To determine the use of the *Caenorhabditis* Sieve's impact on reproduction, grow age-synchronous N2 animals to day 2 of adulthood at 25°C.

2.4.5.2 60 h after egg lay, transfer animals to new NGM plates with either a platinum pick or the *Caenorhabditis* Sieve and give them 4 h to recover (dry the sieved plates for 20 - 30 min).

2.4.5.3 After recovery, individually plate the animals via an eyelash pick to NGM plates, give them 24 h to lay eggs, and remove the animals. Allow the progeny on each plate to develop under normal conditions at 25°C for another 24 h.

Note: An eyelash pick is a human eyelash secured to the end of a Pasteur pipette with nail polish and sterilized with ethanol.

2.4.5.4 Count the number of viable F1 generation individuals. Perform a statistical analysis using a T-test with $\alpha = 0.05$.

Note: Viable offspring are considered to be eggs that successfully hatch and begin their development through the regular larval cycles.

2.4.6 Fluorescent reporter stress response assays

2.4.6.1 Perform three commonly used fluorescent reporter assays to detect potential markers of stress: a DAF-16::GFP translocation into the nuclei of cells in a strain [TJ356- zIs356 (pDAF-16::DAF-16-GFP;rol-6)][20]; an hsp-16.2 expression [TJ375- gpIs1 (hsp-16.2p::GFP)][21]; and a sod-3 expression [CF1553-muIs84([pAD76]sod-3p::GFP+rol-6[su1006])][22].

2.4.6.2 For each assay, culture age-synchronous animals from the three treatment groups at 20°C and examine them at day 3 of adulthood: use a negative control (on a daily basis, transfer a group of animals manually with a platinum pick), a positive control (on a daily basis, transfer a group of animals manually with a platinum pick plus an established stressor), and the *Caenorhabditis* Sieve (pass the animals through the sieve and allow them to recover for 30 min on NGM just before imaging).

2.4.6.3 In the DAF-16::GFP assay, heat shock the positive control animals at 37°C for 30 min before imaging[20]. For the hsp-16.2 assay, heat shock the positive control animals for 90 min, 20 h before imaging[21]. For the sod-3 assay, treat the positive control animals with 100 mM paraquat for 4 h before imaging[22].

2.4.6.4 Harvest the worms immediately with an eyelash pick and mount them to a coverslip with 1 µL of a 36% poloxamer 407 surfactant solution to immobilize the worms.

2.4.6.5 Sandwich the mounted worms with another coverslip. Mount the two coverslips to a standard glass microscopy slide and image the worms using an 8X magnification on an inverted fluorescent microscope (for an overall magnification of 80X) and a constant exposure with a FITC filter.

2.4.6.6 To detect any differences between the three groups in the DAF-16::GFP assay, categorize the animals based on the location of the DAF-16::GFP reporter (nuclear if the reporter translocated to nuclei, cytosolic if the reporter located in cytosol, and intermediate if the reporter located in both nuclei and cytosol).

2.4.6.7 Compare the results using an ordinal logistics statistical model in statistical analysis software. For the hsp-16.2 and the sod-3 expression assays, use a one-way ANOVA with $\alpha = 0.05$ and Tukey's *post hoc* tests with $\alpha = 0.05$ to compare the total fluorescence of the head region.

2.5 REPRESENTATIVE RESULTS:

The *Caenorhabditis* Sieve consists of 2 screw caps, securing an area of woven nylon monofilament mesh smaller than the body diameter of the desired developmental age, used to extract live populations of organisms using a simple washing technique. It attaches to standard conical tubes and uses the mesh screen to mechanically sort animals by body diameter, leaving the desired animals in the tube ready for further maintenance and

experimentation (*e.g.*, transfer or genetic harvest). A gentle manual washing with the *Caenorhabditis* Sieve is quick, approximately 5 min per 60 - 100 mm plate, and the organisms are easily recovered from the mesh.

Percentage yield of animals following *Caenorhabditis* Sieve use:

To establish the percentage yield of the *Caenorhabditis* Sieve, devices were tested with both 20 µm and 50 µm pore-size meshes on adult animals. A mean yield of a > 90% successful animal transfer was achieved for both mesh sizes tested (**Table 2.1**).

Monofilament mesh with different size gaps may be used to separate animals of different life stages. Mesh with 20 µm gaps is appropriate for washing away developing embryos and larval stages smaller than the fourth larval stage, retaining the latter (L4; with an average body diameter of 32 µm) and any animals in later life stages, while mesh with 50 µm gaps will allow all other life stages aside from adults (with an average body diameter of 70 µm) to be washed away (**Table 2.2**).

***Caenorhabditis* Sieve use does not impact healthspan metrics**

Motility: In *C. elegans* the normal sinusoidal movement (*i.e.*, motility) declines with age[18] and is a marker of overall health. To determine if the *Caenorhabditis* Sieve influenced motility, motility scores were compared for pick, FUDR, and *Caenorhabditis* Sieve treatment groups on days 2, 4, 6, and 8 of adulthood. All the animals across every group (N = 10/group) exhibited normal and spontaneous movement patterns (Class A) at multiple ages throughout adulthood (days 2, 4, 6, and 8 of adulthood; $p > 0.05$ for multiple comparisons on all days, **Figure 2.3**).

Pharyngeal pump rate: The ability of *C. elegans'* pharyngeal muscles to pump declines with age and is another biomarker of healthspan[23]. To determine if the *Caenorhabditis* Sieve influenced the animals' pharyngeal pump rate, pick, FUDR, and *Caenorhabditis* Sieve treatment groups were compared on days 2, 4, 6, and 8 of adulthood (n = 8 to 10 per group). There was a significant difference between the animals that underwent the picking and FUDR methods on days 6 ($p < 0.001$) and 8 ($p < 0.001$). Also, there was a significant difference between the sieve and FUDR groups on days 6 ($p < 0.001$) and day 8 of adulthood ($p < 0.001$). However, there was no statistically significant difference between the pick and the *Caenorhabditis* Sieve groups for any day ($p > 0.05$, **Figure 2.4**), indicating that the sieve does not impact this measure of healthspan.

Gentle touch response: Response to mechanical stimulus is a physiological marker to assess aging or general health[24,25]; thus, the impact of different transfer methods on both the anterior and the posterior gentle touch responses were tested. There was no statistically significant difference between the pick, FUDR, and *Caenorhabditis* Sieve treatment groups (n = 8/group), either anteriorly or posteriorly, for any day of testing ($p > 0.4$ for all comparisons; **Figures 2.5A** and **2.5B**).

Fecundity: To establish whether or not the *Caenorhabditis* Sieve influenced the amount of viable progeny produced by *C. elegans*, the individual offspring produced in a 24 h period during day 3 of adulthood was counted and

compared (n = 20 to 22 per group). The use of the *Caenorhabditis* Sieve did not significantly impact the number of progeny produced when compared to a pick treatment group ($p = 0.61$, **Figure 2.6**).

Molecular reporter assays:

DAF-16 nuclear translocation: In *C. elegans*, the activation of the transcription factor DAF-16 is associated with increased stress resistance[26]. The nuclear localization of DAF-16 was examined in a transgenic nematode strain TJ356, which expresses DAF-16 fused to a green fluorescent protein (DAF-16::GFP)[20]. Under normal growth conditions, DAF-16::GFP is localized primarily in the cytosol, but under various stressors (*e.g.*, heat stress), it is rapidly translocated into the nucleus[20]. To test the impact of sorting with the *Caenorhabditis* Sieve on DAF-16 translocation, DAF-16::GFP localizations were compared in age-matched day-5 adults in a positive control group (heat stress), a negative control group (manual transfer via pick), and a *Caenorhabditis* Sieve treatment groups (n = 10/group). The transfer with the *Caenorhabditis* Sieve did not affect the nuclear translocation of DAF-16::GFP, and showed a similar phenotype to the negative control animals ($p > 0.05$, **Figure 2.7**).

***hsp-16.2* reporter:** Small heat shock proteins like HSP-16.2 are biomarkers of a stress response, and they are highly expressed during an exposure to heat shock or oxidative stress agents[21,27]. The TJ375 strain has a GFP reporter gene fused with an hsp-16.2 promoter that is not active under normal conditions[21]. However, after an exposure to a heat shock, HSP-16.2 protein expression is induced, and the animals display high levels of GFP expression[21]. To test the involvement of the *Caenorhabditis* Sieve on an HSP-16.2-mediated stress response, the fluorescence density in the pharynx region (n = 10 animals/group) of age-matched animals was compared in day-5 adults between a positive control group (heat stress), a negative control group (picking), and a *Caenorhabditis* Sieve treatment group. The transfer with the *Caenorhabditis* Sieve did not significantly induce the expression of HSP-16.2::GFP (hsp-16.2::gfp) when compared to the negative control ($p > 0.05$, **Figure 2.8**).

***sod-3* reporter:** In *C. elegans*, the anti-oxidant gene that codes for superoxide dismutase 3 (SOD-3) is up-regulated during oxidative stress[28]. The *C. elegans* strain CF1553 expresses green fluorescent protein (GFP)-labeled SOD-3 promoter, whose expression is induced by oxidative stressors, such as paraquat[5]. To test the involvement of the *Caenorhabditis* Sieve sorting on the antioxidant response in *C. elegans*, the fluorescence density in the head region of age-matched day-5 adults was compared between a positive control population (100 µM paraquat treatment), a negative control population (manual picking), and a *Caenorhabditis* Sieve-transferred population. The transfer with the *Caenorhabditis* Sieve did not significantly induce the expression of sod-3::gfp when compared to the negative control ($p > 0.05$, **Figure 2.9**).

2.6 DISCUSSION:

Herein, we introduced the design and use of the accessible, effective *Caenorhabditis* Sieve as a tool for sorting and maintaining *C. elegans*. This tool has several advantages to manually picking individual animals, washing populations, chemical treatments (*e.g.*, FUDR), and more expensive methods of segregating animals. First, the

Caenorhabditis Sieve efficiently and quickly (less than 20 min) sorts progeny from large mixed populations of animals (**Table 2**). Also, the use of the tool has no detectable toxic effects on the animals' healthspan (**Figures 3 - 6**), does not induce well-described genetic stress reporters (**Figures 7 - 9**), and reduces the amount of foreign chemical that could influence the applied treatment to the culture plates or any molecular assay thereafter. Its ease of use is a significant advantage; a researcher at any stage in their education can be trained to use it (**Figures 1** and **2**; **Protocol**).

The materials required for the fabrication and use of the sieve (*e.g.*, pipettes, buffers) are readily available in standard research laboratories; thus, if broken, the *Caenorhabditis* Sieve is not expensive to replace or repair (**Supplemental Table 2.3**). The self-constructed nature of the *Caenorhabditis* Sieve allows it to be a versatile tool: it can be constructed with mesh sizes appropriate for different *C. elegans* developmental stages and phenotypes. The *Caenorhabditis* Sieve may also be used in assays conducted in other nematode species or when isolating small organisms, provided the appropriate mesh size is used upon manufacture.

In addition to the benefits this tool provides for *C. elegans* population maintenance, the Sieve may be used to clean animals before their use in other experimental applications. For example, with the development of microfluidics to conduct *C. elegans* research comes the issue of chip use and cleaning. Depending on the amount of bacteria attached to the animals, special precautions need to be taken so as not to clog the microfluidic chip, rendering it unusable[29]. Often when *C. elegans* are transferred to a microfluidic chip, residue from the bacterial lawn is brought with them. This residue can and does clog the microfluidic channels, making the chip malfunction, which then requires cleaning or replacement. The device constructed in this protocol offers a method for not only harvesting synchronized animals for microfluidics, but also for cleaning the animals prior to their insertion into a microfluidic device. By removing the debris and bacterial residue, taken up when collecting animals, the microfluidic channels are less prone to malfunction, thus increasing the operational life of individual chips and the subsequent throughput of research being conducted with them.

2.7 ACKNOWLEDGMENTS:

The authors would like to thank Heather Currey for her initial contribution to the study design, and Dr. Swarup Mitra for his critical review of the manuscript. We would also like to thank Dr. Michael B. Harris for comments, refinements and assistance in producing the demonstration of this methodology. The strains were provided by the Caenorhabditis Genetics Center, which is funded by the NIH Office of Research Infrastructure Programs (P40 OD010440). The research reported in this publication was supported by the National Institute of General Medical Sciences of the National Institutes of Health under Award Numbers UL1GM118991, TL4GM118992, or RL5GM118990 and by an Institutional Development Award (IDeA) from the National Institute of General Medical Sciences of the National Institutes of Health under grant number 5P20GM103395-15. The content is solely the responsibility of the authors and does not necessarily represent the official views of the National Institutes of Health. UA is an AA/EO employer and educational institution and prohibits illegal discrimination against any individual:

www.alaska.edu/titleIXcompliance/nondiscrimination.

2.8 DISCLOSURES:

The authors have nothing to disclose. The authors declare that the research was conducted in the absence of any commercial or financial relationships that could be construed as a potential conflict of interest.

2.9 REFERENCES:

1. *C. elegans* Sequencing Consortium. Genome sequence of the nematode *C. elegans*: a platform for investigating biology. *Science.* **282** (5396), 2012-2018 (1998).

2. Herman, M. A. Hermaphrodite cell-fate specification. *WormBook.* 1-16, doi:10.1895/wormbook.1.39.1 (2006).

3. Stiernagle, T. Maintenance of *C. elegans*. *WormBook.* 1-11, doi:10.1895/wormbook.1.101.1 (2006).

4. Chalfie, M., Hart, A. C., Rankin, C. H., Goodman, M. B. Assaying mechanosensation. *WormBook.* doi:10.1895/wormbook.1.172.1 (2014).

5. Van Raamsdonk, J. M., Hekimi, S. Deletion of the Mitochondrial Superoxide Dismutase sod-2 Extends Lifespan in *Caenorhabditis elegans*. *PLoS Genetics.* **5** (2), e1000361 (2009).

6. Van Raamsdonk, J. M., Hekimi, S. FUdR causes a twofold increase in the lifespan of the mitochondrial mutant gas-1. *Mechanisms of Ageing Development.* **132** (10), 519-521 (2011).

7. Gandhi, S., Santelli, J., Mitchell, D. H., Stiles, J. W., Sanadi, D. R. A simple method for maintaining large, aging populations of *Caenorhabditis elegans*. *Mechanisms of Ageing Development.* **12** (2), 137-150 (1980).

8. Aitlhadj, L., Stürzenbaum, S. R. The use of FUdR can cause prolonged longevity in mutant nematodes. *Mechanisms of Ageing and Development.* **131** (5), 364-365 (2010).

9. Davies, S. K., Leroi, A. M., Bundy, J. G. Fluorodeoxyuridine affects the identification of metabolic responses to daf-2 status in Caenorhabditis elegans. *Mechanisms of Ageing Development.* **133** (1), 46-49 (2012).

10. Feldman, N., Kosolapov, L., Ben-Zvi, A. Fluorodeoxyuridine improves *Caenorhabditis elegans* proteostasis independent of reproduction onset. *PLoS One.* **9** (1), e85964 (2014).

11. Pulak, R. Techniques for analysis, sorting, and dispensing of C. elegans on the COPAS flow-sorting system. *Methods Molecular Biology.* **351**, 275-286 (2006).

12. Argon, Y., Ward, S. *Caenorhabditis elegans* fertilization-defective mutants with abnormal sperm. *Genetics.* **96** (2), 413-433 (1980).

13. Lee, S. J., Kenyon, C. Regulation of the longevity response to temperature by thermosensory neurons in *Caenorhabditis elegans*. *Current Biology.* **19** (9), 715-722 (2009).

14. Klass, M. R. Aging in the nematode *Caenorhabditis elegans*: major biological and environmental factors influencing life span. *Mechanisms of Ageing Development.* **6** (6), 413-429 (1977).

15. Zhang, B. *et al.* Environmental Temperature Differentially Modulates *C. elegans* Longevity through a Thermosensitive TRP Channel. *Cell Reports.* **11** (9), 1414-1424 (2015).

16. Michaelson, L. *C. elegans*: A Practical Approach. Ian A. Hope (ed.). Oxford University Press, Oxford. 1999. Pg. 281. ISBN 0 19 963738 5. *Heredity.* **85** (1), 97-100 (2000).

17. Brenner, S. The genetics of *Caenorhabditis elegans*. *Genetics.* **77** (1), 71-94 (1974).

18. Herndon, L. A. *et al.* Stochastic and genetic factors influence tissue-specific decline in ageing *C. elegans*. *Nature.* **419** (6909), 808-814 (2002).

19. Calixto, A., Chelur, D., Topalidou, I., Chen, X., Chalfie, M. Enhanced neuronal RNAi in *C. elegans* using SID-1. *Nature Methods.* **7** (7), 554-559 (2010).

20. Henderson, S. T., Johnson, T. E. daf-16 integrates developmental and environmental inputs to mediate aging in the nematode *Caenorhabditis elegans*. *Current Biology.* **11** (24), 1975-1980 (2001).

21. Rea, S. L., Wu, D., Cypser, J. R., Vaupel, J. W., Johnson, T. E. A stress-sensitive reporter predicts longevity in isogenic populations of *Caenorhabditis elegans*. *Nature Genetics.* **37** (8), 894-898 (2005).

22. Libina, N., Berman, J. R., Kenyon, C. Tissue-specific activities of *C. elegans* DAF-16 in the regulation of lifespan. *Cell.* **115** (4), 489-502 (2003).

23. Keith, S. A., Amrit, F. R., Ratnappan, R., Ghazi, A. The *C. elegans* healthspan and stress-resistance assay toolkit. *Methods.* **68** (3), 476-486 (2014).

24. Scerbak, C., Vayndorf, E. M., Hernandez, A., McGill, C., Taylor, B. E. Mechanosensory neuron aging: Differential trajectories with lifespan-extending alaskan berry and fungal treatments in *Caenorhabditis elegans*. *Frontiers in Aging Neuroscience.* **8**, 173 (2016).

25. Vayndorf, E. M. *et al.* Morphological remodeling of *C. elegans* neurons during aging is modified by compromised protein homeostasis. *npj Aging and Mechanisms of Disease.* **2**, 16001 (2016).

26. Murakami, S., Johnson, T. E. A genetic pathway conferring life extension and resistance to UV stress in *Caenorhabditis elegans*. *Genetics.* **143** (3), 1207-1218 (1996).

27. Abbas, S., Wink, M. Green Tea Extract Induces the Resistance of *Caenorhabditis elegans* against Oxidative Stress. *Antioxidants* (Basel). **3** (1), 129-143 (2014).

28. Yanase, S., Hartman, P. S., Ito, A., Ishii, N. Oxidative stress pretreatment increases the X-radiation resistance of the nematode *Caenorhabditis elegans*. *Mutation Research.* **426** (1), 31-39 (1999).

29. Chung, K., Crane, M. M., Lu, H. Automated on-chip rapid microscopy, phenotyping and sorting of *C. elegans*. *Nature Methods.* **5** (7), 637-643 (2008).

2.10 FIGURES AND TABLES:

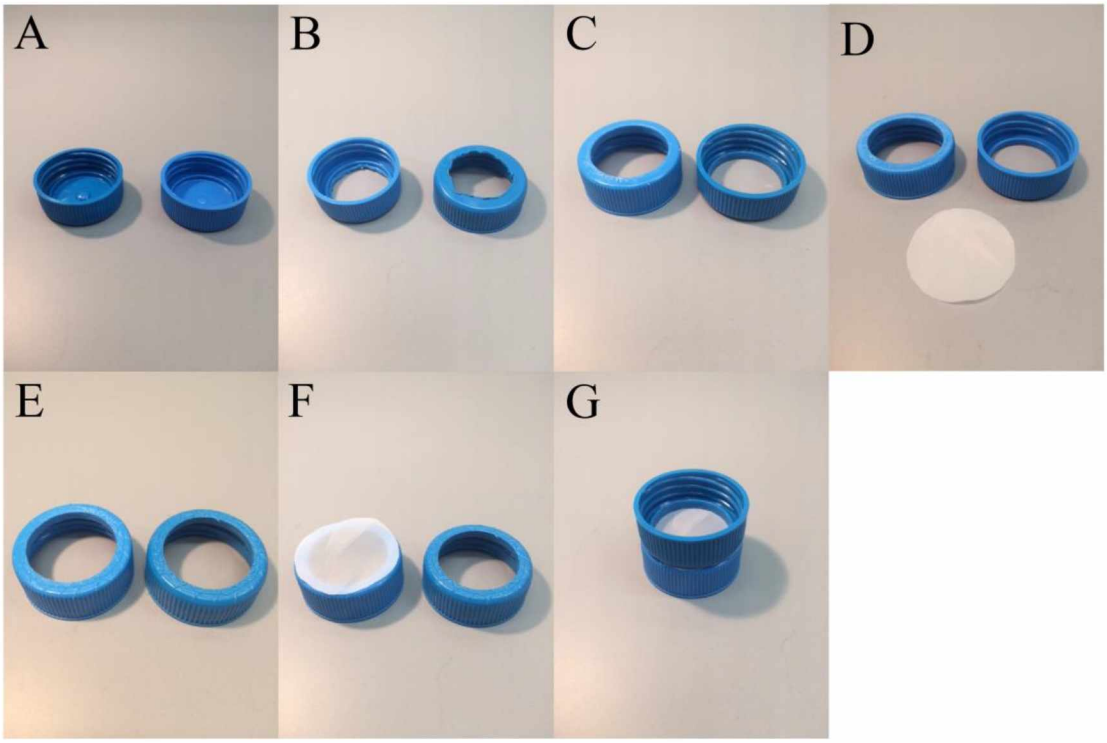

Figure 2.1. ***Caenorhabditis*** **Sieve construction.** The progression of the 'do-it-yourself' manufacture of the tool is shown. These panels show **(A)** two 50 mL conical tube caps **(B)** whose centers have been removed, **(C)** cut edges smoothed, and **(D - F)** who are fitted with monofilament mesh corresponding to the desired life stage of *C. elegans* (see Protocol for details). **(G)** The completed sieve is also shown.

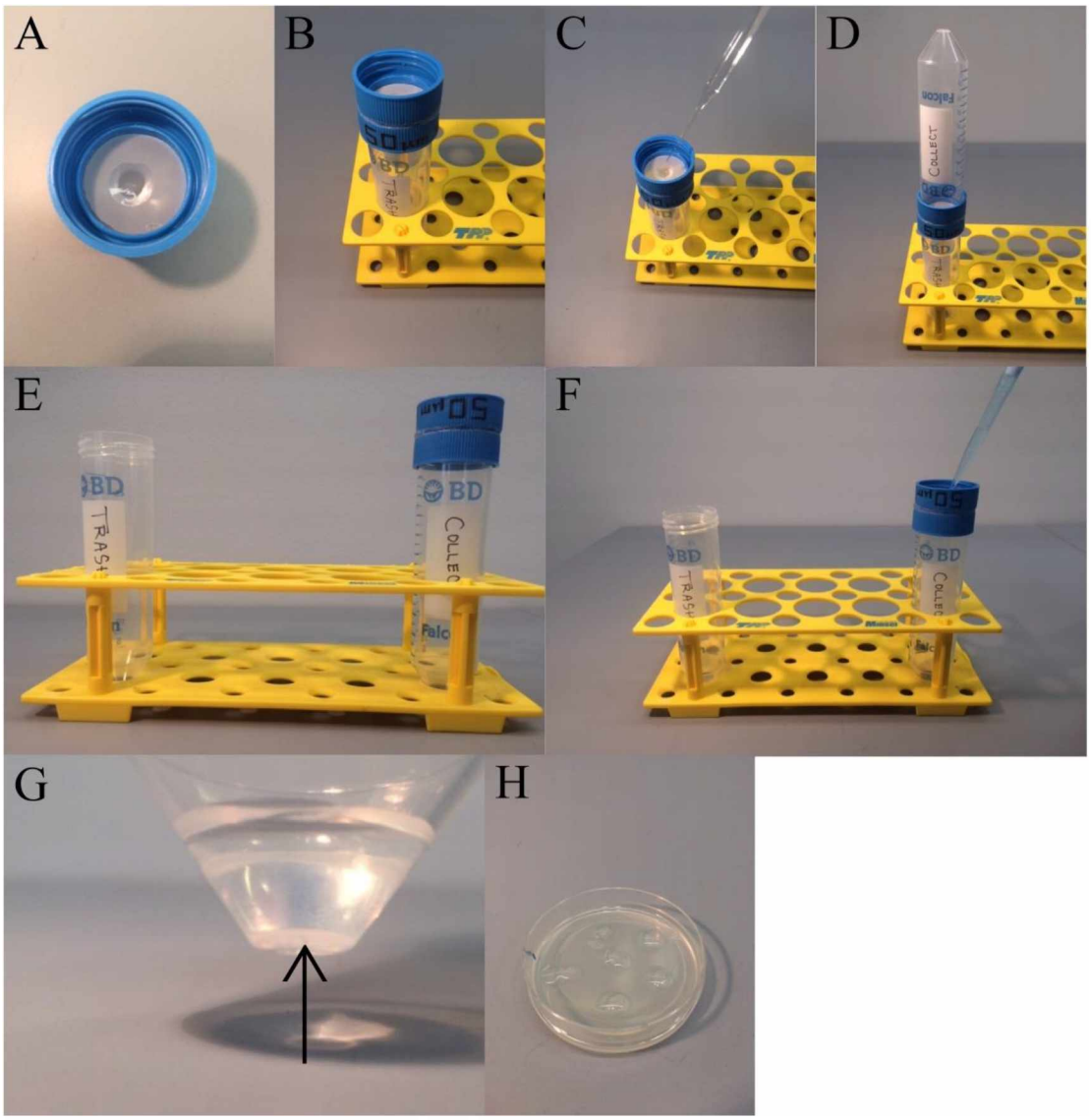

Figure 2.2. Step-by-step image representation of *Caenorhabditis* Sieve use. (**A**) The sieve is pre-wet with a drop of M9 solution, and (**B**) fit on top of a 50 mL conical tube. (**C**) 1 mL of M9 solution with worms is pipetted on the topside of the sieve, (**D**) a 50 mL conical tube is placed on top of the sieve with the worms facing the inside of the tube, and (E) the sieve with a newly attached upper tube is quickly flipped over. (**G**) The sieve is rinsed with M9 carrying the desired animals into the new 50 mL tube and the worms are allowed to settle by gravity to the bottom of the tube. (**H**) The worms are pipetted and placed as droplets on a fresh NGM plate.

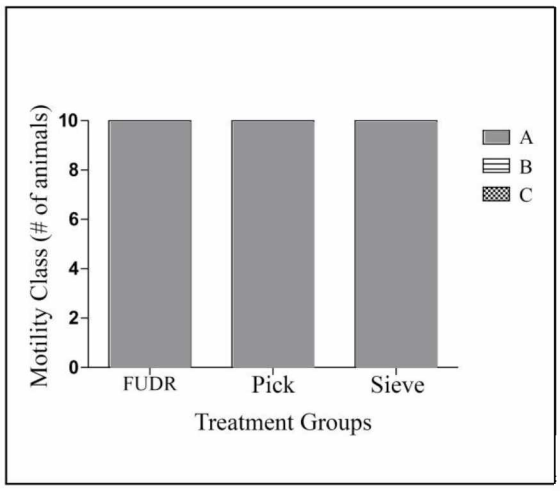

Figure 2.3. *Caenorhabditis* Sieve did not impact motility throughout lifespan. This figure shows the motility class distribution of animals at days 2, 4, 6, and 8 of adulthood for pick, FUDR, and *Caenorhabditis* Sieve treatment groups, all days tested had the same distribution. Class A animals moved normally and spontaneously, class B animals moved abnormally and may have required prodding, and class C animals were unable to

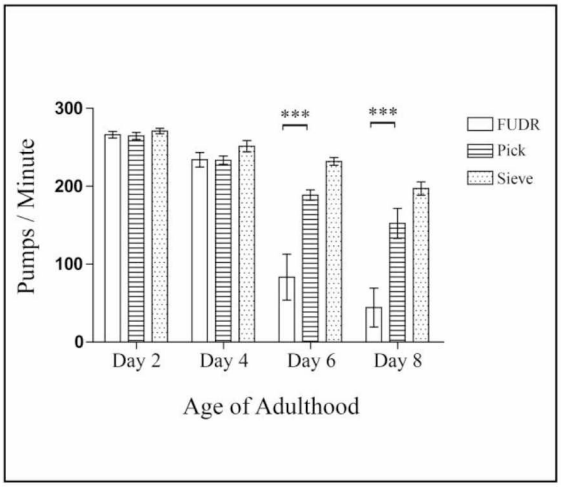

Figure 2.4. *Caenorhabditis* Sieve use did not impact pharyngeal pumping throughout the lifespan. This figure shows the pharyngeal pump rates of pick, FUDR, and *Caenorhabditis* Sieve treatment groups, compared on days 2, 4, 6, and 8 of adulthood. The asterisks denote a significance between the pick, sieve, and FUDR treatment groups for the days specified (*** $p < 0.05$). There was no difference between the *Caenorhabditis* Sieve and the pick group ($p > 0.05$). Two replicates (N = 10 ani-

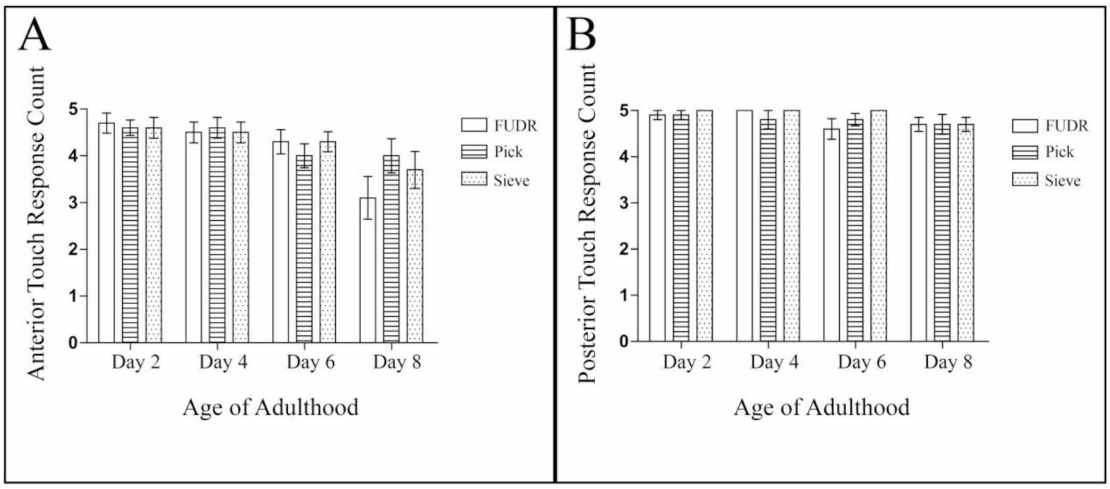

Figure 2.5. *Caenorhabditis* Sieve use did not impact anterior touch response throughout lifespan. These panels show (**A**) the anterior and (**B**) the posterior touch response count of pick, FUDR, and *Caenorhabditis* Sieve treatment groups compared on days 2, 4, 6, and 8 of adulthood. Two replicates were conducted with N = 10 for each treatment group and compared with a one-way ANOVA and a Bonferroni post-test ($p = 0.4$ and $p = 0.9$ for anterior and posterior, respectively). The bars represent the mean ± the standard error of the mean.

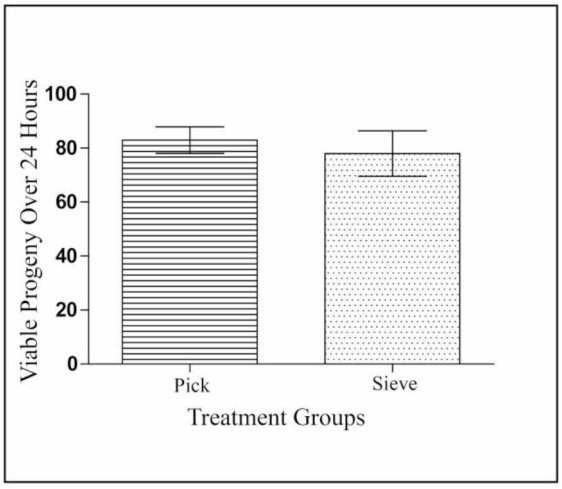

Figure 2.6. *Caenorhabditis* Sieve did not impact the amount of viable progeny on day 3 of adulthood. This figure shows the viable progeny from 24 h egg-laying period, spanning day 3 of adulthood for parent animals. The bars represent the mean ± the standard error of the mean. N = 20 - 22 animals from at least two separate biological replicates per treatment group. The treatment groups are compared with a t-test, ($p > 0.05$).

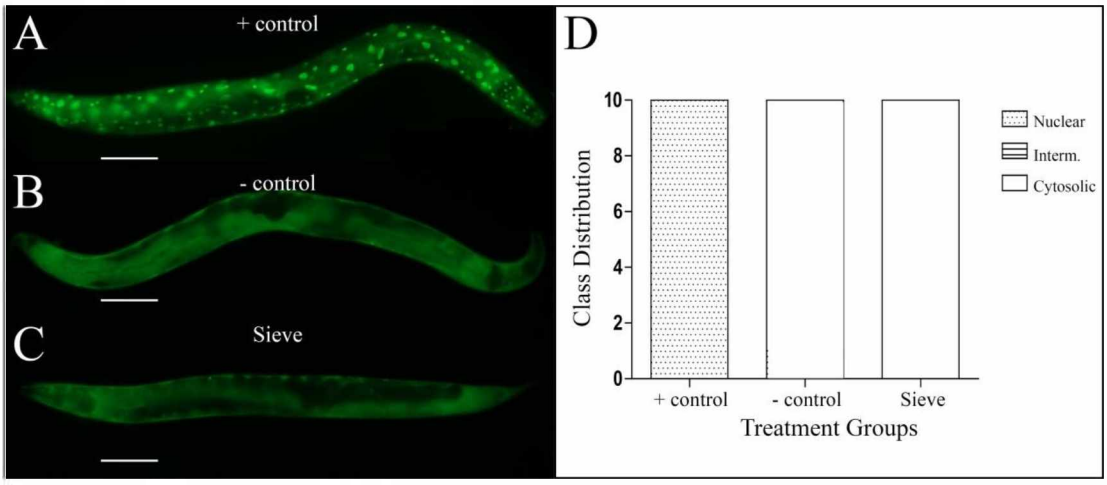

Figure 2.7. *Caenorhabditis* Sieve did not affect nuclear translocation of DAF-16::GFP. These panels show representative images of the DAF-16 translocation of (**A**) a heat shock group (the positive control), (**B**) a pick group (the negative control), and (**C**) a *Caenorhabditis* Sieve treatment group. Scale bars represent approximately 50 μm. (**D**) The animals in the positive control group displayed an activation of the DAF-16 nuclear translocation. The *Caenorhabditis* Sieve did not induce a nuclear translocation and displayed cytosolic fusion protein similar to the animals in the negative control group. N = 10 animals per treatment group from at least three separate biological replicates. The treatment groups were compared with a one-way ANOVA and a Tukey's post hoc test. The scale bar is 100 μm.

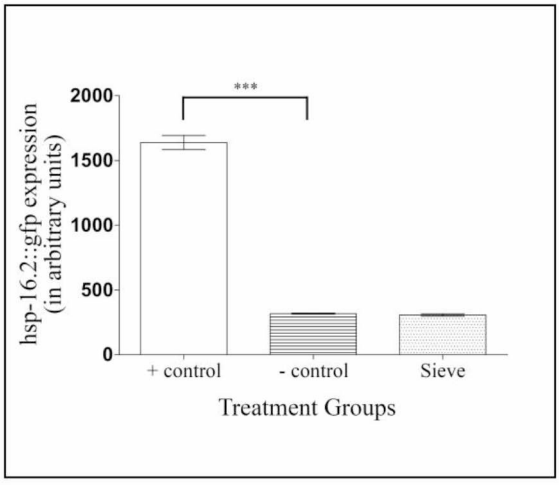

Figure 2.8. *Caenorhabditis* Sieve did not affect the expression of hsp-16.2::gfp. The HSP-16.2 expressions (in arbitrary fluorescence units) of a heat shock group (the positive control), a pick group (the negative control), and a *Caenorhabditis* Sieve treatment group are compared. The asterisks denote a high expression of hsp-16.2::gfp for the positive control group which was significantly different from the other treatment groups (*** $p < 0.05$). The *Caenorhabditis* Sieve did not affect the hsp-16.2::gfp expression and displayed fluorescence intensities similar to animals in the negative control group ($p > 0.05$). Three replicates were conducted with N = 10 for each treatment group and compared with a one-way ANOVA and a Tukey's *post hoc* test.

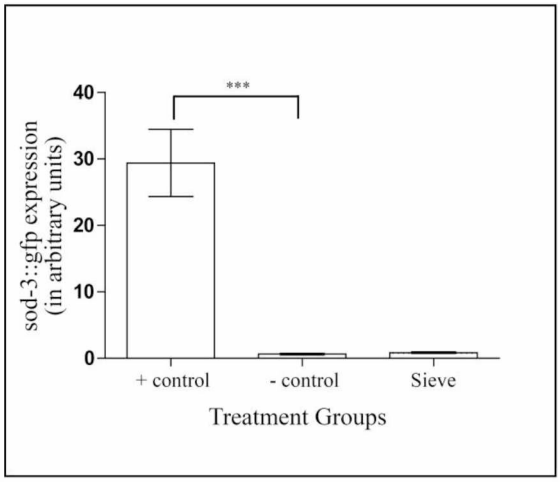

Figure 2.9. *Caenorhabditis* Sieve did not affect the expression of sod-3::gfp. The SOD-3 expressions (in arbitrary fluorescence units) of a 100 μM paraquat group (the positive control), a pick group (the negative control), and a *Caenorhabditis* Sieve treatment group are shown. The asterisks denote a high expression of sod-3::gfp for the positive control group which was significantly different from the other groups (*** $p < 0.05$). The *Caenorhabditis* Sieve did not affect the sod-3::gfp expression and displayed fluorescence intensities similar to the animals in the negative control group ($p > 0.05$). Three replicates were conducted with N = 10 for each treatment group and compared with a one-way ANOVA and a Tukey's *post hoc* test.

Mesh size	N=50	N=100
20 μm	95.33%	NA
50 μm	99.00%	93.33%

Table 2.1. Percentage yield of mesh sizes. This table shows the results of a 20 μm device tested with N = 50 adults for 3 replicates and a 50 μm device tested with N = 50 adults for 2 replicates and with N = 100 for 3 replicates.

Mesh Size	Dev. Stage	Body Diameter
20 μm	Larval Stage 4	~35 μm
50 μm	Day 1 Adult	~70 μm

Table 2.2. Mean body diameter. This table displays the mean body diameter acquired by averaging 3 measurements equally spread across each worm for 15 animals at each measured life stage.

Name of Material/ Equipment	Company	Catalog Number	Comments/Description
Safety glasses	Uline	S-21076	
Protective heat resistant gloves	Grainger	Item # 3AT17 Mfr. Model # 3AT17 Catalog Page # 1703	
50 mL conical tubes	Falcon	14-432-22	Tubes and lids will be used
Synthetic nylon mesh	Dynamic Aqua-Supply Ltd.	NTX20 and NTX50	Select pore size for application
Cyanoacrylate glue	Scotch Super Glue Liquid	SAD114	
Pliers	Vampliers	VMPVT-001-8	Used to hold lids while cutting
Dremel tool with circular file	Lowe's	Item # 525945 Model # 100-LG	Used to clean hole that was cut
FuDR	Sigma	F0503	
M9 Chemical (NaCl, Na_2HPO_4, KH_2PO_4, $MgSO_4$)	Sigma	S7653, RES20908-A7, 1551139, M7506	
NGM plate chemicals (Bactopeptone, Agar, KH2PO4, K2HPO4, CaCl2,Cholesterol, Streptomycin)	BD Biosciences (bactopeptone) , Lab express (agar), Sigma (rest)	BD bioscience 211677, Lab Express 1001, Sigma 1551139, 1551128, C1016, C8667, S6501	
Pluronic® F-127	Sigma	P2443	
Paraquat dichloride hydrate	Sigma	36541	
Step drill bit	Huele	B06Y25PFMZ	Other brands will work so long as they cut up to 1 in

Supplemental Table 2.3. List of material and supply. List of materials and supplies used to construct the *Caenorhabditis* Sieve and proof-of concept experiments.

GENERAL CONCLUSION:

Insulin Ligands Influence Morphology of Mechanosensory Neurons

The results presented in Chapter 1 show that ILPs influence the morphology of mechanosensory neurons in *C. elegans*. There was inconsistency in the results, in that the second round of RNAi did not produce changes in neuronal aberrations similar to the first and third rounds. The second round of RNAi resulted in a single change in *Neurite Branches* while the first and second rounds resulted in multiple changes in multiple *Somatic Outgrowth* types. The similarity in the outcome of rounds 1 and 3 provides some support for the hypothesis, *knockdown of similar ILP subfamily members will result in similar phenotypic aberrations in neurons,* as the ILP re-screen candidates were primarily from the β sub-family of ILPs, and knockdown of those β sub-family members produced similar shifts in neuronal aberrations. Of emphasis from this study, is that these identified ILPs are considered important for promoting neuronal aberrancy to that seen in what is considered normal levels in regular, aging morphology. Their knockdown was causative of the observed decrease in morphological aberrations. This is most likely due to agonist behavior at the DAF-2 receptor to which they bind. This agonist-like behavior observed in the chosen ILPs is plausible as the absence of these possible agonists would produce a decrease in DAF-2 signaling and subsequent increase in DAF-16 translocation, which has been shown to decrease neuronal aberrancy in mechanosensory neurons[17]. Knockdown of antagonist ILPs, on the other hand, would produce no change in IR activity as the agonist ILPs out-compete them already, or would increase receptor activity from agonist ILP behavior going unchecked. This unchecked agonist behavior causing an inhibition of the DAF-16 pro-longevity transcription factor, and an increase in neuronal aberration[28,30,32,39]. Also, several β subfamily members are known to have agonist behavior on the DAF-2 receptor through dauer modulation, such as INS-2, INS-3, INS-4, INS-6, INS-7, and DAF-28[28,32,33,59]. Interestingly, two β sub-family ILPs are known to display antagonistic behavior, INS-1[33,34], the closest *C. elegans* homolog to human insulin, and INS-7[45]. INS-7 displays both agonistic and antagonistic behavior depending on the observed outcome, such as dauer prevention[27] or learning[45], respectively. This variable role supports a context-based function of ILPs[47], and the idea of a spatiotemporal "block-design" that is responsible for orchestrating overall ILP expression in specific tissues under specific environmental and cellular conditions[35]. This further highlights that more research is necessary on the ligand-receptor binding interaction to fully understand ILP signaling. Because of the experimental endpoint context and tissue specificity of ILP activity, understanding the direct binding activity of ILPs to the IR receptor and any inter-ILP binding competition would greatly contribute to understanding of how those context-specific activities are achieved. This understanding would fill in the gap at the start of the IIS pathway with elucidation of the molecular sterics of different ILPs on the IR binding sites. Molecular studies of more direct IIS pathway responses and mRNA expression levels over time are proposed to paint a more accurate picture of how the IR responds to individual ILPs and which ILPs will play long term roles in neuronal aging. The results presented in this study indicate specific ILPs, and the β subfamily in particular, to be responsible for maintaining normal mechanosensory neuron morphology. Therefore, these ILPs should be considered as starting points for future work that focuses on neuronal aging and neurodegeneration, and as potential candidates for further molecular study into ligand-receptor binding.

***Caenorhabditis* Sieve: A Low-Tech Instrument and Methodology for Sorting Small Multicellular Organisms**

Results garnered from Chapter 2, show a successful introduction of a new technology designed for research laboratory use. The original goal of designing and producing a tool and accompanying protocol that is an affordable, efficient, rapid, and accurate alternative method for transferring large numbers of animals at particular developmental stages between culture plates was met. This is evidenced by the *Caenorhabditis* Sieve's adoption as a transfer methodology by other researchers in the shared laboratory space the device was designed in, for either transferring via its primary intent or cleaning *C. elegans* as per an alternative intended purpose. Even more evidence that the initial goals were met is the reproduction and implementation of the device in the research laboratory of Dr. Michael B. Harris at California State University, Long Beach, for use in an upstart newly established *C. elegans* laboratory. Along with this adoption by other researchers, was the frequent use of the *Caenorhabditis* Sieve in a teaching environment where several undergraduate researchers successfully used the device and protocol. These outcomes highlight the simplicity of comprehension and use by researchers with little laboratory experience or experience with the *Caenorhabditis* Sieve. They also bolster a broad reaching impact on the greater research community that this tool provides.

This novel technology and the ability it has to fill a gap in basic research tools through its simplicity, efficacy, and cost effectiveness allowed the parent university, University of Alaska Fairbanks, to file a patent and license the technology with the biomedical research company NemaMetrix for further research and development to bring the device to market and mass production in the hopes of advancing scientific progress.

Thesis Contributions

Both chapters 1 and 2 of this thesis contribute to the advancement of science. Chapter 1 identifies a list of ILPs that are responsible for the occurrence of normal age-related morphology changes in neurons. This list of ILPs and resulting data on the relative shifts in morphology changes, when the expression of each is individually knocked down, helps to clarify the role of those ILPs as either agonists or antagonists to the DAF-2 receptor. Chapter 1 also presents future research avenues to further understand IIS and its influence on neuronal aging and metabolic signaling overall. Chapter 2 introduced a new laboratory tool that facilitates the use of assays utilizing small organisms that would otherwise be unfeasible. Together, the application of the *Caenorhabditis* Sieve from chapter 2 can be applied to the research avenues described in chapter 1 to acquire further knowledge on the IIS pathway. The *Caenorhabditis* Sieve can assist in the proposed genetic screen, using *C. elegans daf*-16::*gfp* reporter strain, by allowing for larger numbers of animals to be maintained for each RNAi treatment group. Additionally, by removing the tedious and time consuming process of hand transferring individual animals the proposed screen could be conducted in a smaller amount of time as animal transfer in different treatment groups would not need to be staggered over multiple days to account for transfer time. The *Caenorhabditis* Sieve can also assist in the proposed research of *C. elegans* ILP mRNA expression by allowing researchers to use and maintain the large numbers of *C. elegans* required for each group used for genetic material harvesting, and additionally by keeping those groups of *C. elegans* free of mixed population and bacterial genetic contamination. By using these thesis chapters in concert with

one another researchers can dig deeper into the mechanics and functionality of the IIS pathway. By facilitating these future research endeavors down the proposed paths, this thesis as a whole serves to contribute to the advancement of IIS understanding, and by direct extension, a better understanding of the aging process that underlies neurodegeneration.

BIBLIOGRAPHY:

1. Yankner, B., Lu T., Loerch, P. The aging brain. *The Annual Review of Pathology: Mechanisms of Disease*. (3), 41–66 (2008). DOI: 10.1146/annurev.pathmechdis.2.010506.0920442008

2. Bishop, N.A., Lu, T., Yankner, B.A. Neural mechanisms of ageing and cognitive decline. *Nature* **464** (7288), 529–535 (2010). DOI: 10.1038/nature08983

3. Fjell, A.M., Walhovd, K.B. Structural brain changes in aging: courses, causes and cognitive consequences. *Reviews in the Neurosciences*. **21** (3), 187–221 (2010). PMID: 20879692

4. Knobloch, M., Mansuy, I.M. Dendritic spine loss and synaptic alterations in Alzheimer's disease. *Molecular Neurobiology*. **37** (1), 73–82 (2008). DOI: 10.1007/s12035-008-8018-z

5. https://www.alz.org/alzheimers-dementia/facts-figures

6. http://parkinson.org/Understanding-Parkinsons/Causes-and-Statistics/Statistics

7. http://www.alsa.org/about-als/facts-you-should-know.html

8. https://www.cdc.gov/DiseasesConditions/

9. Vilchez, D., Saez, I., Dillin, A. The role of protein clearance mechanisms in organismal ageing and age-related diseases. *Nature Communications*. **2014** (5), 5659 (2014).

10. Mattson, M. P., Chan, S. L., Duan, W. Modification of brain aging and neurodegenerative disorders by genes, diet, and behavior. *Physiol. Rev*. **2002** (82), 637–672 (2002).

11. Samuelson, A., Carr, C., Ruvkun, G. Gene activities that mediate increased life span of *C. elegans* insulin-like signaling mutants. *Genes and Development*. **21** (22), 2976-2994 (2007). DOI: 10.1101/gad.1588907

12. Kaletsky, R., Murphy, C. The role of insulin/IGF-like signaling in *C. elegans* longevity and aging. *Disease models & mechanisms*. **3** (10), 415-419 (2010). DOI: 10.1242/dmm.001040

13. Kannan, K., Fridell, Y. Functional implications of *Drosophila* insulin-like peptides in metabolism, aging, and dietary restriction. *Frontiers in physiology*. **4** (October), 288 (2013). DOI: 10.3389/fphys.2013.00288

14. Suh, Y. et al. Functionally significant insulin-like growth factor I receptor mutations in centenarians. *Proceedings of the National Academy of Sciences of the United States of America*. **105** (9), 3438-3442 (2008). DOI: 10.1073/pnas.0705467105

15. Pan, C., Peng, C., Chen, C., McIntire, S. Genetic analysis of age-dependent defects of the *Caenorhabditis elegans* touch receptor neurons. *Proceedings of the National Academy of Sciences of the United States of America.* **108** (22), 9274-9 (2011). DOI: 10.1073/pnas.1011711108

16. Tank, E., Rodgers, K.E., Kenyon, C. Spontaneous Age-Related Neurite Branching in *Caenorhabditis elegans*. *The Journal of neuroscience: the official journal of the Society for Neuroscience*. **31** (25), 9279-88 (2011). DOI: 10.1523/JNEUROSCI.6606-10.2011

17. Toth, M. et al. Neurite Sprouting and Synapse Deterioration in the Aging *Caenorhabditis elegans* Nervous System. *The Journal of neuroscience: the official journal of the Society for Neuroscience*. **32** (26), 8778–8790 (2012). DOI: 10.1523/JNEUROSCI.1494-11.2012

18. van Exel, E. et al. Insulin-like growth factor-1 and risk of late-onset Alzheimer's disease: findings from a family study. *Neurobiology of Aging*. **35** (2014), 725.e7-725.e10 (2014). DOI: 10.1016/j.neurobiolaging.2013.08.014

19. Steen, E. et al. Impaired insulin and insulin-like growth factor expression and signaling mechanisms in Alzheimer's disease- is this type 3 diabetes? *Journal of Alzheimer's Disease*. **7** (2005), 63-80. DOI: 10.3233/JAD-2005-7107

20. Gami, M.S., Wolkow, C. Studies of *Caenorhabditis elegans* DAF-2/insulin signaling reveal targets for pharmacological manipulations of lifespan. *Aging Cell*. **2006** (5), 31-37 (2006). DOI: 10.1111/j.1474-9726.2005.001888.x

21. Paradis, S., Ruvkun, G. *Caenorhabditis elegans* Akt/PKB transduces insulin receptor-like signals from AGE-1 PI3 kinase to DAF-16 transcription factor. *Genes and Development*. **12** (16), 2488-98 (1998). PMID: 9716402

22. Paradis, S., Ailion, M., Toker, A., Thomas, J., Ruvkun, G. A PDK1 homolog is necessary and sufficient to transduce AGE-1 PI3 kinase signals that regulate diapause in *Caenorhabditis elegans*. *Genes and Development*. **13** (11), 1438-1452 (1999). DOI: 10.1101/gad.13.11.1438

23. *C. elegans* Sequencing Consortium. Genome sequence of the nematode *C. elegans*: a platform for investigating biology. *Science.* **282** (5396), 2012-2018 (1998).

24. Herman, M. A. Hermaphrodite cell-fate specification. *WormBook.* 1-16, doi:10.1895/wormbook.1.39.1 (2006).

25. Hobert O. Neurogenesis in the nematode *Caenorhabditis elegans* (October 4, 2010), *WormBook*, ed. The *C. elegans* Research Community, WormBook, doi/10.1895/wormbook.1.12.2

26. Brenner, S. The genetics of *Caenorhabditis elegans*. *Genetics*. **77** (1), 71-94 (1974). DOI: 10.1002/cbic.200300625

27. Stiernagle, T. Maintenance of *C. elegans*. *WormBook.* 1-11, DOI:10.1895/wormbook.1.101.1 (2006).

28. Murphy, C.T. et al. Genes that act downstream of DAF-16 to influence the lifespan of *Caenorhabditis elegans*. *Nature*. **424** (6946), 277-284 (2003). DOI: 10.1038/nature01789

29. Klass, M. Aging in the nematode *Caenorhabditis elegans*: Major biological and environmental factors influencing life span. *Mechanisms of Ageing and Development*. **1977** (6), 413-429 (1977).

30. Cohen, E., Dillin, A. The insulin paradox: Aging, proteotoxicity and neurodegeneration. *Nature Reviews Neuroscience*. **9** (10), 759-767 (2008). DOI: 10.1038/nrn2474

31. Nollen, E. et al. Genome-wide RNA interference screen identifies previously undescribed regulators of polyglutamine aggregation. *Proceedings of the National Academy of Sciences*. **101** (17), 6403-6408 (2004). DOI: 10.1073/pnas.0307697101

32. Murphy, C.T., Hu, P.J. Insulin/insulin-like growth factor signaling in *C. elegans* (December 26, 2013), *WormBook*, ed. The *C. elegans* Research Community, WormBook, DOI:/10.1895/wormbook.1.164.1

33. Hung, W., Wang, Y., Chitturi, J., Zhen, M. A *Caenorhabditis elegans* developmental decision requires insulin signaling-mediated neuron-intestine communication. *Development*. **141** (8), 1767-1779 (2014). DOI: 10.1242/dev.103846

34. Pierce, S. et al. Regulation of DAF-2 receptor signaling by human insulin and ins-1, a member of the unusually large and diverse *C. elegans* insulin gene family. *Genes and Development*. **15** (6), 672-86 (2001). DOI: 10.1101/gad.867301

35. Ritter, A., et al. Complex expression dynamics and robustness in *C. elegans* insulin networks. *Genome Research*. **23** (6), 954-65 (2013). DOI: 10.1101/gr.150466.112

36. Matsunaga, Y., Iwasaki, T., Kawano, T. Diverse insulin-like peptides in *Caenorhabditis elegans*. *International Biology Review*. **1** (1), 1-15 (2017). DOI: 10.18103/ibr.v1i1.1276

37. Li, W., Ruvkun, G. daf-28 encodes a *C. elegans* insulin superfamily member that is regulated by environmental cues and acts in the DAF-2 signaling pathway. *Genes and Development*. **17** (7), 844-858 (2003). DOI: 10.1101/gad.1066503

38. Kao, G. et al. ASNA-1 Positively Regulates Insulin Secretion in *C. elegans* and Mammalian Cells. *Cell*. **128** (3), 577-587 (2007). DOI: 10.1016/j.cell.2006.12.031

39. Scerbak, C. et al. Insulin signaling in the aging of healthy and proteotoxically stressed mechanosensory neurons. *Frontiers in Genetics*. **5** (July), 1-14 (2014). DOI: 10.3389/fgene.2014.00212

40. Ward, C., Menting, J.G., Lawrence, M.C. The insulin receptor changes conformation in unforeseen ways on ligand binding: Sharpening the picture of insulin receptor activation. *Bioessays*. **2013** (35), 945-954 (2013) DOI: 10.1002/bies.201300065

41. Whittaker, L., Hao, C., Fu, W., Whittaker, J. High Affinity Insulin Binding: Insulin Interacts with Two Receptor Ligand Binding Sites. *Biochemistry*. **47** (48), 12900 (2008). DOI: 10.102/bi801693h

42. Duret L., et al. New Insulin-Like Proteins with Atypical Disulfide Bond Pattern Characterized in *Caenorhabditis elegans* by Comparative Sequence Analysis and Homology Modeling. *Genome Research*. **1998** (8), 348-353 (1998). DOI: 10.1101/gr.8.4.348

43. Varewijck, A.J., Janssen, J.A.M.J.L. Insulin and its analogues and their affinities for the IGF1 receptor. *Endocrine-Related Cancer*. **19** (5), F63-F75 (2012). DOI: 10.1530/ERC-12-0026

44. Hung, W. et al. Attenuation of insulin signaling contributes to FSN-1 mediated regulation of synapse development. *The EMBO journal*. **32** (12), 1745-60 (2013). DOI: 10.1038/emboj.2013.91

45. Chen, Z. et al. Two Insulin-like Peptides Antagonistically Regulate Aversive Olfactory Learning in *C. elegans*. *Neuron*. **77** (3), 572-585 (2013). DOI: 10.1016/j.neuron.2012.11.025

46. Matsunaga, Y., Gengyo-Ando, K., Mitani, S., Iwasaki, T., Kawano, T. Physiological function, expression pattern, and transcriptional regulation of a *Caenorhabditis elegans* insulin-like peptide, INS-18. *Biochemical and Biophysical Research Communications*. **423** (3), 478-83 (2012). DOI: 10.1016/j.bbrc.2012.05.145

47. Fernandes de Abreu, D.A. et al. An Insulin-to-Insulin Regulatory network Orchestrates Phenotypic Specificity in Development and Physiology. *PLOS Genetics*. **10** (3), e1004225 (2014). DOI: 10.1371/journal.pgen.1004225

48 Baugh, R.L., Kurhanewicz, N., Sternberg, P.W. Sensitive and Precise Quantification of Insulin-Like mRNA Expression in *Caenorhabditis elegans*. *PloS one*. **6** (3), 18086 (2011). DOI: 10.1371/journal.pone.0018086

49. Chen, Y., Baugh, R. Ins-4 and daf-28 function redundantly to regulate *C. elegans* L1 arrest. *Developmental Biology*. **394** (2), 314-326 (2014). DOI: 10.1016/j.ydbio.2014.08.002

50. Michaelson, L. *C. elegans*: A Practical Approach. Ian A. Hope (ed.). Oxford University Press, Oxford. 1999. Pp. 281. ISBN 0 19 963738 5. *Heredity*. **85** (1), 97-100 (2000).

51. Chalfie, M., Hart, A. C., Rankin, C. H., Goodman, M. B. Assaying mechanosensation. *WormBook*. DOI:10.1895/wormbook.1.172.1 (2014).

52. Van Raamsdonk, J. M., Hekimi, S. FUdR causes a twofold increase in the lifespan of the mitochondrial mutant gas-1. *Mechanisms of Ageing Development.* **132** (10), 519-521 (2011).

53. Gandhi, S., Santelli, J., Mitchell, D. H., Stiles, J. W., Sanadi, D. R. A simple method for maintaining large, aging populations of *Caenorhabditis elegans*. *Mechanisms of Ageing Development.* **12** (2), 137-150 (1980).

54. Aitlhadj, L., Stürzenbaum, S. R. The use of FUdR can cause prolonged longevity in mutant nematodes. *Mechanisms of Ageing and Development.* **131** (5), 364-365 (2010).

55. Davies, S. K., Leroi, A. M., Bundy, J. G. Fluorodeoxyuridine affects the identification of metabolic responses to daf-2 status in *Caenorhabditis elegans*. *Mechanisms of Ageing Development.* **133** (1), 46-49 (2012).

56. Feldman, N., Kosolapov, L., Ben-Zvi, A. Fluorodeoxyuridine improves *Caenorhabditis elegans* proteostasis independent of reproduction onset. *PLoS One.* **9** (1), e85964 (2014).

57. Pulak, R. Techniques for analysis, sorting, and dispensing of C. elegans on the COPAS flow-sorting system. *Methods Molecular Biology.* **351**, 275-286 (2006).

58. Chung, K., Crane, M. M., Lu, H. Automated on-chip rapid microscopy, phenotyping and sorting of *C. elegans*. *Nature Methods*. **5** (7), 637-643 (2008).

59. Hua, Q., et al. A divergent INS protein in *Caenorhabditis elegans* structurally resembles human insulin and activates the human insulin receptor. *Genes and Development*. **17** (June), 826-831 (2003). DOI: 10.1101/Gad.1058003